Analysis of endocytosis at eisosomes

Dissertation zur Erlangung des Doktorgrades
der Fakultät für Biologie
der Ludwig-Maximillians-Universität
München

vorgelegt von

Michael Rehman

München 2011

Erstgutachter: Prof. Dr. Stefan Jentsch
Zweitgutachter: Prof. Dr. Charles David
Tag der mündlichen Prüfung: 19 .09.2011

Eherenwörtliche Versicherung

Ich versichere hiermit ehrenwörtlich, dass die vorgelegte Dissertation von mir selbstständig und ohne unerlaubte Hilfe angefertigt ist.

München, den ....

(Unterschrift)

Erklärung

Hiermit erkäre ich,

☐ Dass die Dissertation nicht ganz oder in wesentlichen Teilen einer anderen Prüfungskomission vorgelegt worden ist

☐ Dass ich mich anderweitig einer Doktorprüfung ohne Erfolg **nicht** unterzogen habe

München, den ....

(Unterschrift)

Diese Dissertation wurde von Prof. Dr. Stefan Jentsch betreut. Die Dissertation wurde eingereicht am

Tag der mündlichen Prüfung:

Table of Contents

1.List of publications

N E Ziolkowska, L Karotki, **M Rehman,** J T Huiskonen, T C Walther. " *Eisosome-driven plasma membrane organization is mediated by BAR domains".* Nat Struct Mol Biol (**2011**)

Rehman, M.[*], Aguilar, P. S.[*], Frohlich, F.[*], Shales, M.[*], Ulitsky, I., Olivera-Couto, A., Braberg, H., Shamir, R., Walter, P., Mann, M., Ejsing, C. S., Krogan, N. J.,Walther, T. C. (**2010**). "*A plasma-membrane E-MAP reveals links of the eisosome with sphingolipid metabolism and endosomal trafficking.*" Nat Struct Mol Biol 17(7): 901-908. (* = equal contribution)

Choudhary, C., Kumar, C., Gnad, F., Nielsen, M. L., **Rehman, M.,** Walther, T. C., Olsen, J. V., Mann, M. (**2009**). "*Lysine acetylation targets protein complexes and co-regulates major cellular functions.*" Science 325(5942): 834-840.

2.Abbreviations

AAA-ATPase	ATPase associated with various cellular activities
BAR	Bin1/Amphiphysin/Rvs (161,167)
CHX	Cycloheximide
CPY	Carboxypeptidase-Y
DNA	Deoxyribonucleic acid
EDTA	Ethylenediaminetetraacetic acid
E-MAP	Epistatic miniarray profile
FM4-64	N-(3-triethylammoniumpropyl)-4-(6-(4-(diethylamino)phenyl)hexatrienyl)pyridinium dibromide
FRAP	Fluoroscence recovery after photpbleaching
G418	Geniticin disulphate
GFP	Green fluorescent protein
HRP	Horse radish peroxidase
IP	Immunoprecipitation
Kan	Kanamycin
kDa	kilo-Daltons
LB	Luria Bertini media
LY	Lucifer yellow
MAT	Mating type
MCC	Membrane compartment occupied by Can1
MCP	Membrane compartment occupied by Pma1
MCT	Membrane compartment occupied by TORC2
PAGE	Polyacrylamide gel electrophoresis
PBS	Phosphate buffered saline
PCR	Polymerase chain reaction
PEG	Polyethylene glycol
RFPmars	Red fluorescent protein Mars
RT	Room temperature
SC	Synthetic complete
SDS	Sodium dodecyl sulphate
SILAC	Stable isotope labelling of amino acids in cell culture
WT	Wildtype
YP	Yeast peptone media

3.Abstract

The yeast plasma membrane contains at least three microdomains – membrane compartment containing Pma1 (MCP), membrane compartment containing TORC2 (MCT) and membrane compartment containing Can1 (MCC). Eisosomes underlie the MCC domain defined by the marker protein arginine permease (Can1). Eisosomes are large protein assemblies composed of Pil1 and Lsp1 proteins, of which Pil1 is essential for plasma membrane organization. We found that the uncharacterized AAA-ATPase protein Yta6 dynamically colocalizes with eisosomes. Yta6 physically interacts with eisosome components, specifically with Pil1. In *PIL1* deletion cells, Yta6 is unable to localize normally to the plasma membrane. Yta6 foci colocalize with the intermediates of FM4-64 on the plasma membrane. The number of these intermediates is increased upon overexpression of Yta6. Overexpressed Yta6 is also able to rescue the defects of endocytosis in cells devoid of amphiphysins. Together rescue experiments and colocalization of a protein cargo Hxt3 with eisosomes suggest that Yta6 likely plays a role in endocytosis at eisosomes. To identify genes whose products function together with eisosome components, we independently carried out a genetic interaction study (epistatic mini array profile) which revealed the protein Emp70. *EMP70* showed the strongest correlation in genetic profile with *PIL1*. Emp70 localizes to a subset of eisosomes in addition to its localization in endosomes and vacuoles. We found eisosomes are required for normal numbers of Emp70 plasma membrane foci. Deletion of Emp70 misdirected endosomal protein Kex2 to vacuole, implicating its essential role in maintaining the architecture of the endosomal compartment. In summary, Yta6 likely plays a role in initiation of endocytosis at eisosomes and Emp70 during intracellular trafficking from plasma membrane to vacuole.

4.Introduction

4.1.Plasma membrane organization

4.1.1.Plasma membrane structure

The plasma membrane has a bilayered structure composed of lipids and proteins. The ratio of lipid to protein varies depending on the type of cellular membrane, type of organism, and type of cell. The three main types of lipids present in the membranes are phosphoglycerides, sphingolipids and cholesterol. Phosphoglycerides account for more than half of the lipid of most membranes. The distribution of these lipids in the membrane is asymmetric; the outer leaflet contains mostly phosphatidylcholine and sphingolipids and the inner leaflet contains primarily phosphatidylethanolamine, phosphatidylserine and minor amounts of phosphatidylinositol. Phosphatidylcholine is one of the lipids which serve as the bulk structural element of biological membranes. Due to its cylindrical nature, it does not induce curvature of membrane but is required for membrane transport and fusion processes. In addition, it has a role in signaling via the generation of DAG. Phosphatidylethanolamine is another major component of membranes. It is required for assembly of many membrane proteins by acting as a chaperone during their folding. Phosphatidylserine is only a minor component of most membranes and plays an important role in regulation of apoptosis. Sphingolipids are derivatives of sphingosine have been estimated to compose >30% in the plasma membrane (Patton and Lester, 1991). The various sphingosine based lipids have additional groups esterified to the terminal alcohol of the sphingosine moiety e.g. if the substitution is

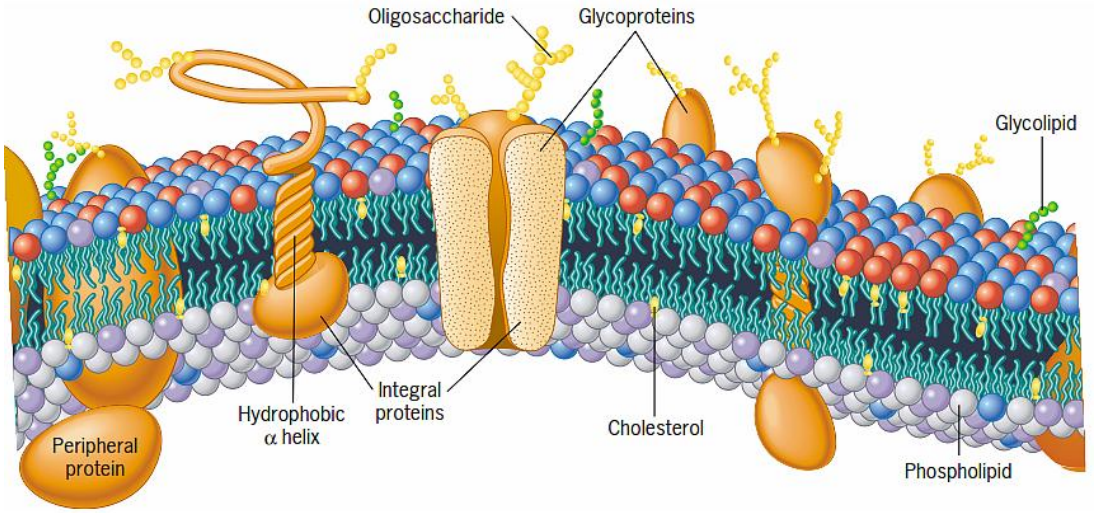

Fig 1. General organization of the plasma membrane. The external surface of most membrane proteins and lipids contain short chains of sugars. The two leaflets of the bilayer contain different lipids. The outer leaflet is thought to contain microdomains ("rafts") consisting of clusters of specific lipid species (Karp, 2004).

phosphocholine, the molecule is sphingomyelin, if the substitution is a carbohydrate, the molecule is called glycolipid. Sphingolipids in general perform structural role in the membranes. In addition to providing structural integrity to the membrane they also have important role in cell signaling and in particular some e.g. sphingomyelin is required for myelin sheath formation. Last important component of membranes is the sterol cholesterol, which in certain animal cells may constitute up to 50% of the total lipid in the plasma membrane. The hydrophobic rings of cholesterol molecule are flat and rigid, and they interfere with movements of fatty acid tails of the phospholipids. Thus, sterols provide rigidity to the membrane (Alberts, 2002).

The model for the organization of lipids and proteins in the membrane has undergone many revisions. In 1935, Danielli and Davson proposed that the

plasma membrane was composed of lipid bilayer, lined by globular proteins and lipid bilayer penetrated by protein lined pores for transport. This model was replaced by the 'fluid mosaic model' proposed by Singer and Nicolson which states that - membranes are two dimensional fluids in which proteins are embedded (Singer and Nicolson, 1972; Vanderkooi and Green, 1970; Vereb et al., 2003) **(Fig 1)**. This model is now considered a 'central dogma' of membrane biology. The structure and arrangement of membrane proteins in the fluid mosaic model differ from that of previous models in that they occur as mosaic of discontinuous particles that penetrate lipid sheet. Most importantly, in the fluid mosaic model the components are mobile and capable of coming together to engage in various types of transient or semipermanent interactions (Frye and Edidin, 1970).

For several years after the acceptance of fluid mosaic model it was assumed that proteins are the only key players for membrane functionality e.g. in transport, cell signaling, and lipids have a passive role. Biochemical studies suggested the existence of a higher order organization of proteins and lipids in the membrane called 'lipid rafts' (Simons and Vaz, 2004). Lipid rafts are membrane microdomains formed by high concentration of sphingolipids and cholesterol. The tight packing of lipids in rafts confers resistance to solubilization by non-ionic detergents at low temperatures. The size of rafts *in vivo* is not yet established however, much evidence now suggests them to be in the range of 25 to 75 nm (Lingwood and Simons, 2010; Mayor and Rao, 2004). According to the lipid raft hypothesis, different lipids found in the plasma membranes have

different propensity to associate with each other due to differing biophysical characteristics of the lipid. This causes phase separation which results in the formation of distinct and stable domains by membranes. The combinatorial association of different types of sphingolipids with cholesterol further accounts for raft diversity (Simons and Gerl, 2010) **(Fig 2)**. In recent years two types of lipid rafts have been proposed: planar lipid rafts and non-planar lipid rafts (Allen et al., 2007). Both types are enriched in sphingolipids and cholesterol. Planar rafts are continuous with the plasma membrane, do not show invaginations and often contain flotilin proteins. Non-planar rafts are made by caveolin proteins, the so called 'caveolae' (Allen et al., 2007). Both types of rafts are proposed to cause localized cell signaling by recruiting specific proteins necessary for signal transduction (Wachtler and Balasubramanian, 2006). They also provide cells with a mechanism for sorting in the exocytic pathway (Lingwood and Simons, 2010).

4.1.2.Differences between yeast and higher eukaryotes plasma membrane organization

The yeast plasma membrane appears simpler in composition compared to mammalian cells. The inner leaflet of *S cerevisiae* is enriched in PE, PI, PS. In contrast to higher eukaryotes, in which cholesterol is the most abundant sterol, the yeast plasma membrane contains mainly ergosterol and minor amounts of zymosterol. A striking feature of the yeast plasma membrane is the anomalously slow mobility of lipids and proteins therein. This slow mobility does not appear to depend on the cell wall or actin cytoskeleton as the mobility is only mildly

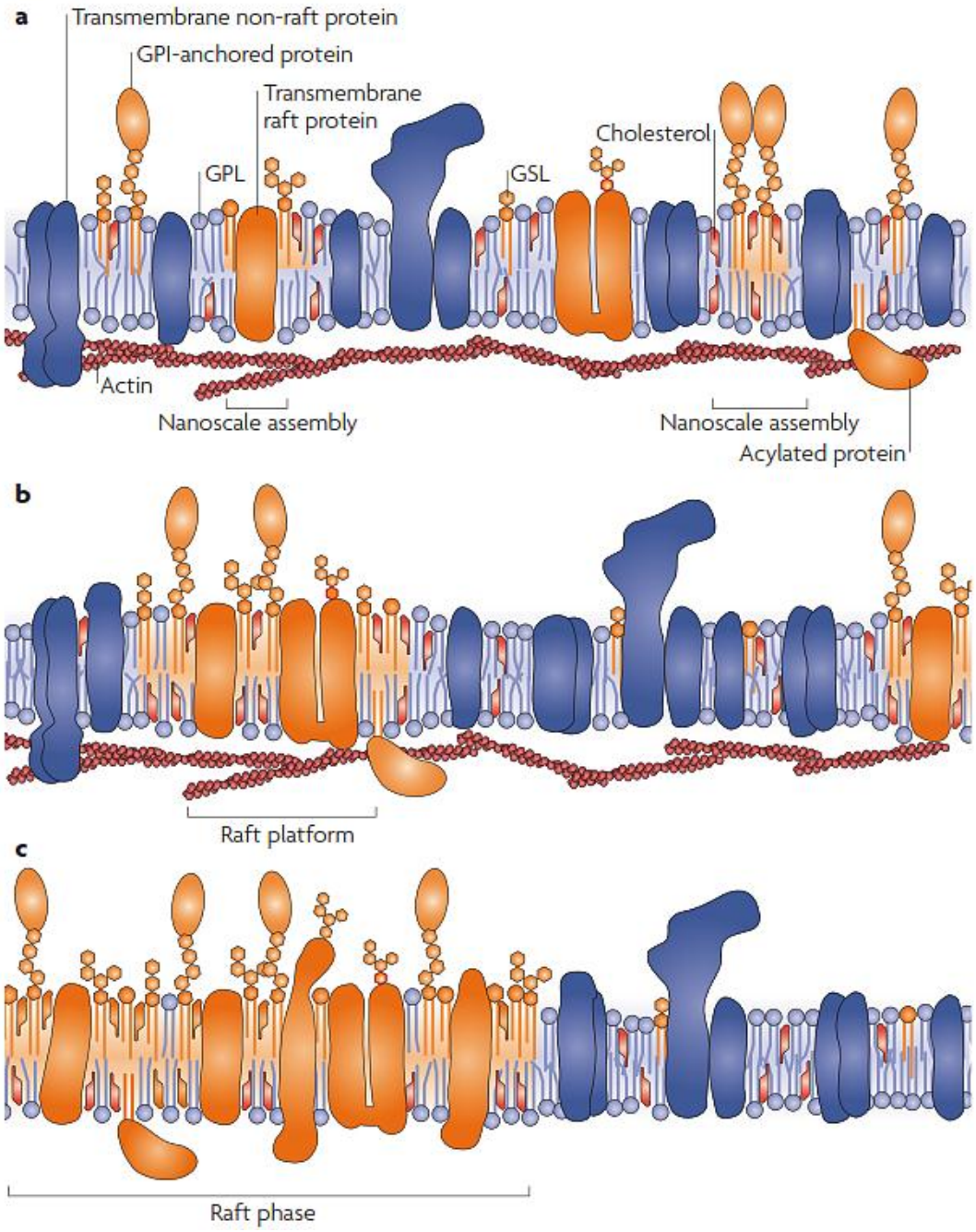

Fig 2.Raft based heterogeneity in cell membranes. (a) Nanoscale assemblies of lipids and proteins can be modulated by actin structures. (b) Signaling and trafficking events initiate formation of raft platforms. (c) Micrometre sized rafts are observed in model systems like giant unilamellar vesicles and giant plasma membrane vesicles. (Simons and Gerl, 2010)

affected in spheroplasts (Valdez-Taubas and Pelham, 2003; van der Rest et al., 1995; van Meer, 2002).

The organization of proteins and lipids on the yeast plasma membrane shows many similarities with mammalian cells but also possesses some unique features. Early studies from Kai Simon's lab showed that the yeast plasma membrane contains lipid rafts. In yeast, lipid rafts are composed of sphingolipids, ergosterol, inositolphosphoceramide and its mannosylated derivatives. Lipid rafts in yeasts were identified on the basis of insolubility in 1% Triton X-100 at 4 ^{0}C and thus called detergent resistant membranes (DRM) (Schuck et al., 2003). This assay, though reproducible, suffers from possibilities of artifacts. One limitation of this method is that partial insolubility need not arise from differences in detergent sensitivity of coexisting domains, but could also instead arise due to differences in the detergent sensitivity of the two leaflets. Further, it has been recently observed that Triton X-100 promotes the formation of ordered domains in model bilayers, so the presence of detergents may induce segregation of components of the membrane bilayer. Current advances in microscopy have allowed the direct visualization of these lipid rafts by specific marker proteins. Three domains are now well recognized on the yeast plasma membrane. They are named after marker proteins that predominantly localize there **(Fig 3)**.

The first identified microdomain in yeast was found to contain the highly expressed yeast transporter – Pma1. Pma1 was found in the DRM fraction.

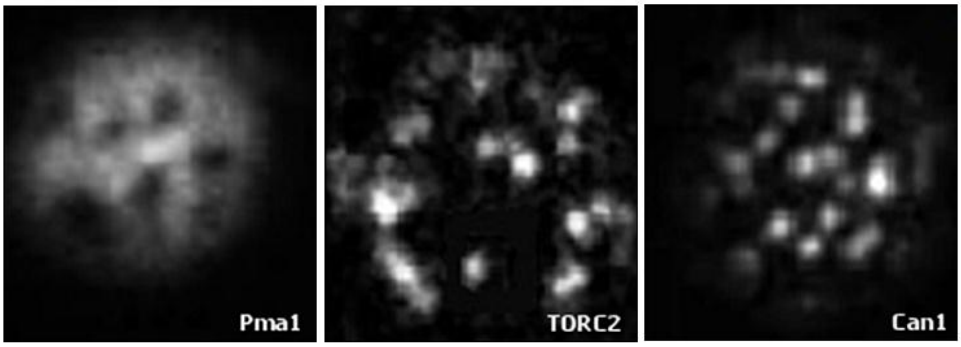

Fig 3. Yeast plasma membrane shows at least three kinds of mutually exclusive domains. MCP (occupied by Pma1) shows network like organization, MCT (occupied by TORC2) shows punctate organization and MCC (occupied by Can1) shows punctate organization (modified from (Berchtold and Walther, 2009; Malinska et al., 2003)).

Microscopy studies showed that Pma1 forms network like pattern in the plasma membrane and thus was called 'membrane compartment occupied by Pma1' or MCP. MCP domain covers a large area of the plasma membrane. Pma1 in this domain freely moves within the plane of the membrane (Grossmann et al., 2007; Malinska et al., 2003).

The second most studied domain is called MCC domain after the arginine transporter Can1 that localizes there. Can1 in the MCC forms large patches of roughly 300 nm diameter that appear as elongated membrane furrows by freeze-fracture electron microscopy (Stradalova et al., 2009). It also behaves like typical raft proteins as it found to be present in the DRM. The definition of raft has been much discussed in many reviews and they are much smaller than 300 nm so it is suggested that Can1 fluorescence in the MCC region is due to raft clustering. Consistent with the raft hypothesis, a sterol labeling dye filipin has been observed to colocalize with Can1 foci (Grossmann et al., 2007; Wachtler et

al., 2003). MCC is also very stable and shows extremely low mobility if any. This is observed in FRAP experiments where the bleached region does not recover over the course of many minutes (Malinska et al., 2004). The organization of this domain is independent of actin cytoskeleton as observed after treating cells with Latrunculin A (Malinska et al., 2004). Recently it has been observed that MCC domains correspond to furrow like invaginations. These invaginations are elongated and do not colocalize with actin patches. Furthermore, membrane potential changes affect the organization of MCC domain (Malinska et al., 2003).

Finally, the last well characterized domain is formed by the TORC2 complex - MCT domain. MCT consists of small, mobile foci distinct from MCC. All TORC2 components localize as oligomeric foci to the plasma membrane, with two to six copies of the subunits of the complex. In contrast to the MCP and MCC domains, MCT components are highly dynamic. They show short range lateral movement on the plasma membrane. The other events that contribute to the dynamic movement of TORC2 are: appearance, disappearance, fusion and splitting of foci. Interestingly, TORC2 foci at the plasma membrane do not colocalize with actin patches and actin is not required for its motility (Berchtold and Walther, 2009).

4.2.Endocytosis

Endocytosis is a universal process occurring in all cell types from bacteria to mammalian cells. It can be defined as: 'A complex process that controls the

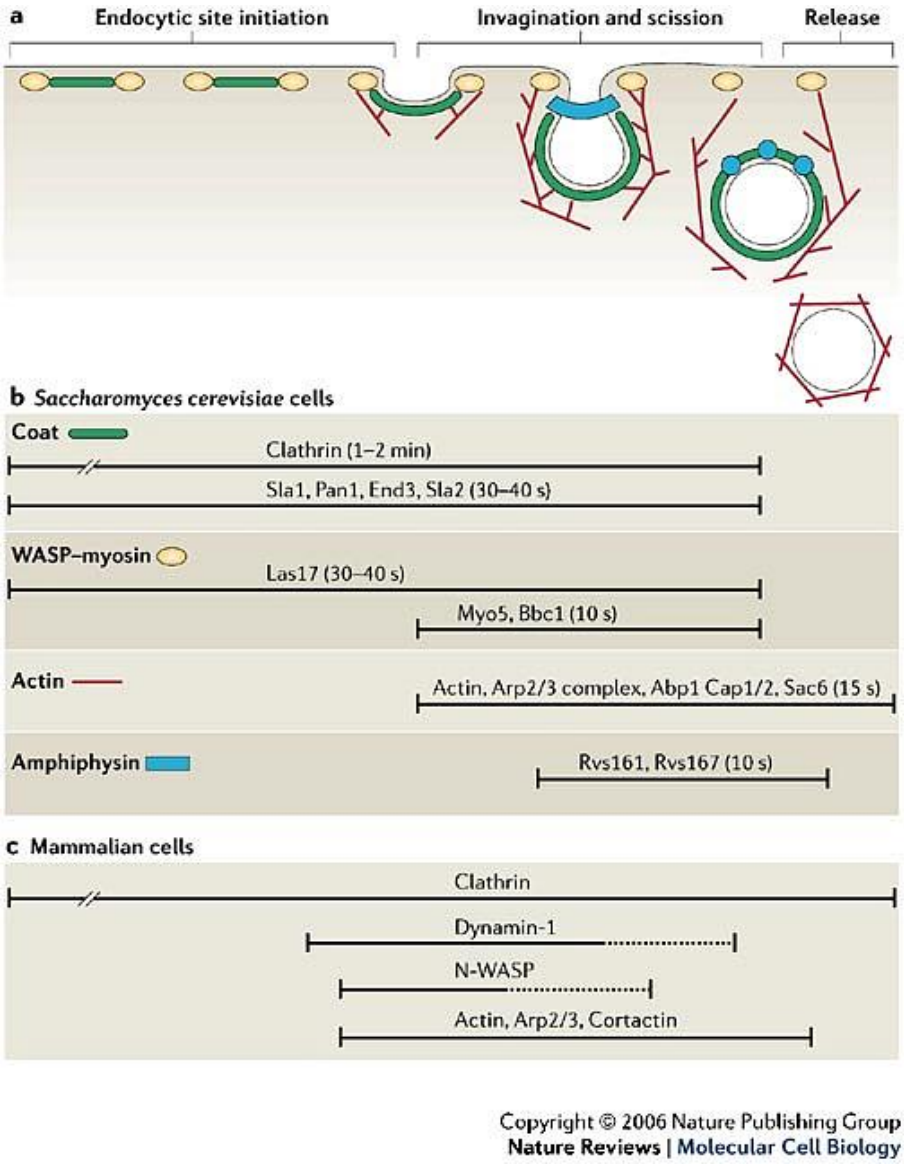

Fig 4. Canonical endocytic pathway in yeast. (a) The four protein modules that are involved in endocytic internalization in yeast are shown: coat complex (green), WASP-myosin complex (yellow), actin network (red) and amphiphysin complex (blue). Components of these different protein modules are assembled and disassembled dynamically. (b) The temporal localization of the constituent proteins for each module in yeast. (c) The approximate temporal localization of proteins during endocytic internalization in mammalian cells. Dashed lines indicate ambiguity in the time frame of the protein dynamics. Endocytic protein modules have not been defined for mammalian cells (Kaksonen et al., 2005).

composition of the plasma membrane, nutrient uptake and regulation of cell signaling' (Ayscough, 2005). The word complex in this definition says that it is not a single step process but requires multiple steps for it to be successful. For any endocytic process to occur at least three steps are required. First, the site of endocytosis is chosen. In eukaryotes, this is facilitated by proteins of the clathrin family, FCHO domain containing proteins, receptor clustering and other mechanisms. Clathrin and clathrin adaptors are central to the formation of clathrin coated pits (CCP). Then there has to be a tubular invagination at the site where endocytosis is initiated. This step in many organisms is mediated by clathrin and amphiphysins. Finally, there scission occurs. In most organisms this step is mediated by dynamin proteins. Yeast serves as a great model system to study these processes because many of the endocytic effectors are conserved between yeast and higher eukaryotes (Engqvist-Goldstein and Drubin, 2003).. The most studied pathway is the actin dependent pathway. Recent studies have shown that this route can be resolved into four modules on the basis of their timing of arrival at the site of endocytosis – coat module, actin module, WASP module and amphiphysin module **(Fig 4)**.

4.2.1.Actin patch dependent endocytosis in yeast

The first step in the actin dependent pathway is mediated by proteins of the coat module. Coat module proteins initiate cargo recruitment and invagination. These processes are mediated independently of actin but their disassembly requires actin polymerization. Assisting in this process is a multimeric protein called clathrin, which consists of three heavy chains and three light chains

noncovalently bound to form a symmetric complex called a triskelion. The exact role of clathrin in yeast is still under debate due to lack of *in vivo* evidence for the formation of clathrin coated pits and clathrin coated vesicles in yeast. Besides, it appears that *CHC1* is the only gene in yeast encoding a clathrin heavy chain. *chc1Δ* mutants are viable but grow worse than wildtype cells.

Actin polymerization is important as it is needed for membrane internalization. The proteins of the second module initiate this important step of actin polymerization. This module is composed of WASP homolog Las17, Myo5 and Bbc1. The motor activity of myosin and the assembling actin drive the invagination inward. It remains immobile at the plasma membrane at the site where actin is being polymerized and disassembles after the coat movement when actin is depolymerized. Myo5 mutants are defective in fluid phase endocytosis and exhibit an increased number of invaginations on the membrane. Bbc1 and Sla1 regulate coat-complex internalization at endocytic sites, possibly by regulating actin nucleation via Las17 or Myo3/5 (Kaksonen et al., 2005).

Proteins of the third module, Rvs161 and Rvs167, are then recruited which contribute to the release of the forming vesicle. These two proteins belong to the amphiphysin family (Lombardi and Riezman, 2001). Amphiphysins are composed of BAR (Bin-Amphiphysin-Rvs) - domains. BAR domains sense membrane curvature and assist in membrane tabulation (Habermann, 2004). Both Rvs161 and Rvs167 have highly conserved BAR domain but only Rvs167

has the other conserved SH3 domain. SH3 domain binds proline rich regions and is involved in cell signaling. They have a mobile fraction in the cytosol and also form transient foci on the plasma membrane. These foci also colocalize with actin patches (Youn et al., 2010). Rvs- proteins *in vivo* form homodimers or heterodimers. They both play a role in endocytosis but Rvs167, because it has an SH3 domain, also functions in cell division, which is mechanistically not very clear (Youn et al., 2010). These proteins are suggested to be required for the scission of the internalizing vesicles. Mutants of *RVS*- show retraction of the coat complex after the initial internalization movement (Jonsdottir and Li, 2004). Even though the amphiphysins are important for endocytosis, many studies in recent years have found that its defects can be overcome by mutating the genes involved in sphingolipid metabolism (Morgan et al., 2009). Germann et al performed a suppressor screen using Rvs161 as bait and revealed proteins involved in sphingolipid-dependent suppressor pathway (Germann et al., 2005). They found mutants of *SUR1*, *SUR2*, *SUR3* and *SUR4* genes having the ability to suppress the endocytic defects in *RVS*-mutants. All these could rescue defects in the single mutants and also the double mutants. Sur1 is a catalytic subunit of MIPC synthase. It forms a complex with Csg2 and functions in the spingolipid biosynthesis. Sur2 is a sphinganine C4 – hydroxalase, catalyses the conversion of sphinganine to phytosphinganine in the spingolipid biosynthesis. Sur4 is an elongase in the sphingolipid biosynthesis, synthesizes very long chain 20-26-carbon fatty acids from C18-CoA. Sur3 is physically unmapped. Another protein of SUR (suppressor of RVS) family – Sur7, has been found to suppress the defects in the amphiphysin mutants upon overexpression (Germann et al., 2005;

Lombardi and Riezman, 2001; McCourt et al., 2009; Morgan et al., 2009). Mechanism of action of many of these proteins is not clear and also which step of endocytosis do they suppress.

Amphiphysins only bend the membrane for invagination but next step of scission is required to pinch off vesicle for intracellular trafficking. Proteins in the fourth module, actin module, are suggested to perform this task. Actin assembly forces may contribute in this process as evidenced by the presence of dense actin filaments called 'actin patches' around early vesicles. Actin patch movement provides the force needed to direct the invaginating plasma membrane into the cell against turgor pressure (Aghamohammadzadeh and Ayscough, 2009) . The first observation of actin patches dates back to 1984 observation by Kilmartin et al (Drubin et al., 1988; Kilmartin and Adams, 1984). They used antibodies to check for actin localization during cell cycle. Later studies used fluorescent reporters to detect actin patches. Yeast cells show three types of actin structures: the actin ring during cytokinesis, actin cables and actin patches. The actomyosin ring in yeast starts early during cell cycle in G1 phase; its contraction is coordinated temporally and spatially with septum formation; surprisingly, the cells without actomyosin structure can divide, albeit less efficiently. Actin cables are polarized structures in dividing cells oriented towards mother-bud axis. These cables act as tracks on which the vesicle moves towards the bud. Actin patches are 0.1 to 0.2 μm in diameter and localize to the cell cortex. In the non-dividing cells they are distributed everywhere in the cell, while in the dividing cells oriented towards the mother bud axis. Each cell has about

10 to 100 patches. Actin patches are dynamic and localize with endocytic cargo. The patches show a lifetime of approximately 15 seconds. At the molecular level these actin patches are made of branched actin filaments. Actin patch formation and movement appears to require actin polymerization nucleated by Arp2/3. Ultrastructure studies have shown that they patches colocalize with membrane invaginations. Genetic studies have shown that mutants of actin patch components (e.g. *act1-1, myo3Δmyo5Δ, sla1Δ*) have defects in cell wall assembly and they grow larger than WT cells (Drubin et al., 1988; Smith et al., 2001).

4.2.2.Eisosomes organize yeast plasma membrane and are static sites of endocytosis

Eisosomes underlie the MCC compartment on the plasma membrane. They are large immobile protein complexes present on yeast plasma membrane. Each cell has about 25 to 45 eisosomes. The core proteins that compose eisosomes are – Pil1 and Lsp1. Pil1 and Lsp1 are 72% similar and the homologs are conserved across fungal kingdom. Each eisosome foci comprises of 2000 – 5000 proteins of each type. Eisosome proteins Pil1 and Lsp1 specifically interact with each other in a 1:1 ratio **(Fig 5)**. *PIL1* deletion mutant shows a striking phenotype – a complete loss of the membrane organization. This has been observed in thin section electron micrographs and also by colocalization of a plasma membrane marker dye with a fluorescently tagged protein. *PIL1* mutants show the so-called 'eisosome remnants'. These remnants vary from cell to cell but are 1 to 5 per

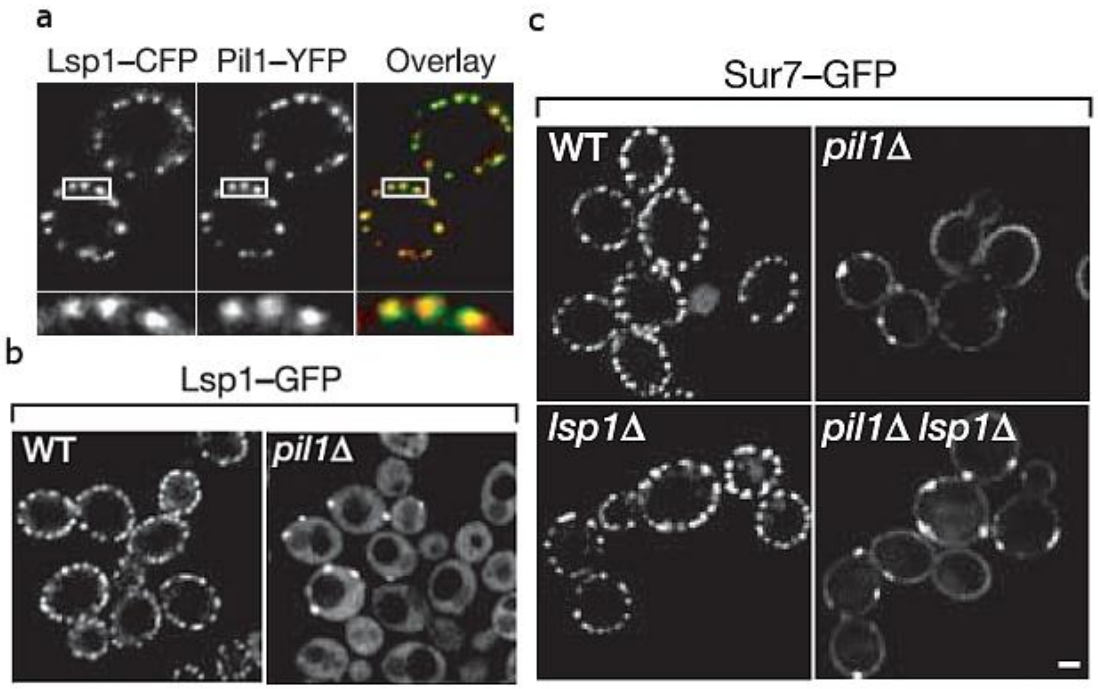

Fig 5. Eisosomes organize plasma membrane. (a) Mid section of a cell is shown to represent the colocalization of eisosomes proteins Pil1 and Lsp1. (b) Mid sections of cells expressing Lsp1-GFP in WT, *pil1Δ* are shown. (c) Mid sections of cells expressing Sur7-GFP in WT, *pil1Δ, lsp1Δ, pil1Δlsp1Δ* are shown (modified from (Walther et al., 2006)).

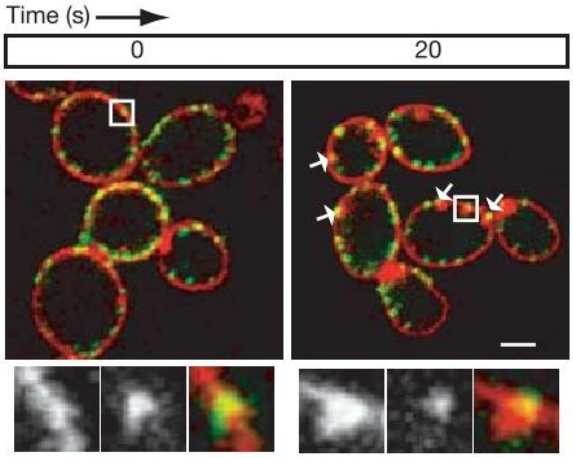

Fig 6. Eisosomes are sites of endocytosis. Mid sections of cells expressing Pil1 (green) is shown and early intermediates of FM4-64 (red). All FM4-64 intermediates colocalize with eisosomes (modified from (Walther et al., 2006).

cell. However, how and why only Pil1 causes this misorganization is still unclear, as Pil1 and Lsp1 show strong similarity but only one gives this phenotype (Walther et al., 2006).

Apart from eisosome's membrane organizing property, they also colocalize with FM4-64 early intermediates at the plasma membrane **(Fig 6)**. This colocalization suggests their role in endocytosis, as FM4-64 is an endocytic tracer which is known to traffic from plasma membrane to endosomal pathway to vacuoles. FM4-64 serves a good example of lipid cargo. The colocalization of eisosomes with Hxt2 intermediates of internalization suggest that also protein cargo is internalized at eisosomes. Mammalian cells show a wide variety of mechanisms of endocytosis and it is likely that yeast also has another pathway which is independent of actin patches. This is supported by: (a) observation of zero colocalization of eisosomes and actin patch marker Abp1, (b) The plasma membrane FM4-64 intermediates localization is unaffected in cells treated with LatA. The presence of two pathways could either allow spatial regulation, cargo selective or temporal regulation in endocytosis. Intriguingly, these intermediates of FM4-64 form only a few eisosomes – approximately about 4 in 40 eisosomes. Experiments with Ste3-HA internalization have shown that eisosome mutants have defects in endocytosis, so it conceivable that a pathway of endocytosis originates at eisosomes.

4.3.Intracellular trafficking from plasma membrane to vacuoles

4.3.1.Sorting from the plasma membrane to vacuole

During intracellular trafficking the internalized cargo along with its coat is first trafficked to early endosomes. At this step, the cargo can be either destined to vacuoles or recycled to the plasma membrane. An important post translational modification occurs in many cargoes early during internalization – ubiquitinylation. It is the addition of 76 amino acid polypeptide, ubiquitin, to the epsilon amino group of lysine residues in the target proteins. Polyubiquitin chain serves as signal triggering endocytosis to early endosomes (Dupre et al., 2004; Lin et al., 2008). Following their internalization, all endocytic ubiquitinylated yeast plasma membrane cargoes are transported through several endocytic intermediates known as post Golgi endosomes or late endosomes. There they meet membrane proteins from Golgi apparatus where cargoes are sorted into distinct domains depending on whether it is for recycling or degradation. Cargo destined for vacuoles is sorted into vesicles which are budded into the interior of the late endosomes resulting in the formation of multivesicular bodies (MVB) (Katzmann et al., 2002). After fusion of MVBs with the vacuole, the vesicles are released into the lumen of the vacuole and proteins associated with them are degraded by vacuolar hydrolases **(Fig 7)**.

4.3.2.AAA-ATPases for disassembly of complexes

The sorting of the MVB is mediated by a set of proteins called class E vps (vacuolar protein sorting). The mutants of the members of this class accumulate

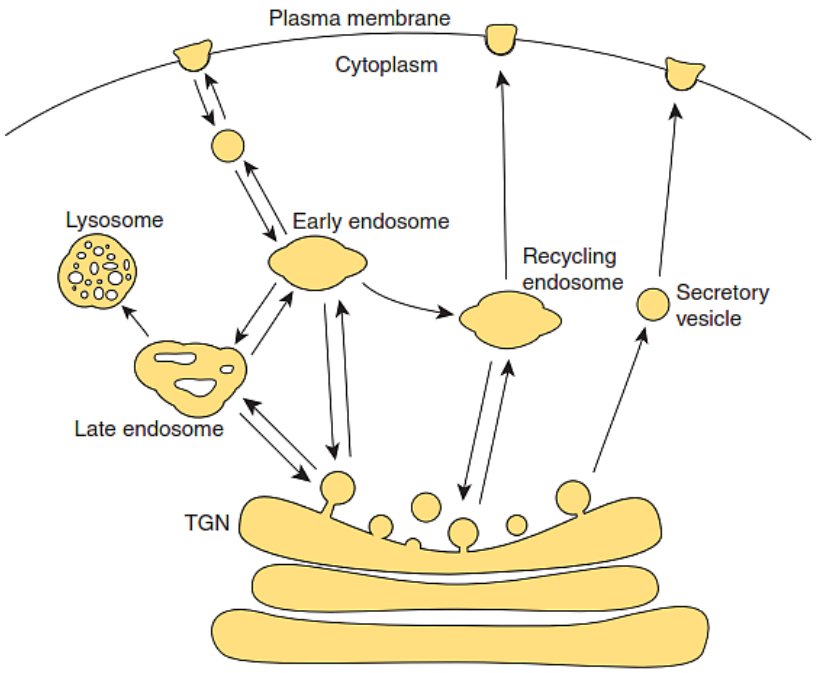

Fig 7. The schematic shows the intracellular trafficking in a typical cell. It shows cargo trafficking through early, late and recycling endosomes (Orlando and Guo, 2009).

endosomal membranes and exhibit defects in the formation of MVB vesicles (Hurley and Emr, 2006). Among class E vps proteins, yeast Vps4 has been shown to play an essential role in the morphological and functional organization of the endocytic system and is required for efficient transport from early to late endosomes. Vps4 is a member of AAA-ATPase family and ATP binding regulates the association of Vps4 with endosomal compartment (Wendland et al., 1998) **(Fig 8)**.

AAA–ATPases are universally present in all organisms from bacteria to metazoans. Just like other P type ATPases, the characteristic features of AAA-ATPases are:

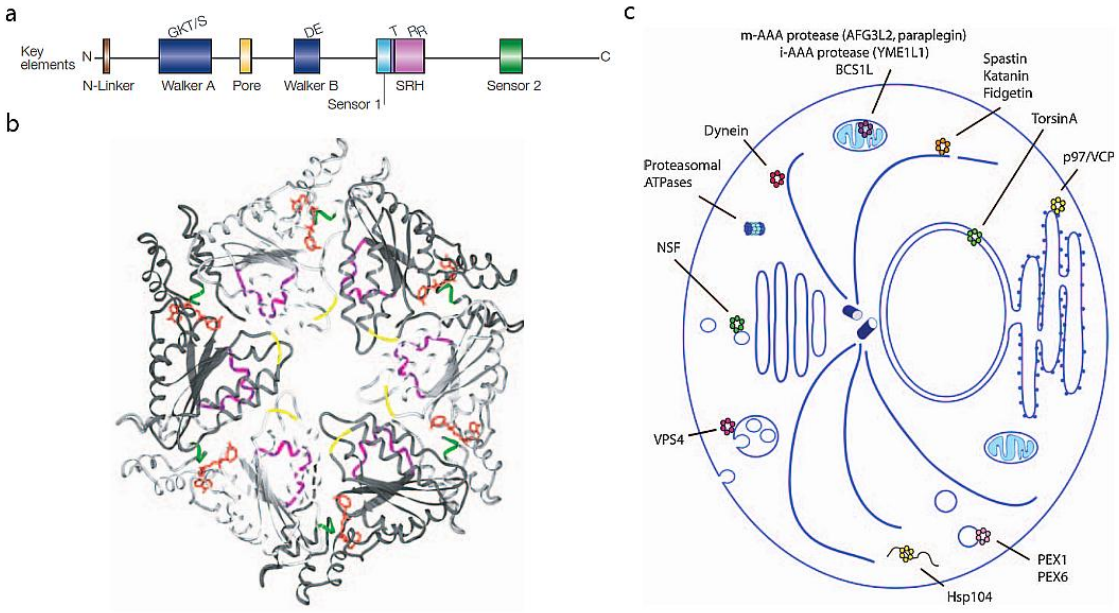

Fig 8. AAA-ATPases in yeast. (a) Organization of domains in AAA-ATPase proteins. (b) Hexameric oligomer of AAA-ATPase NSF. (c) Localization of yeast AAA-ATPase proteins (Hanson and Whiteheart, 2005; White and Lauring, 2007).

Walker A, Walker B, sensor 1, sensor 2 (Frickey and Lupas, 2004) (Hanson and Whiteheart, 2005). The Walker A motif is involved in the phosphate binding of ATP, walker B motif is involved in the metal binding and ATP catalysis, sensor 1 is involved in detection of nucleotide binding and ATP hydrolysis. Members of AAA family assemble into ring-like oligomers that carry out non-covalent conformational modifications of stable proteins and protein-protein complexes. The chaperone like activity of AAA-ATPases promotes assembly and disassembly of target protein complexes. This function is primarily achieved by application of mechanical force on the host protein. Some proteins have only a single AAA domain and others such as dyenin have more than one domain per protein. The oligomers of the AAA proteins can be either hexamers or heptamers. Yeast has

about 50 AAA+ proteins involved in diverse functions (Frickey and Lupas, 2004; Hanson and Whiteheart, 2005; Langer, 2000; Vale, 2000). AAA-ATPases perform many functions in the cell **(Fig 8)**. Many AAA-ATPase proteins function as regulatory subunits of the eukaryotic 26S proteasome – a complex which catalyzes the ATP dependent degradation of ubiquitinated proteins. AAA module also primes the assembly of various membranes targeting protein complex during membrane fusion. For example, NSF is AAA-ATPase which is used for recycling of cis SNARE complexes. NSF performs a chaperone like function to dissociate otherwise stable complexes of vesicle and target membrane SNAP receptors after one round of fusion to facilitate the next round (Dalal et al., 2004). Other activities associated with AAA modules include peroxisome biogenesis, assembly of mitochondrial membrane proteins, cell cycle control, mitotic spindle formation, cytoskeletal interactions, vesicle secretion, signal transduction, and transcription.

AAA-ATPases have been found in almost every organelle in yeast. Yeasts have at least 24 classical AAA proteins (Frickey and Lupas, 2004). They are either involved as regulatory subunits of proteasome, involved in intramitochrondrial protein sorting, important factors for membrane fusion process or involved in endosomal trafficking (Ammelburg et al., 2006; Hanson and Whiteheart, 2005). A previous study found the AAA-ATPase Yta6 localizing to the cell cortex (Beach and Bloom, 2001). Yta6 has a AAA-ATPase domain at the C-terminus. There is no detectable known domain according to current bioinformatic analysis. As expected, the AAA-ATPase domain shows high sequence similarity with other

AAA-ATPase domains. Yta6 shows maximum similarity to Spastin and Katanin proteins, which in higher eukaryotes are involved in microtubule severing (Connell et al., 2009; Hartman et al., 1998). At present the function of Yta6 remains completely uncharacterized.

4.4. Aims

Previous work showed that early intermediates of FM4-64 localize to the plasma membrane independently of actin patches, but are dependent on eisosomes. In the wildtype cells eisosomes were observed to colocalize with FM4-64 intermediates and the intermediates of Hxt2. This suggested the possibility of alternative pathway of endocytosis independent of actin patches.

The goals of this work were to understand the mechanisms of endocytosis at eisosomes. We took a candidate approach by studying two proteins – Yta6 and Emp70. To understand the role of Yta6 in the biology of eisosomes we decided to carry out biochemical experiments to know its interacting partners. We carried out microscopy by confocal and TIR-FM to accurately determine the localization of Yta6 in relation to eisosomes. Finally, to know its involvement in endocytosis, we performed many types of endocytosis assays. To functionally annotate Emp70, we performed live cell imaging of Emp70 with eisosomes to obtain quantitative values for its localization with eisosomes. Emp70 was earlier predicted to be a endosomal protein (Schimmoller et al., 1998). To this end, we carried out microscopy and biochemical assays to determine if it is required for endocytosis, recycling or for maintenance of intracellular compartments.

5.Materials and methods

5.1.Computational and data analyses

NCBI / Pubmed and Google / GoogleScholar were used for most literature search. DNA/protein sequences of interest were extracted from SGD database. In case of alignment or making phylogenetic trees or other sequence manipulation, following softwares were used: NCBI BLAST, Uniprot, ExPaSy, SMART, NCBI ORF finder, Geneious, APE.

Data obtained were either created in Microsoft office Excel or GraphPad Prism. Using their internal options graphs, trendlines or plots were drawn. When standard deviation was mentioned, it was manually incorporated. Histograms were all drawn using the 'Data analysis' Add-ins of Microsoft office Excel. All tests of significance were performed in GraphPad Prism using its automated method.

5.2.Microbiological and genetic techniques

5.2.1.Bacteria techniques

Chemically competent cells for transformation were prepared according to standard protocols. Briefly, a single colony was grown in 200 mL LB media for 2-3 hrs with vigorous shaking (37 ^{0}C, 370 rpm). This was in triplicate, and done till OD reached 0.6. The cultures were then chilled on ice for 30 mins. Cells suspension was then applied into two 500 ml sterile centrifuge tubes and centrifuged at 3000 rpm for 10 min at 4 ^{0}C. Pelleted cells were washed with the original volume of ice-cold ddH_2O, and spin at 3000 rpm for 10 min at 4 ^{0}C.

Washed cells were resuspended with 200 ml (about 1/3 of original volume) of sterile, ice-cold 0.1 M $CaCl_2$ by gentle pipetting. They were left on ice for 1-2hrs before spinning down at 3000 rpm for 10 min at 4 ^{0}C. Cells were then resuspended in 6 ml of sterile, ice-cold 0.1 M $CaCl_2$ 15% glycerol (1/100 of the original volume). 10-50 μl of cells was aliquoted by dispensing into sterile microcentrifuge tubes (the tubes should be placed on dry ice previously in order to freeze cell immediately). Finally, aliquots were frozen at -70 ºC until use.

For molecular biology cloning related work the XL1Blue or DH5alpha *E coli* strains were used. pTOPO, pET, yeast shuttle vectors were transformed and standard protocols were followed. For protein expression related work BL21 strain of *E coli* was used. For transformation, following procedure was followed: an aliquot of competent cells was put on ice and mixed with 1 μg of DNA solution followed by incubation for 15 mins there, a heat shock was given for 90 sec and vial was put back on ice for another 30 sec, then 300 μl of LB media was added and vial was put on 37 ^{0}C incubator. Finally, after 30 mins cells were plated.

5.2.2.Yeast techniques

5.2.2.1.Gene tagging and deletion

Gene tagging with fluorescent reporter proteins or non-fluorescent tags was performed by transformation PCR – product (Janke et al., 2004; Longtine et al., 1998). This method was also used to create yeast strains with gene deletions. It relies on homologous recombination of the transformed PCR product with the

regions in the yeast genome. The positive cells were identified by microscopy, western blotting or colony PCR.

5.2.2.2.Yeast transformation

A LioAc based method was used for all yeast transformation methods. First a culture of 5 ml was started from a single colony on plate for overnight. Early morning another 50 ml culture was started using the overnight culture from 0.2 OD. After the culture reached 0.7 to 0.8 OD, it was pelleted. The pellet was mixed with 10 μl of PCR product or 1-2 μg of plasmid DNA and 100 μl of 0.2 M LioAc (Sigma), followed by addition of 400 μl of PEG 4000 (Serva). This mix was incubated at room temperature before addition of 20 μl of DMSO and then heat shock at 42 ^{0}C for 20 mins. After heat shock cells were washed with YPD and incubated at 30 ^{0}C for more than 4 hrs, before plating on plates with appropriate resistance or auxotrophy.

5.2.2.3.Yeast growth assays

Two types of growth assays were used to check for growth defects in yeast strains. In the growth assay on plates, serially diluted cells were plated starting from 0.2 OD cells. The plates contained appropriate chemical related to the experiment and were incubated at 30 ^{0}C or as per the experiment requirements. In the growth assay in culture, an automated machine connected to software for growth measurement was used. The software allowed to export to a .csv file which was used to show growth curves using Microsoft Excel.

5.2.2.4.Yeast mating and sporulation

To mate a- and α- types of yeast, they were first individually grown to mid log phase. Small amount of culture of each type was then pelleted, mixed in 20μl and incubated on plate till any zygotes were visible when observed in microscope. These zygotes were manually separated from each other on the dissection microscope, and incubated at 30 ^{0}C for three days to grow. Upon growth a small amount was put for overnight culture in YPD media. The culture was then pelleted and put in rich sporulation media, incubated at 30 ^{0}C for few days. Upon visible sporulation the spores were dissected using the dissection microscope. For tetrad dissection following protocol was followed: centrifuge 100 μl of sporulation culture, resuspend in 20 μl of zymolase buffer with 2 μl of zymolyase, incubate at RT for 15 mins, add 100 μl zymolase buffer to stop the reaction, perform dissection at the microscope and let spores grow at 30 ^{0}C. The mating type was tested using the mating type PCR which a- and α- type gave different band sizes upon PCR amplication. Amplification was performed using following primer: F (AGTCACATCAATCGTTTATGG), R – a specific (GCACGGAATATGGGACTACTTCG), R – α- specific (ACTCCACTTCAAGTAA-GAGTTTG). A band of 544 bp is expected from Mat a- type strain while from Mat α- 404 bp band is expected.

5.2.2.5.Yeast genomic DNA isolation

To isolate genomic DNA from yeast 5.0 OD cells were pelleted, then resuspended in 200 μl of breaking buffer (2% Triton X-100, 1% SDS, 100 mM NaCl, 10 mM Tris-Cl pH 7.5, 1 mM EDTA). Small amount of zirconium beads were

added and cells were lysed by vortex for 8 mins. 200 µl of Phenol-chloroform (1:1) was added and mixed. This was spin down for 10 mins at RT and upper layer was transferred to another eppendorf. 10 µl of sodium acetate was then added, followed by equal amount of isopropanol. This was put on rotator for 10 mins for precipitates to form, followed by spin down. The genomic DNA containing pellet was then dissolved in water and stored.

5.2.2.6.Yeast lysate preparation

For general purpose yeast lysate preparation following method was used. 5.0 OD cells were pelleted. To denature proteins and cell wall 8 M urea was added. A small amount of zirconium beads were added to this and they were vortexed for 8 mins. This was followed by addition of 20 µl of 20% SDS and 20% 5X Lamelli buffer. The mix was then heated at 65 ^{0}C for 5 mins before loading 20 µl in the PAGE.

5.2.2.6.Yeast DNA preparation for colony PCR

1 ml of yeast culture was pelleted and 40 µl water was added. A small amount of zirconium beads were added before vortex for 8 mins. 1 µl of that mix was then used for PCR reaction as template. PCR reaction of 25 µl containing – water (16 µl), 10X Buffer (2.5 µl), 25 mM $MgCl_2$ (3 µl), F primer (1.5µl of 10 pM), R primer (1.5µl of 10 pM), DNA template (1 µl) and Taq polymerase (1 µl), was performed.

5.3. Microscopy

5.3.1.Imaging

For fluorescence microscopy, yeast cells were grown to an OD_{600nm} = 0.6 in YPD media at 30 ^{0}C and observed in SC media unless and otherwise stated. Cells were mounted onto coverslips previously coated with concanavalin-A and directly imaged with an ANDOR / TiLL iMIC CSU22 spinning disk confocal microscope, 100X 1.4 NA oil immersion objective. For quantification of the relative numbers of Yta6 molecules making foci, the individual images of Yta6-GFP, Cse4-GFP, and Spc105-GFP were collected with same settings.

For FRAP experiments, the FRAP module of the Andor software was used. ROI of interest were selected. After initializing the time lapse imaging, the selected ROI were bleached with high power laser. Using ImageJ data was imported to Microsoft excel and manually the curves were created.

5.3.2. Image processing

We collected 16-bit images using Andor Image iQ 1.9 in the linear range of the camera. For presentation, images were filtered with a smoothening filter averaging two pixels, converted to 8-bit images and cropped using ImageJ (http://rsb.info.nih.gov/ij/) or a Guassian filter plugin with .75 pixels was used. For quantitation of colocalization, we collected stacks and extracted four-dimensional images for individual cells. Turboreg plugin of ImageJ was used to correct for drift of cell in making movie of colocalization of Hxt3-RFPmars and

Lsp1-RFPmars. Quantification was always performed on original images. Finally, images were put together using Adobe Illustrator.

5.4. Assays

5.4.1.FM4-64 uptake assay

Cells exponentially growing at an OD_{600} = 0.7 (1 ml) were harvested, resuspended in 50 µl of medium and chilled on ice for 5 min. FM4-64 was added to a final concentration of 10 µM and incubated for another 10 min. Cells were washed with ice-cold medium, resuspended and incubated for different time points, after which cells were killed by 10 mM NaN_3 and 10 mM NaF and immediately analyzed by microscopy.

5.4.2.Actin staining by phalloidin

Phalloidin staining was performed to stain actin structures in yeast. Following procedure was followed: Grow an overnight culture, next morning inoculate again starting at 0.2 OD till mid log phase, spin down 200 µl of cells and fix with 3.6% formaldehyde for 30 mins at ice cold temperature, spin down at 1200 rpm to wash out the formaldehyde, resuspend in PBS with 5 µM phalloidin, incubate for 30 mins at ice cold temperature, wash out phalloidin and perform microscopy.

5.4.3.CPY secretion assay

The CPY secretion colony blot assay was performed as described using anti-CPY antibodies (Invitrogen-A6428) (Mullins and Bonifacino, 2001).

5.4.4.Can1 degradation assay

For Can1 localization and western blot analysis cells were grown in log phase in SC-Arginine medium containing 1.5% raffinose and 0.5% glucose. To induce Yta6 overexpression, cells were then shifted to galactose containing medium for 4 hrs followed by addition of 150 μM CHX. The addition of CHX was taken as 0 time point followed by observation or preparation of cells for western blotting as described previously (Frohlich et al., 2009). Equal amounts were loaded on PAGE.

5.4.5.Hxt3 degradation assay

Cells expressing Hxt3-GFP in wildtype or in mutants were grown in 2% glucose containing YP media. To induce degradation, the cells were transferred to media containing 2% galactose. Equivalent of cells were harvested at mentioned and prepared for either microscopy or western blotting.

5.5.Molecular biology techniques

5.5.1.PCR

Polymerase chain reaction (PCR) was used to amplify fragments of DNA. PCR was performed for either gene cloning, gene tagging / deletion using PCR method, making mutants or colony PCR from yeast. For a 50 μl reaction following was used: water (32 μl), 10X Buffer (5 μl), 25 mM $MgSO_4$ (6 μl), 10 mM dNTP (3 μl), 10 pM forward primer (3 μl), 10 pM reverse primer (3 μl), DNA polymerase (1 μl), Template (1 μl). Except for colony PCR and gene tagging /

deletion, where Taq polymerase was used, Phusion polymerase was used (Finnzymes).

5.5.2.Restriction digestion and ligation

For cloning purposes DNA was digested according to standard procedures. Appropriate restriction enzymes (obtained from NEB or fermentas) were used to specifically digest DNA and create sticky / blunt ends suitable for ligation. After over 2 hr digestion, the mix was run on 1% TAE agarose gel. Using methods and protocols from Qiagen, DNA was extracted and ligation was performed. T4 DNA ligase from Fermentas was used in all cases for ligation performed overnight at 16 ^{0}C.

5.5.3.DNA sequencing

All sequencing was performed at the Core Facility (Max Planck Institute of Biochemistry) using an ABI 3730 sequencing machine. A volume of 7 μl containing – 100 ng DNA, 1 μl of 10 pM primer and water was provided to the facility. Facility performed the sequencing reaction with the DYEnamic ET terminator cycle sequencing kit (Amersham-Pharmacia) according to manufacturer's instructions.

5.6.Biochemical techniques

5.6.1.Western blotting

For all western blotting procedures a 10% PAGE was used unless otherwise stated. The gel was first incubated in transfer buffer containing methanol. Dry blotting or wet transfer was used to transfer proteins to the nitrocellulose

membrane. The membrane was then blocked with 5% milk, incubated with primary antibody according to the company suggestions, washed with TBST with tween, incubated with HRP conjugated secondary antibody for 1 hr and washed last time with TBST with tween. The washed blot was incubated with a solution to cause chemiluminisence which was imaged in the Fiji image reader setup.

List of antibodies:

Primary antibody	Company
Anti-HA	SantaCruz biotech
Anti-Myc	SantaCruz biotech
Anti-GFP	Molecular probes
Anti-GFP	SantaCruz biotech
Anti-CPY	Invitrogen
Secondary antibody	Company
Anti-mouse	SantaCruz biotech
Anti-rabbit	SantaCruz biotech

5.6.2.Mass spectometry

Protein extracts from 70 ODs of 'light' and 'heavy' labeled cells were obtained as described (Walther et al., 2007). For immunopurification, equivalent amounts of proteins were incubated with anti-GFP AB-conjugated magnetic nanobeads (Miltenyi Biotech) for 5 mins at 4 ^{0}C and loaded on µMacs columns (Miltenyi Biotech) in a magnetic µMacs Separator (Miltenyi Biotech), washed three times with 1 ml of lysis buffer with 1% (v/v) Triton-X100, three times with 1 ml of lysis buffer without Triton X-100 and eluted by TEV cleavage. Eluates were mixed, diluted 5x in 8 M urea, reduced for 20 min at room temperature (22 ^{0}C) in 1 mM DTT and then alkylated for 30 min by 5.5 mM iodoacetamide in the dark. Then, the eluates were digested, desalted and concentrated as described. Peptides were separated on-line using an Easy nLC system (Proxeon Biosystems, Odense,

Denmark). Samples (5 µl) were loaded as described. Peptides were eluted with a segmented gradient of 2–60% solvent B for 102 mins with a constant flow of 250 nl min^{-1}. The HPLC system was coupled to an LTQ-Orbitrap Velos mass spectrometer (Thermo Fisher Scientific) via a nanoscale LC interface (Proxeon Biosystems). The spray voltage was 2.2 kV, and the temperature of the heated capillary was 180 ^{0}C. Survey full scan spectra (m/z = 300–1600) were acquired in positive ion mode with a resolution of 60,000 at m/z = 400 after accumulation of 1,000,000 ions. Up to ten most-intense ions were sequenced by collision-induced dissociation in the LTQ. Precursor ion charge-state screening was enabled, and all unassigned charge states as well as singly charged peptides were rejected. The dynamic exclusion list was restricted to a maximum of 500 entries with a maximum retention period of 90 secs and a relative mass window of 10 p.p.m. Orbitrap measurements were performed enabling the lock mass option for survey scans to improve mass accuracy. Data were acquired using the Xcalibur software (version 2.1.0, Thermo Fisher Scientific) and MaxQuant, version 1.0.1. The data was searched against the yeast database concatenated with reversed copies of all sequences and supplemented with frequent contaminants using Mascot (version 2.2.0, Matrix Science). Carbamidomethylated cysteines were set as fixed, whereas oxidation of methionine and N-terminal acetylation were set as variable modifications. Maximum allowed mass deviation for MS/MS peaks and missed cleavages were 0.5 and 3 Da, respectively. Maximum false-discovery rates (FDR) were 0.01 both on peptide and protein levels. Minimum required peptide length was six residues. Proteins with at least two peptides were considered identified (Walther et al., 2007).

5.6.3.Lipid isolation

Two methods of lipid isolation were used. For the cold lipid extraction method (non-radioactive), 25 ml cultures of the appropriate strains were incubated with shaking at 30 ^{0}C to OD 0.5. To serve as controls for the success of the method, Myriocin / Aureobasidin was added independently to wildtype strains for 1 hr. Cells were harvested and washed. They were lysed in 1 ml lysis buffer and transferred to glass vials. A small amount of zirconium beads was added and tubes were vortex for 2 mins, followed by incubation at 60 ^{0}C for 20 mins. The extracts were then spinned down at 3000 rpm for 10 mins and dried under nitrogen gas, max 40 ^{0}C. Dried pellet was resuspended in 500 µl water - saturated butanol and 250 µl of waster was added. This mix was vortexed and then spinned down at 4000 rpm for 5 mins. The upper organic phase was then transferred to a new glass vial and let dry under nitrogen gas. During the drying time, the silica plates (Whatman) were activated. Silica plates were heated for 10 mins in microwave and then let cool. On the silica plates, the 100 µl lipids mixed in $CHCL_3$/MetOH/water was dropwise loaded. To run the plate, the TLC plate was dipped in 3 cm TLC solution in a closed glass chamber. The TLC was performed for 2 hrs. To develop, the TLC plate was dipped in cerium molybdate stain and heated at 200 ^{0}C.

For the radioactive method following procedure was performed. Cells were grown in synthetic media containing either glucose (SC-Glu) or galactose (SC-Gal) for 6 h to OD~0.7, washed twice and resuspended in SC-Ser and SC-Gal-Ser. Aureobasidin A treatment was started 20 min prior to labelling. Cells were

labeled with [^{3}H] serine for 90 mins and normalized by OD. Lipid extraction, mild alkaline hydrolysis and desalting were performed as described in (Guan and Wenk, 2006). The dried lipid extracts were reconstituted in chloroform:methanol:water (16:16:5, v/v/v), applied to a silica LK6D thin-layer chromatography (TLC) plate (Whatman) and resolved in chloroform:methanol:4.2 N ammonium hydroxide (9:7:2, v/v/v). Radioactive bands were visualized by Kodak Biomax MR film (Sigma-Aldrich) after EN3HANCE (PerkinElmer) treatment.

5.7. Preparation of yeast ultrathin sections and electron microscopy

Cells were grown in yeast peptone dextrose medium to 0.7 - 0.8 OD. 10 OD of cells were harvested by centrifugation. Cells were fixed by a solution containing 1% Glutaraldehyde, 0.2% Paraformaldehyde in PBS for 50 mins, followed by washing twice with 0.9% NaCl. Pellet was then resuspended in 2% $KMnO_4$ and incubated at room temperature for 45 mins, followed by dehydration through graded alcohols – 50%, 70%, 80%, 90%, 95%, 100% (10 – 15 mins each). This was followed by incubation in propylene oxide for 15 mins twice, then embedding media / propylene oxide (1:1), Embedding media / propylene oxide (1:1), embedding media / propylene oxide (2:1) and finally with embedding medium overnight. Embedding media (R1165) was obtained from Agar Scientific Ltd, England. Sectioning was done with a Reichert Ultracut (Leica/ Reichert, Vienna, Austria). A poststaining step was performed using 1% Uranyl acetate (prepared in filtered water) for 30 mins at room temperature. Electron

microscopy images were taken with a Philips CM 120 (FEI / Philips, Eindhoven, Netherlands). Adjustments of image size, brightness and contrast were performed on GIMP and ImageJ.

5.8. Composition of buffers and media used

Laemmli sample buffer:
- 2% (w/v) SDS
- 20% (v/v) glycerol
- 100 mM Tris base
- 60 mM EDTA
- 0.1% (w/v) bromophenol blue

DNA loading buffer
- 40% sucrose
- 1 mg Bromophenol blue

50X TAE
- 2 M Tris
- 50 mM EDTA

10X SDS PAGE Running buffer
- 25 mM Tris, pH 8.3
- 192 mM Glycine
- 0.1%SDS

50X Stock Solution of TAE Buffer:
- 57.1 ml glacial acetic acid
- 242 g Tris base
- 100 ml of 0.5M EDTA

Add water to 1L and adjust pH to 8.5 with KOH

Coomassie brilliant blue solution:
- 20% (v/v) methanol
- 10% (v/v) acetic acid
- 0.1% (w/v) Coomassie Brilliant Blue R-250

Destaining solution:
- 20% (v/v) methanol
- 10% (v/v) acetic acid

Transfer buffer:
- 250 mM Tris base
- 1.92 M glycine
- 0.1% (w/v) SDS
- 20% (v/v) methanol

TBST:
- 25 mM Tris-HCl, pH 7.5
- 137 mM NaCl
- 2.6 mM KCl

Stripping buffer:
- 4% (w/v) SDS
- 100 mM beta-mercaptoethanol
- 62.5 mM Tris/HCl, pH 6.8

• 0.1% (v/v) Tween 20

LB-medium (and plates)
• 1% (w/v) tryptone (Difco)
• 0.5% (w/v) yeast extract (Difco)
• 1% (w/v) NaCl
• 1.5% (w/v) agar (plates)
• sterilized by autoclaving

SC-media/plates:
• 0.67% (6.7 g/l) yeast nitrogen base (Difco)
• 0.2% (2 g/l) drop out amino acid mix
• 2% (20 g/l) glucose, raffinose, or galactose
• 2% (20 g/l) agar (for plates)
• sterilized by autoclaving

Lipid lysis buffer
• 95% ethanol/water/diethylether-/pyridine/NH_4Cl (15:15:5:1:0.018)

YPD:
• 1% (10 g/l) yeast extract (Difco)
• 2% (20 g/l) bacto-peptone (Difco)
• 2% (20 g/l) D-(+)-glucose
• 2% (20 g/l) agar (for plates)
• sterilized by autoclaving

Sporulation media:
• 1% glucose
• 7.3 mM KH2PO4

TLC running buffer solution
• 180 ml $CHCL_3$/MetOH/4.2N NH_4OH (9:7:2)

Cerium molybdate stain (Hanessian's stain)
• 5 g $CeSO_4$
• 25 g $(NH_4)\ Mo_7O_{24}\ 4xH_2O$
• 50 ml sulfuric acid
• 450 ml water

5.9. Yeast strain list

TWY138	*Mat**a** ura3 trp1 leu2 his3 ade2 can1-100*	Walther et al 2006
TWY250	*Matα ura3 trp1 leu2 his3 ade2 can1-100 rvs161Δ::KAN*	Walther,TC
TWY252	*Matα ura3 trp1 leu2 his3 ade2 can1-100 rvs167Δ::KAN*	Walther, TC
TWY425	*Matα ura3 trp1 leu2 his3 ade2 can1-100 yta6Δ::KAN*	Walther,TC

TWY471	*Matα his3 leu2 lys2 ura3 Yta6-TAP::KAN*	Ghaemmaghami, S et al 2003
TWY821	*Mata ura3 trp1 leu2 his3 ade2 can1-100 Yta6-GFP::HIS*	This study
TWY834	*Matα ura3 trp1 leu2 his3 ade2 can1-100 Sla1-RFPMars::NAT*	This study
TWY965	*Matα ura3 trp1 leu2 his3 ade2 can1-100 Yta6-TAP::KAN*	This study
TWY971	*Mata ura3 trp1 leu2 his3 ade2 can1-100 GAL inducible N-term GFP Yta6 (gigYta6)*	This study
TWY980	*Matα ura3 trp1 leu2 his3 ade2 can1-100 gigYta6::HIS pil1Δ::NAT*	This study
TWY1011	*Matα ura3 trp1 leu2 his3 ade2 can1-100 Sla1-RFPMars::NAT gigYta6::HIS*	This study
TWY1158	*Mata his3 leu2 lys2 ura3 Can1-GFP::HIS*	Huh et al, 2003
TWY1205	*Mata ura3 trp1 leu2 his3 ade2 can1-100 GAL inducible N-term HA tagged Yta6(giHAYta6)*	This study
TWY1234	*Matα ura3 trp1 leu2 his3 ade2 can1-100 Yta6-TAP::KAN, Pil1-Myc::HIS*	This study
TWY1235	*Matα ura3 trp1 leu2 his3 ade2 can1-100 Yta6-TAP::KAN Lsp1-Myc::HIS*	This study
TWY1238	*Matα ura3 trp1 leu2 his3 ade2 can1-100 Yta6-TAP::KAN, Pil1-Myc::HIS lsp1Δ::NAT*	This study
TWY1239	*Matα ura3 trp1 leu2 his3 ade2 can1-100 Yta6-TAP::KAN Lsp1-Myc::HIS pil1Δ::NAT*	This study
TWY1321	*Matα ura3 trp1 leu2 his3 ade2 can1-100 Yta6-GFP::HIS pil1Δ::NAT*	This study
TWY1533	*Matα his3 leu2 lys2 ura3 Can1-GFP::HIS giHA-Yta6::KAN*	Huh et al, 2003
TWY1742	*Matα ura3 trp1 leu2 his3 ade2 can1-100 Yta6-GFP::HIS lsp1Δ::HPH*	This study
TWY1743	*Matα ura3 trp1 leu2 his3 ade2 can1-100 gigYta6::HIS lsp1Δ::NAT*	This study
TWY1757	*Matα ura3 trp1 leu2 his3 ade2 can1-100 gigYta6::HIS pil1Δ::NAT lsp1Δ::HPH*	This study
TWY1900	*Matα ura3 trp1 leu2 his3 ade2 can1-100 Hxt2-Mars::NAT Yta6-GFP::KAN*	This study
TWY2042	*Mata ura3 trp1 leu2 his3 ade2 can1-100 gigYta6::HIS, pRS306 Pil1-GFP::URA*	This study
TWY2076	*Matα his3 leu2 lys2 ura3 Can1-GFP::HIS, rvs161Δ::NAT*	This study
TWY2078	*Matα his3 leu2 lys2 ura3 Can1-GFP::HIS, rvs161Δ::NAT giHAYta6::KAN*	This study

TWY2072	*Mat**a** his3 leu2 lys2 ura3 Hxt3-GFP::HIS*	Huh et al, 2003
TWY2207	*Mat**a** his3 leu2 lys2 ura3 Hxt3-GFP::HIS, lsp1△::NAT*	This study
TWY2209	*Mat**a** his3 leu2 lys2 ura3 Hxt3-GFP::HIS, pil1△::HpH*	This study
TWY2211	*Mat**a** his3 leu2 lys2 ura3 Hxt3-GFP::HIS, lsp1△::NAT, pil1△::HpH*	This study
TWY2213	*Mat**a** his3 leu2 lys2 ura3 Hxt3-GFP::HIS, yta6△::NAT*	This study
TWY2215	*Mat**a** his3 leu2 lys2 ura3 Hxt3-GFP::HIS, giHAYta6::KAN*	This study
TWY2216	*Mat**a** his3 leu2 lys2 ura3 Hxt3-GFP::HIS, giHAYta6::Kan, rvs161△::NAT*	This study
TWY2217	*Matα his3 leu2 lys2 ura3 vrp1△::KAN*	Winzeler et al., 1999
TWY2218	*Matα his3 leu2 lys2 ura3 vrp1△::KAN, giHAYta6::HIS*	This study
TWY2224	*Mat**a** his3 leu2 lys2 ura3 Hxt3-GFP::HIS, rvs161Δ::KAN*	This study
TWY2279	*Matα ura3 trp1 leu2 his3 ade2 can1-100 lsp1Δ::NAT, pil1Δ::HPH, Yta6-GFP*	This study
TWY2274	*Matα ura3 trp1 leu2 his3 ade2 can1-100 gigYta6, rvs161Δ::KAN, sla1-RFPmars::NAT*	This study
TWY2272	*Matα ura3 trp1 leu2 his3 ade2 can1-100 rvs161Δ::KAN, sla1RFPmars::NAT*	This study
TWY2229	*Mat**a** his3 leu2 lys2 ura3 Hxt3-GFP::HIS, Lsp1-RFPmars::NAT*	This study
TWY1194	*Mat **a** Kex2-RFP-Mars::NAT^R, EMP70-GFP::KAN^R ura3 trp1 leu2 his3 ade2 can1-100*	This study
TWY1044	*Mat **a** EMP70-GFP::KAN^R SNF7-RFP-Mars::NAT^R ura3 trp1 leu2 his3 ade2 can1-100*	This study
TWY1063	*Mat **a** EMP70-GFP::KAN^R ura3 trp1 leu2 his3 ade2 can1-100*	This study
TWY871	*Mat α EMP70-GFP::KAN^R, LSP1-RFP-Mars::NAT^R ura3 trp1 leu2 his3 ade2 can1-100*	This study
TWY1319	*Mat **a** YLR413w-RFP-Mars::NAT^R, EMP70-gfp::KAN^R ura3 trp1 leu2 his3 ade2 can1-100*	This study
TWY1320	*Mat **a** YLR413w-RFP-Mars:.NAT^R, EMP70-gfp::KAN^R, del_pil1::KANR ura3 trp1 leu2 his3 ade2 can1-100*	This study
TWY1195	*Mat **a** KEX2-GFP::KAN^R, emp70Δ::NAT^R ura3 trp1 leu2 his3 ade2 can1-100*	This study

TWY138	*Mat a ura3 trp1 leu2 his3 ade2 can1-100*	This study
TWY1360	*Mat a emp70Δ::NAT^R ura3 trp1 leu2 his3 ade2 can1-100*	This study
TWY1223	*Mat a vps1Δ::HPH^R ura3 trp1 leu2 his3 ade2 can1-100*	This study
TWY1230	*Mat a tmn1Δ::NAT^R tmn2Δ::HPH^R tmn3Δ::HPH^R ura3 trp1 leu2 his3 ade2 can1-100*	This study
TWY1183	*Mat a VPS5-RFP-Mars::NAT^R, EMP70-GFP::KAN^R ura3 trp1 leu2 his3 ade2 can1-100*	This study
TWY450	*Mat α pil1Δ ::kan ura3 trp1 leu2 his3 ade2 can1-100*	This study
TWY1184	*Mat a tmn2*Δ ::hph *ura3 trp1 leu2 his3 ade2 can1-100*	This study
TWY1182	*Mat α tmn3*Δ ::hph *ura3 trp1 leu2 his3 ade2 can1-100*	This study
TWY1207	*Mat α emp70Δ :: nat, tmn3Δ ::hph*	This study
TWY1206	*Mat a emp70Δ*::nat, *tmn2*Δ ::hph *ura3 trp1 leu2 his3 ade2 can1-100*	This study
TWY1814	*Mat a tmn2*Δ ::hph, *tmn3*Δ *ura3 trp1 leu2 his3 ade2 can1-100*	
TWY1064	*Mat a Emp70-GFP* ::kan, Lsp1-Cherry::HIS *ura3 trp1 leu2 his3 ade2 can1-100*	
TWY1369	Mat a/α *ura3 trp1 leu2 his3 ade2 can1-100* *cdc28*Δ::natNT2	This study
TWY1370	Mat a/α *ura3 trp1 leu2 his3 ade2 can1-100* *cdc28*Δ::natNT2, [pRS316-*CDC28*]	This study
TWY1371	Mat α *ura3 trp1 leu2 his3 ade2 can1-100* *cdc28*Δ::natNT2, [pRS316-*CDC28*]	This study
TWY1372	Mat α *ura3 trp1 leu2 his3 ade2 can1-100* *cdc28*Δ::natNT2, [pRS316-*CDC28*; pRS314]	This study
TWY1373	Mat α *ura3 trp1 leu2 his3 ade2 can1-100* *cdc28*Δ::natNT2, [pRS316-*CDC28*; pRS314-*CDC28*]	This study
TWY1374	Mat α *ura3 trp1 leu2 his3 ade2 can1-100* *cdc28*Δ::natNT2, [pRS316-*CDC28*;pRS314-*cdc28K40R*]	This study
TWY1375	Mat α *ura3 trp1 leu2 his3 ade2 can1-100* *cdc28*Δ::natNT2, [pRS316-*CDC28*; pRS314-*cdc28K40Q*]	This study

TWY1376	Mat a S288c Cdc28-GFP::HISMX6	Huh, Won-Ki et al, Nature 2003

5.10.Yeast vectors

Accession no.	Plasmid	Tag	Marker
P30299	pYM13	TAP	kanMX4
P30300	pYM14	6HA	kanMX4
P30301	pYM15	6HA	HIS3MX6
P30302	pYM16	6HA	hphNT1
P30303	pYM17	6HA	natNT2
P30304	pYM18	9myc	kanMX4
P30305	pYM19	9myc	HIS3MX6
P30306	pYM20	9myc	hphNT1
P30307	pYM21	9myc	natNT2
P30308	pYM22	3HA	klTRP1
P30235	pYM23	3myc	klTRP1
P30236	pYM24	3HA	hphNT1
P30239	pYM27	EGFP	kanMX4
P30240	pYM28	EGFP	HIS3MX6
P30279	pYM-N25	GAL1 Promoter, yeGFP	natNT2
	pYM27.1	RFPmars	natNT2
	pYM27.2	RFPmars	KanMX6
	pFA6a	GAL1 Promoter, GFP	KanMX6
P30347	pFA6-	No tag – deletion	hphNT1
P30346	pFA6-	No tag - deletion	natNT2
	pFA6a	GAL1 Promoter, GFP	HIS3MX6

(Janke et al., 2004; Longtine et al., 1998)

6.Results

6.1. Yta6 is involved in endocytosis

6.1.1. Yta6 dynamically localizes to the plasma membrane

The uncharacterized AAA-ATPase Yta6 was previously found to localize in a peculiar pattern reminiscent of eisosome localization after over-expression (Beach and Bloom, 2001). To test whether endogenous Yta6 localizes to the plasma membrane we created Yta6 with C-terminal GFP fusion using homologous recombination to introduce the corresponding sequence into the genome. When we determined the localization of Yta6-GFP in respect to a plasma membrane marker Hxt2-RFPmars, we found that Yta6 forms foci on the plasma membrane **(Fig 9a)**. We then performed time lapse imaging to determine if Yta6 foci are static or dynamic. It showed that many Yta6 foci remain at the plasma membrane for approximately two minutes before disappearing **(Fig 9b,c).** To know whether Yta6 foci at the plasma membrane exchange with cytosolic Yta6, we performed FRAP (fluorescence recovery after photobleaching) experiments. Three foci were imaged every two seconds. This revealed that Yta6 foci recover in approximately two minutes **(Fig 9d,e)**.

6.1.2. Yta6 forms oligomeric foci on the plasma membrane

Yta6 belongs to the AAA-ATPase family of proteins. These proteins have a highly similar AAA-ATPase domain but unique domains for localization to respective

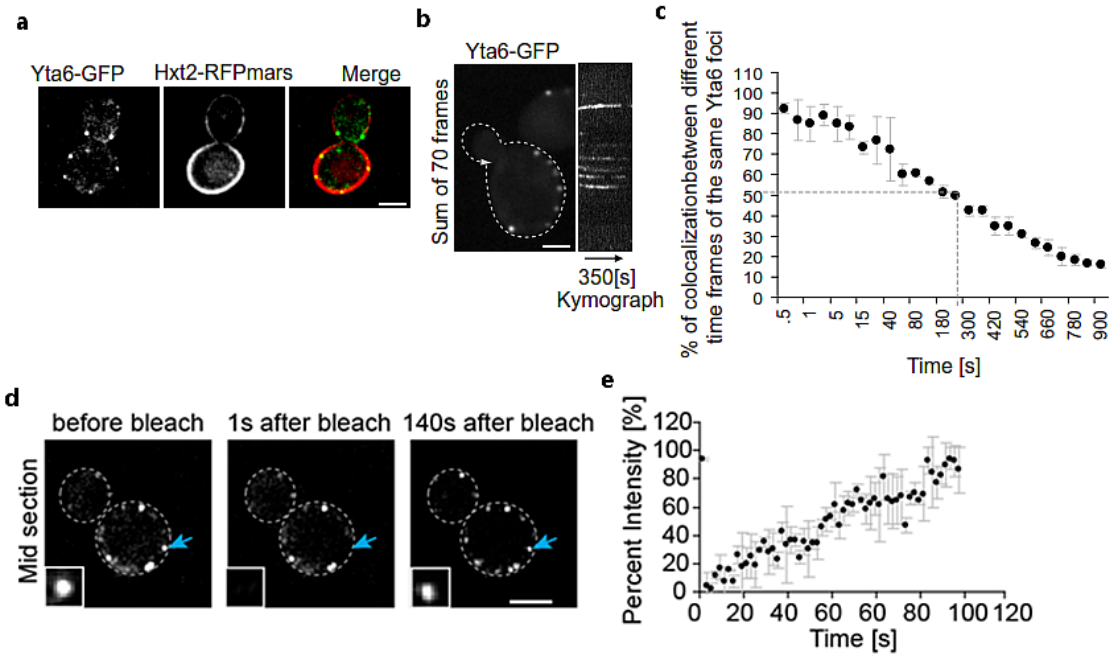

Fig 9. Yta6 dynamically localizes to the plasma membrane. (a) A representative image of endogenous Yta6 tagged with GFP and Hxt2 tagged with RFPmars is shown. A merged image is shown for colocalization. (b) Sum of images of 70 time frames containing Yta6 foci along with kymograph is shown to represent their dynamics. (c) A plot of Yta6 foci disappearance vs time is made to show the residence time of Yta6 foci. (d) Representative images of FRAP of a foci of Yta6 as marked in blue. (e) Quantification of FRAP from three foci (Bar = 2.5 μm).

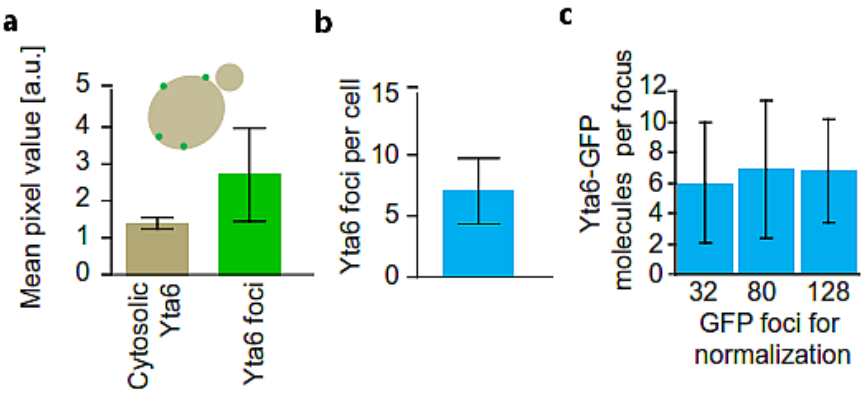

Fig 10. Yta6 forms approximately seven foci per cell. (a) Comparison of the cytoplasmic Yta6 intensity and Yta6 foci intensity is shown which was used to specify Yta6 foci. (b) Quantification of average Yta6 foci per cell. (c) A plot of the average Yta6 foci intensity (n=50) vs average foci intensity of Cse4 (32 molecules; n=20), Spc105 (80 molecules; n=20), and LacI (128 molecules; n=18) is shown. Error bars in all cases indicates standard deviation.

cellular compartments. Most of the AAA-ATPases form oligomers. To know if Yta6 forms oligomers, we used a microscopy based method. First, we determined the brightness of Yta6 foci vs cytosolic signal **(Fig 10a).** Using this quantification we then determined the average number of Yta6 foci per cell **(Fig 10b).** We then compared the brightness of Yta6 foci with foci made by three different proteins: Cse4 (32 molecule foci), Spc105 (80 molecule foci) and LacI repressor (128 molecule foci). Using this method we found that Yta6 forming foci on average contain six of its molecules **(Fig 10c)**.

6.1.3. Regions of Yta6 required for localization to the plasma membrane

AAA-ATPases usually have one or more AAA-ATPase domain and another domain which provides specificity for localization. Yta6 has one AAA-ATPase domain and there is another potential uncharacterized domain at the N-terminus for its localization. To determine if its N-terminus is required for localization to the plasma membrane, we created a mutant without the AAA-ATPase domain. We found that its *GAL*-inducible overexpressed N-terminus (1-456) is sufficient for localization and foci formation at the plasma membrane **(Fig 11)**. To test if AAA-ATPase domain is involved in localization we created a Walker A mutant of *GAL*-inducible overexpressed Yta6 (K517A). This showed that AAA-ATPase of Yta6 affects its localization **(Fig 12)**.

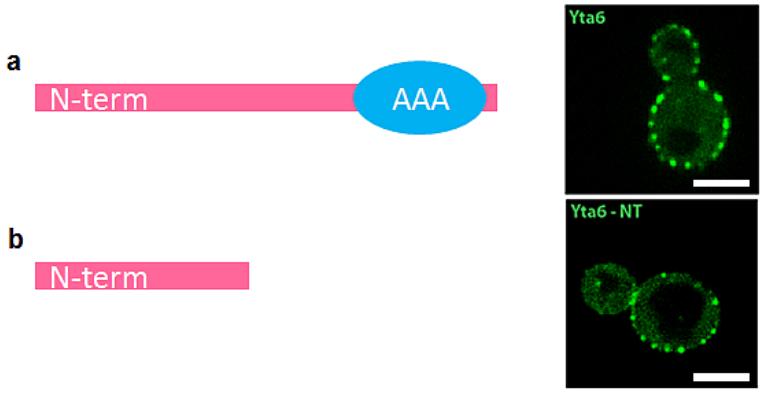

Fig 11. N-terminus of Yta6 is sufficient for its plasma membrane localization. (a) Representative image of WT cell expressing GFP-Yta6 from gal-inducible promoter is shown. (b) Representative image of N term mutant of GFP Yta6 (1-456) from gal-inducible promoter is shown (Bar=2.5 μm).

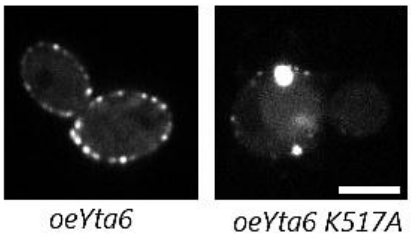

Fig 12. Walker A mutant of Yta6 is unable to normally localize to the plasma membrane. Left panel shows a representative WT cell with GFP-Yta6 from gal-inducible promoter (*oeYta6*). Right panel shows representative picture of a cell expressing mutant Yta6 K517A (Bar = 2.5 μm).

6.1.4. Yta6 forms 'punctae' on the plasma membrane

Confocal microscopy showed dim but specific membrane fluorescence signal in Yta6 GFP expressing cells. To investigate this population at a higher time resolution we used total internal reflection fluorescence microscopy (TIR-FM). It revealed many, transient Yta6 spots that were highly mobile but less bright **(Fig 13)**. Quantification showed that this population of Yta6 localizes to the plasma membrane with a residence time of 60 ms.

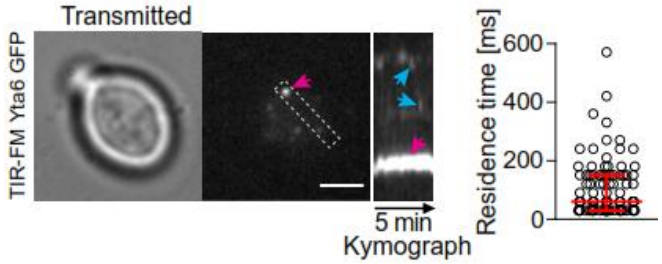

Fig 13. Yta6 shows fast moving punctae. Representative TIR-FM brightfield image and Yta6-GFP along with kymograph for 5 min is shown. The pink arrow is to indicate static foci and blue arrows indicate punctae. Far right panel shows quantification of lifetime of punctae. Error bar indicates 25th percentile, median and 75th percentile (Bar = 2.5 μm).

6.1.5. Yta6 deletion mutant shows canavanine resistance

To determine if Yta6 mutants have any defects, we tested its growth by plating serial dilutions at 37 ^{0}C and 24 ^{0}C. We did not observe any changes in growth under both conditions compared to WT. To test if *yta6*Δ is sensitive to canavanine (3 μg/ml) we compared growth of wildtype BY4741, *yta6Δ* in BY4741 and W303. BY4741 has endogenous Can1 expression but W303 is mutated for Can1, thus served as a control. We found that *yta6*Δ strains are resistant to canavanine **(Fig 14).**

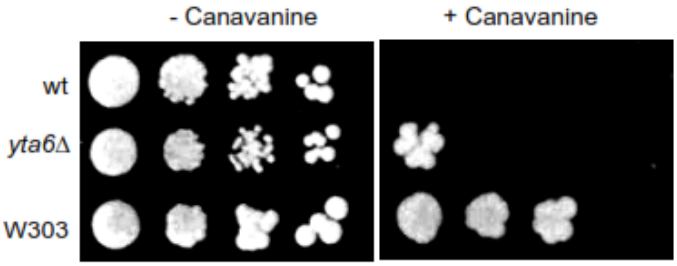

Fig 14. y*ta6Δ* shows resistance to canavanine. Serially diluted cells of wt, *yta6Δ* and W303 were plated on plates with or without 3 μg/ml canavanine to test for its sensitivity.

6.1.6. Yta6 colocalizes with eisosomes

Because the Yta6-GFP signal previously reported was reminiscent of the eisosome pattern, we determined the endogenous localization of Yta6-GFP in respect to eisosomes, marked by Pil1-RFPmars and found it colocalized at a subset of eisosomes in optical top and midsections (88.6 ± 4.2% (SD) Yta6-GFP foci completely overlap with eisosome signal) **(Fig 15)**. The high overlap of Yta6 foci with eisosomes suggests that Yta6 specifically localizes to the eisosomes.

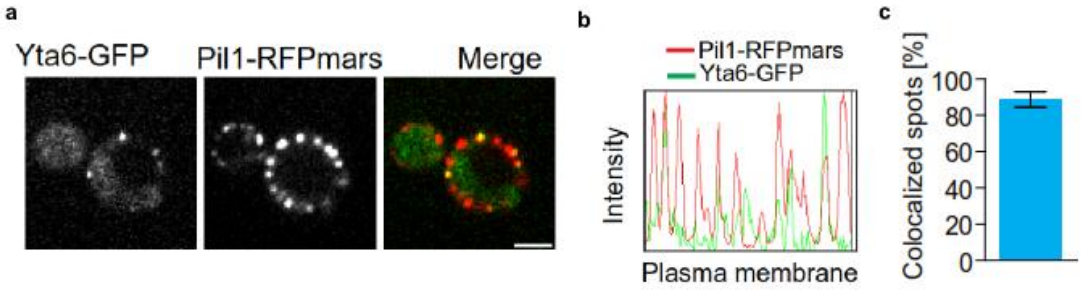

Fig 15. Yta6 colocalizes with eisosomes. (a) Representative image of GFP tagged endogenous Yta6 and RFPmars tagged endogenous Pil1 is shown. Merged image is shown for colocalization. (b) Line scan over the midsection of the mother cell in (a). (c) Quantification of colocalization is shown. Error bar indicates standard deviation. (Bar = 2.5 μm).

6.1.7. Yta6 physically interacts with eisosome core components

To determine whether co-localization of Yta6 and eisosome components is due to a physical interaction between the proteins, we purified Yta6 fused to a tandem affinity purification (TAP) tag from yeast cells by affinity chromatography. We used stable isotope labeling with amino acids in cell culture (SILAC) for the Yta6-TAP tagged strain to discriminate specific interactors from background binders present in eluates from control purifications (Walther et al., 2007).

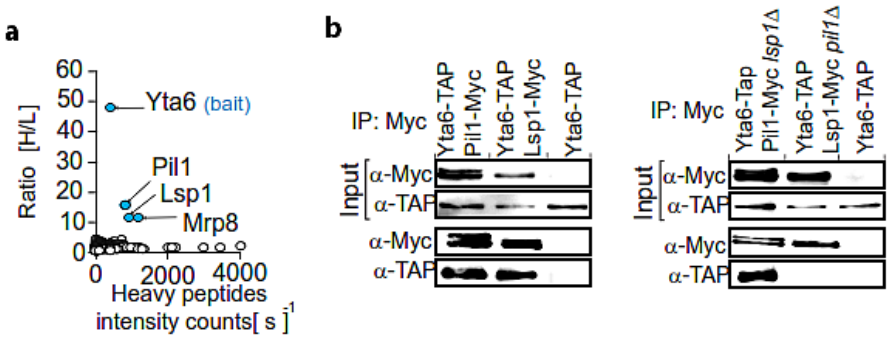

Fig 16. Eisosome components copurify in Yta6 co-immunoprecipitation experiments. (a) Affinity purification of Yta6-TAP expressing cells labeled with Lys8 and untagged control cells labeled with Lys0 were analyzed by quantitative LC-MS/MS. Averaged ratios of heavy to light intensities for proteins are plotted against the intensity of signal from the heavy labeled sample. Significant outliers (P> 0.0000001) for the ratio are shown in blue (b) Yta6 interacts with Pil1 independent of Lsp1. Pil1-Myc and Lsp1-Myc were immunoprecipitated and probed for the presence of Yta6-TAP in WT cells (left panels) or *pil1Δ* or *lsp1Δ* (right panels).

Fig 16 shows that Yta6 had an abundance ratio of roughly 50, indicating that it mostly was purified from labeled cells. We also detected the major eisosome core components Pil1 and Lsp1, as well as the known eisosome binding protein Mrp8 (Wang et al., 2009) with significantly higher ratios than background, indicating that they purify specifically from the strain expressing Yta6-TAP. To independently confirm the interaction between Yta6 and eisosomes, we performed a reverse experiment and immuno-purified Myc-tagged eisosome core components. We specifically found Yta6-TAP in purifications from these cells, but not in the ones performed in parallel from untagged controls. To further test whether Yta6 requires a particular core component for its interaction with eisosomes, we immuno-isolated Pil1-Myc or Lsp1-Myc from cells with a deletion of the other major eisosome component, *LSP1* or *PIL1*, respectively. Comparison of the eluates from each purifications shows that Yta6 requires Pil1, but not Lsp1, for its interaction with eisosomes. From these data, we conclude

that Yta6 directly or indirectly interacts physically with eisosome components and that this is dependent on the presence of Pil1.

6.1.8. Yta6 requires Pil1 for localization to the plasma membrane

To test whether the interaction of Yta6 with eisosomes is required for normal localization of Yta6 at the cell cortex, we investigated endogenously tagged Yta6-GFP in *lsp1*Δ or *pil1*Δ cells by fluorescence microscopy. Consistent with our biochemical data, deletion of *PIL1*, but not *LSP1,* resulted in the loss of foci from the plasma membrane **(Fig 17a)**. However, some residual Yta6-GFP fluorescence remained at the plasma membrane in *pil1*Δ cells and *lsp1*Δ*pil1*Δ cells that was visible only by TIR-FM microscopy **(Fig 17b)**. This most likely indicates that Yta6 is targeted to the cell cortex and then independently interacts with eisosomes there. To validate this hypothesis, we over-expressed GFP-tagged Yta6 and found that it forms foci in wildtype (WT), as well as *lsp1*Δ, *pil1*Δ and *pil1*Δ *lsp1*Δ cells. We also found that Yta6 requires actin for localization to the plasma membrane **(Fig 17c).**

6.1.9. *YTA6* genetically interacts with *PIL1*

To determine if Yta6 shows genetic interaction with Pil1 we used a condition where Pil1 shows phenotype. It has been reported previously that *pil1Δ* is resistant to 5 μM Myriocin (Walther et al., 2007) . Myriocin is an inhibitor of serine palmitoyl transferase, thus it inhibits sphingolipid synthesis. We used this phenotype and made a double mutant of *PIL1* and *YTA6*. We compared the

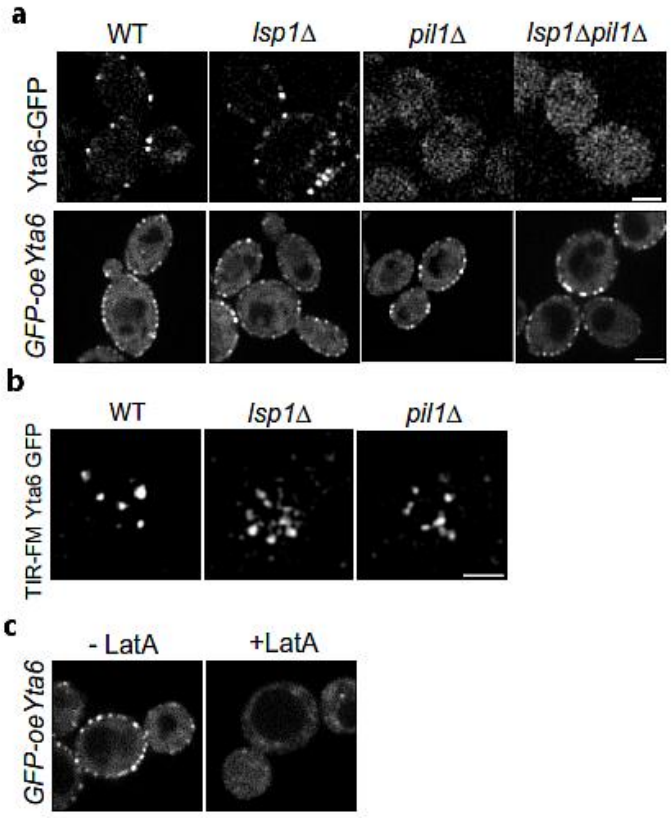

Fig 17. Yta6 has many mechanisms for localizing to the plasma membrane. (a) Endogenous Yta6 requires eisosomes to form foci at the plasma membrane. Representative confocal mid sections of WT, *lsp1*Δ, *pil1*Δ and *lsp1Δpil1Δ* cells expressing endogenous Yta6 (upper panel) or *oeYta6* (overexpressed Yta6- gal inducible) (lower panel) are shown. (b) Yta6 punctae localize independently of eisosome components. (c) Yta6 requires actin for localization to the plasma membrane. Representative confocal mid sections of untreated or cells treated with LatA for 30 mins are shown (Bar = 2.5 μm).

growth of cells in culture of cells with or without Myriocin. We found that Yta6 suppressed *pil1Δ* resistance of growth in Myriocin **(Fig 18).**

6.1.10. Yta6 colocalizes with endocytic sites marked by FM4-64

Yta6 localizes to a subset of eisosomes at any given time. Similarly, FM4-64, a styryl dye widely used as an endocytic tracer forms punctate foci that

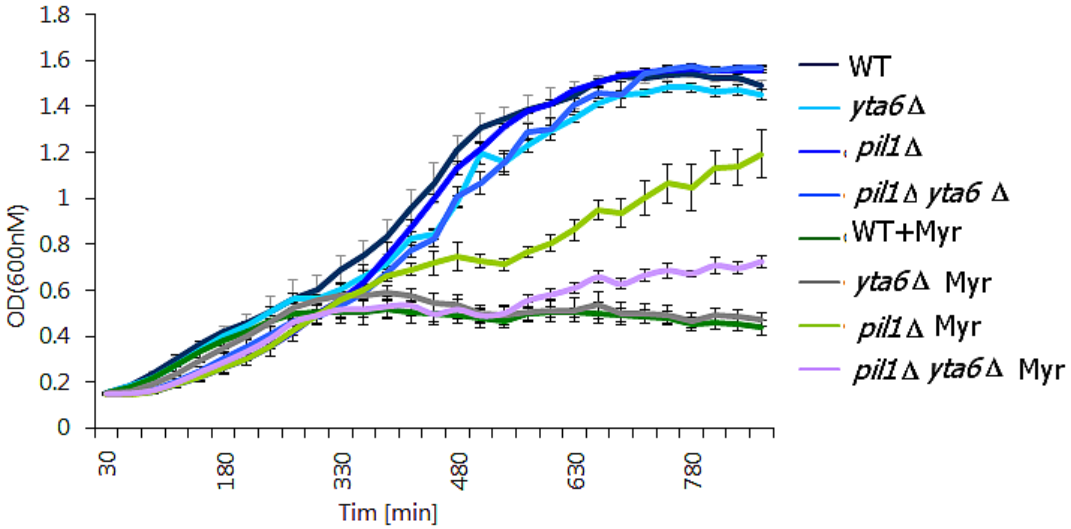

Fig 18. Yta6 is partially required for the suppression of the Myriocin growth defect by Pil1. Growth curves are shown of cells of WT, *yta6Δ*, *pil1Δ*, *yta6Δpil1Δ*, WT + Myr, *yta6Δ* + Myr, *pil1Δ* + Myr, *yta6Δpil1Δ* + Myr. 1 μM Myriocin was used. Error bars indicate standard deviation from three experiments in all cases.

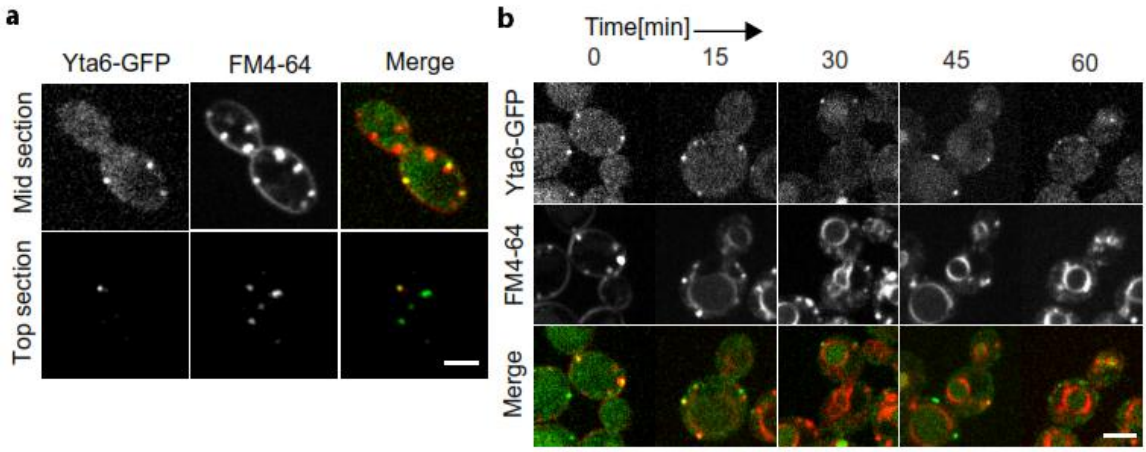

Fig 19. Yta6 colocalizes with endocytic sites marked by FM4-64 foci. (a) Representative confocal mid and top sections of Yta6-GFP localization (green) in respect to plasma membrane FM4-64 intermediates (red) is shown. (b) Yta6-GFP is not internalized with FM4-64. Images of the colocalized signal of Yta6-GFP (green) and FM4-64 (red) during a chase for 60 mins are shown. Bar = 2.5 μm.

colocalize with some but not all eisosomes (Walther et al., 2006). We therefore tested whether Yta6 colocalizing with eisosomes also have FM4-64 foci. We

found that more than 60% of Yta6-GFP foci colocalized with FM4-64 intermediates at the plasma membrane. FM4-64 is primarily used as an endocytic tracer in many cell types. In yeast it is often used to study trafficking from plasma membrane to endosomes to vacuole. Vacuole is the final destination of this dye. To observe if Yta6 is internalized as a cargo we observed its colocalization with the dye at later time points. We found that at later time points during FM4-64 uptake, more and more of the dye was located in the cell interior, where it did not overlap with the Yta6-GFP signal **(Fig 19)**.

6.1.11. Yta6 overexpression induces increased FM4-64 foci formation and endocytosis

The spatial correlation of Yta6 punctae and FM4-64 foci suggests a functional relationship between the two. To test the hypothesis that Yta6 is required for FM4-64 focus formation, we performed FM4-64 uptake pulse-chase experiments in *yta6Δ* cells. At the initial time points of the experiments, we measured a modest but significant and reproducible reduction in the number of FM4-64 foci at the plasma membrane in *yta6*Δ compared to WT control cells **(Fig 20)**. Presumably, this leads to the mild reduction of FM4-64 uptake observed after 60 min of chase. To test whether Yta6 induces the formation of FM4-64 foci, we over-expressed Yta6 from the *GAL*-promoter and counted FM-64 foci at the plasma membrane, as well as uptake of the dye. **Fig 20** shows the dramatic increase in the number of early FM4-64 foci in cells overexpressing Yta6 compared to controls, leading to increased FM4-64 signal at the vacuolar membrane after 60 min chase.

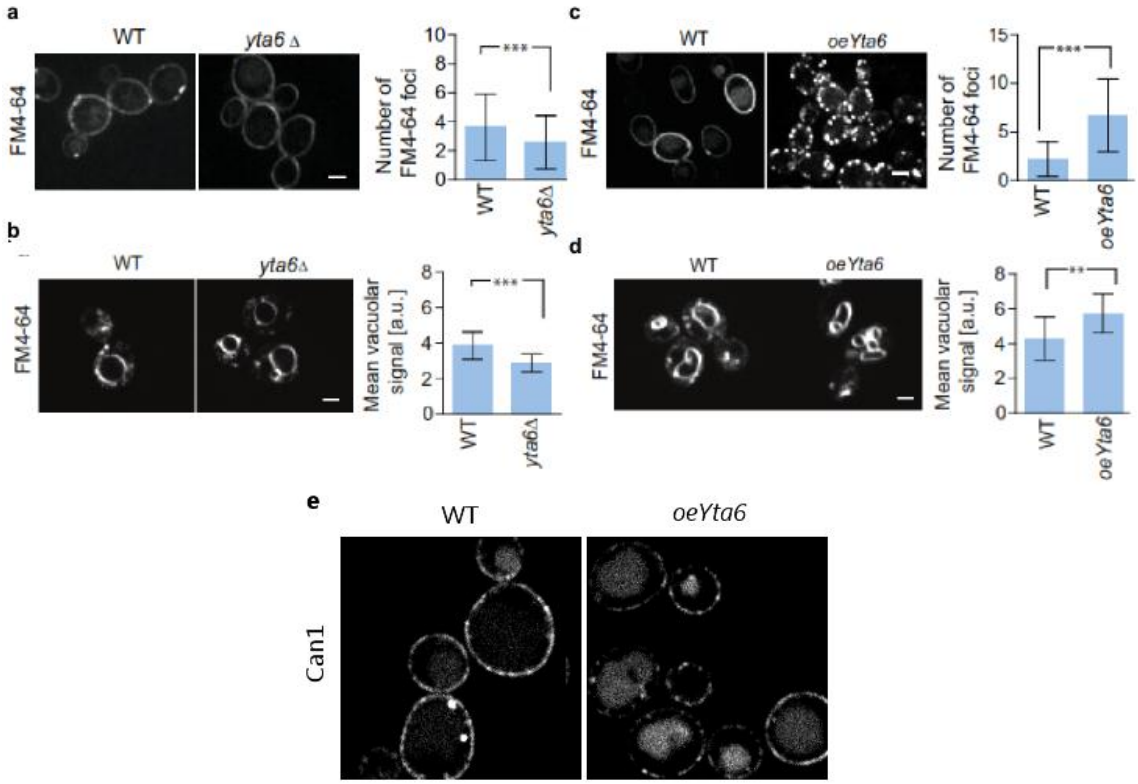

Fig 20. Yta6 overexpression induces increased FM4-64 foci formation and endocytosis. (a) Yta6 deletion mutant shows reduced plasma membrane FM4-64 intermediates. Representative confocal mid sections of the early time point of FM4-64 labeled *yta6Δ* cells are shown. Left panels show representative images, right panel shows quantification of number of FM4-64 foci per cell. (b) Yta6 deletion mutant shows mild reduction in endocytosis. Representative pictures of FM4-64 after chase of 60 mins in WT and *yta6Δ* are shown. (c) Formation of FM4-64 focal intermediates seen early during its uptake is strongly increased in cells overexpressing Yta6 (*oeYta6)*. Left panels show representative images, right panels the number of FM4-64 foci per cell. (d) Representative pictures of FM4-64 after chase of 60 mins in WT and *oeYta6* are shown. (e) Protein cargo Can1 accumulates faster in the vacuoles after a chase for 3 hrs with CHX (Bar = 2.5 μm).

6.1.12. Yta6 is required for membrane swirl formation

The induction of FM4-64 foci formation by Yta6 overexpression provides an opportunity to characterize their structure in more detail. To this end, we analyzed thin sections by transmission electron microscopy, which revealed

many flask-shaped membrane swirls next to the plasma membrane in cells overexpressing Yta6 **(Fig 21)**. These membrane swirls were also present in some sections of WT cells, albeit at a much lower frequency. Due to their localization at the plasma membrane and induction by Yta6 overexpression, we conjecture that these membrane swirls correspond to the FM4-64 foci. Apart from membrane swirls we observed finger-like-projections in the EM pictures. To compare their dimensions we quantified and compared both the swirls and finger-like projections. We also performed the converse experiment where we deleted *YTA6* and observed membrane swirls. In this case we found that their numbers were reduced compared to WT **(Fig 22)**.

6.1.13. Pil1 is required for the increased FM4-64 intermediate formation in overexpression of Yta6

Colocalization of Yta6 and FM4-64 at eisosomes suggests that the induction of foci might be dependent on eisosomes. We tested this model by overexpressing Yta6 in cells where Pil1 is missing and found that this leads to strong reduction of the number of FM4-64 intermediates compared to controls, indicating that eisosomes are required for their Yta6-induced formation. The remaining FM4-64 signal was mostly found in one large cluster that was also labeled by Lsp1-GFP and thus likely represents eisosomes remnants **(Fig 23)**.

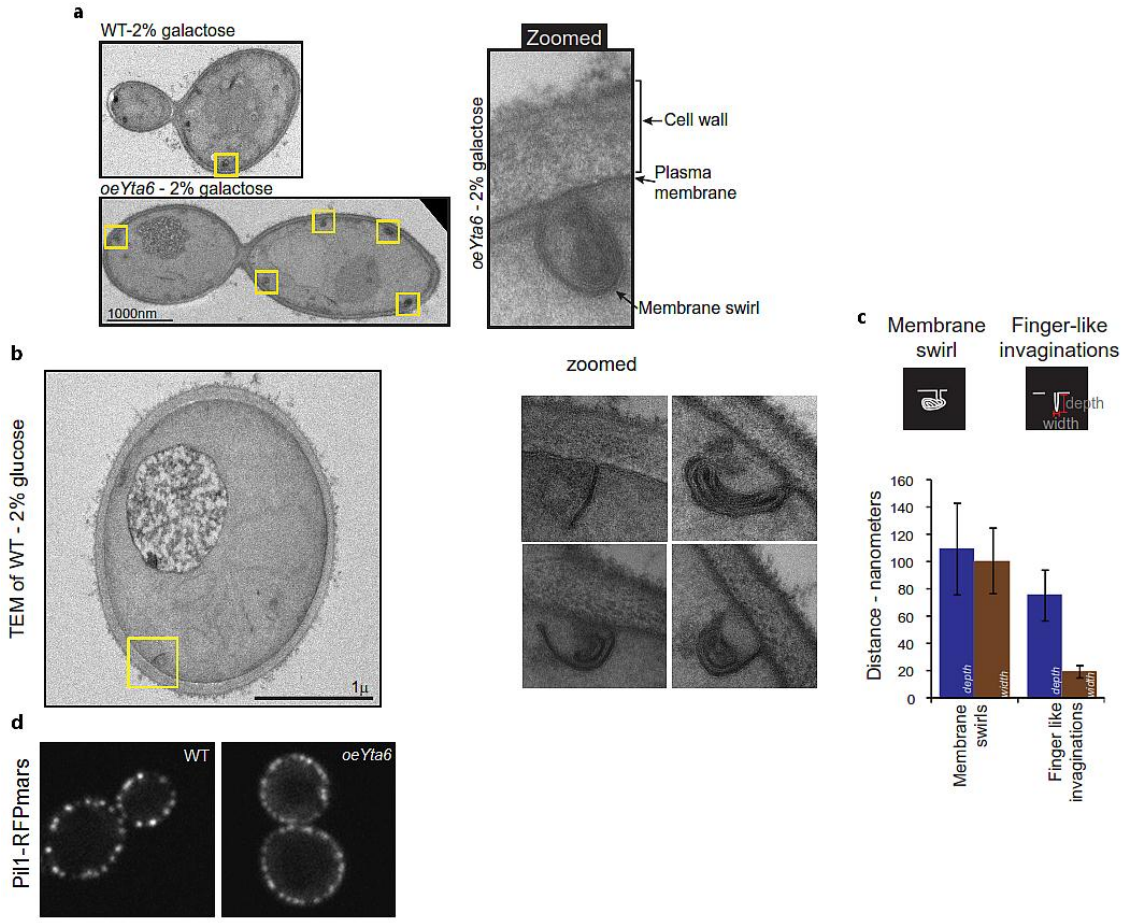

Fig 21. Overexpressed Yta6 shows increased membrane swirls (a) Representative electron micrographs of either WT cells in galactose or *oeYta6* in galactose are shown. Yellow squares show membrane swirls in zoomed view. Right panel shows one zoomed in membrane swirl. (b) A representative WT cell is shown with zoomed finger like projections and membrane swirls are shown on the right panel. (c) Quantification and comparison of membrane swirls with finger-like-projections. (d) *oeYta6* affects the distribution of eisosomes. Left panel shows a WT cell with Pil1-RFPmars. Right panel shows a representative image of a cell overexpressing Yta6 with Pil1-RFPmars.

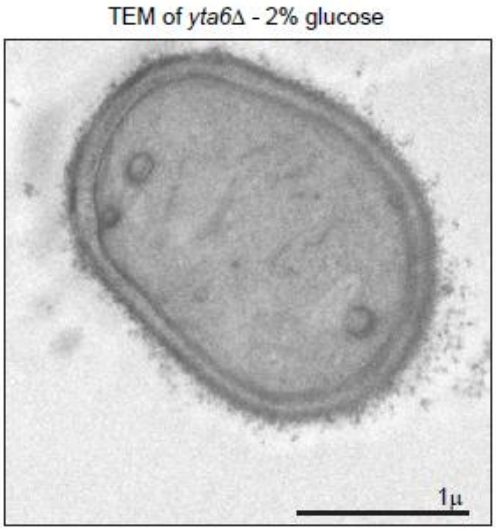

Fig 22. *yta6Δ* cells shows reduced membrane swirls. A representative image of TEM of *yta6Δ* is shown.

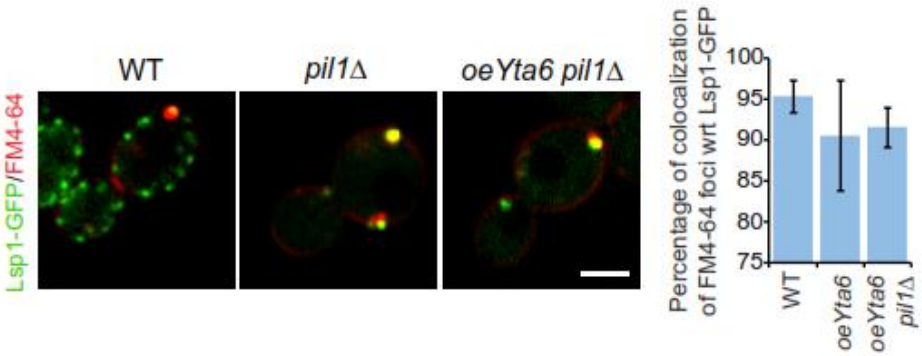

Fig 23. Pil1 is required for the increased FM4-64 intermediate formation in *oeYta6*. Representative confocal midsections are shown of FM4-64 staining with Lsp1-GFP in WT, *pil1Δ,* or *oeYta6pil1Δ (*n=161(wt), 374 (*oeYta6*), 327 (*oeYta6 pil1Δ)).* Right panel shows the quantification (Bar = 2.5 μm).

6.1.14. Yta6 overexpression rescues endocytic defects in yeast amphiphysin mutants

Yta6 overexpression induces FM4-64 foci formation and uptake, but its deletion only mildly affects FM4-64 internalization. In contrast, mutations of many genes encoding actin-patch proteins, which participate in the most studied pathway of endocytosis in yeast, impair FM4-64 uptake (Munn et al., 1995; Young et al., 2002). A possible explanation might be that Yta6 functions in a pathway parallel to actin patches that plays a modest role in FM4-64 endocytosis under normal conditions. To test this hypothesis, we assayed FM4-64 uptake in yeast amphiphysin mutants *rvs161Δ* and *rvs167Δ* cells. Consistent with previous results from other groups, each of these conditions led to a strong reduction of FM4-64 uptake (Douglas et al., 2009; Heese-Peck et al., 2002; Wendland et al., 1996) **(Fig 24)**. Yta6 overexpression reproducibly rescues FM4-64 uptake in *rvs161Δ* and *rvs167Δ* mutants. Absence of the corresponding proteins also led to a reduction of FM4-64 foci. This could be mediated by due to some effect on eisosomes or by Yta6. To test if eisosomes are affected in yeast amphiphysin mutants we observed qualitatively and quantitatively the eisosomes numbers and fluorescence. We did not observe any change **(Fig 25a,b).** We found that Yta6 localization is affected in the amphiphysin mutants suggesting that reduction of foci may be mediated due to reduced Yta6 foci formation **(Fig 25c).** Finally, to ensure that the 4 ^{0}C incubation used for pulse labeling in these experiments has no effect on the results, we performed the FM4-64 assay without incubation on ice and found consistent rescue of the inhibition of FM4-64 endocytosis in *rvs161Δ* cells by Yta6 overexpression **(Fig 26)**.

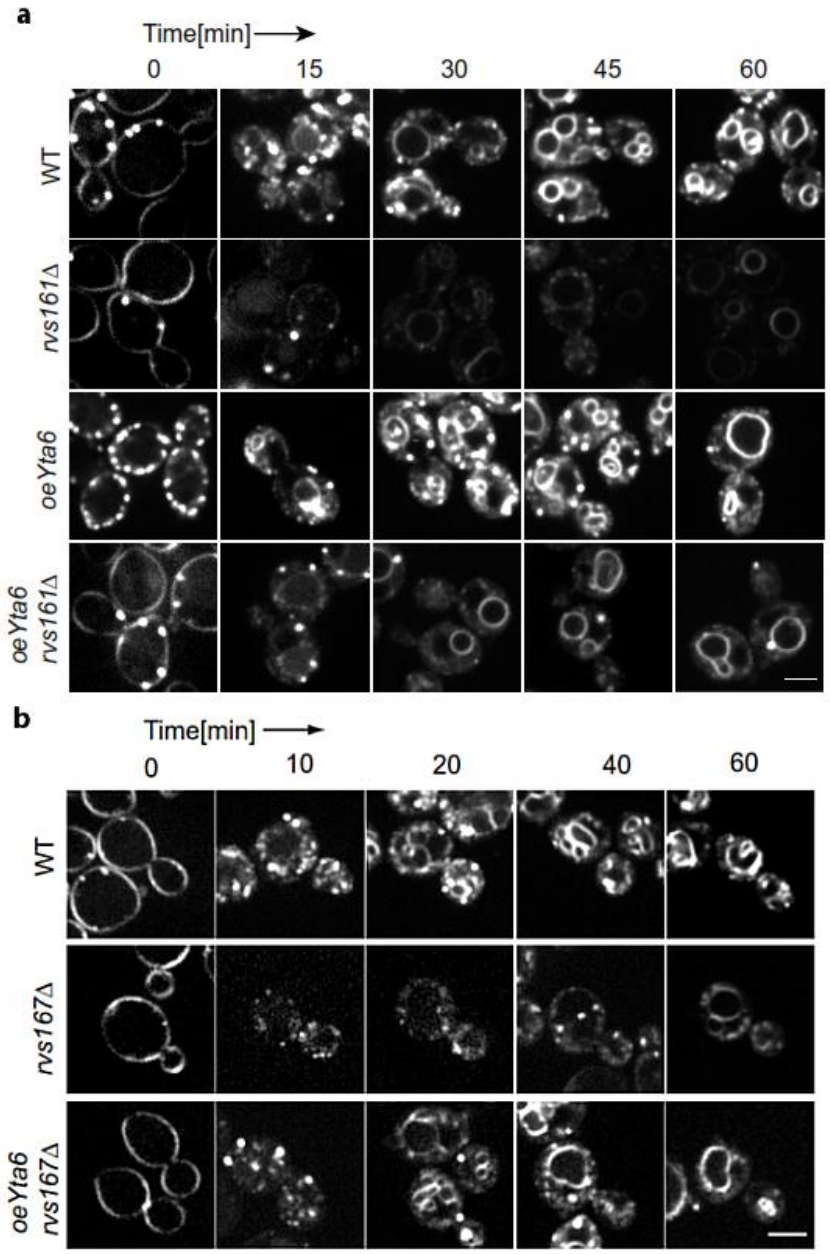

Fig 24. Yta6 overexpression rescues endocytic defects in yeast amphiphysin mutants. (a) Yta6 overexpression rescues FM4-64 uptake defects in *rvs161Δ* cells. Representative confocal midsections of FM4-64 uptake at different time points of a 60 min chase are shown for WT (upper row), *rvs161Δ* (second row from top) cells and cells overexpression Yta6 (*oeYta6,* third row from the top) or overexpressing Yta6 in *rvs161Δ* cells (bottom row) are shown. (b) Yta6 overexpression rescues FM4-64 uptake defects in *rvs167Δ* cells. Representative confocal midsections of FM4-64 uptake at different time points of a 60 min chase are shown for WT, *rvs167Δ*, and *oeYta6rvs167Δ* (Bar = 2.5 μm).

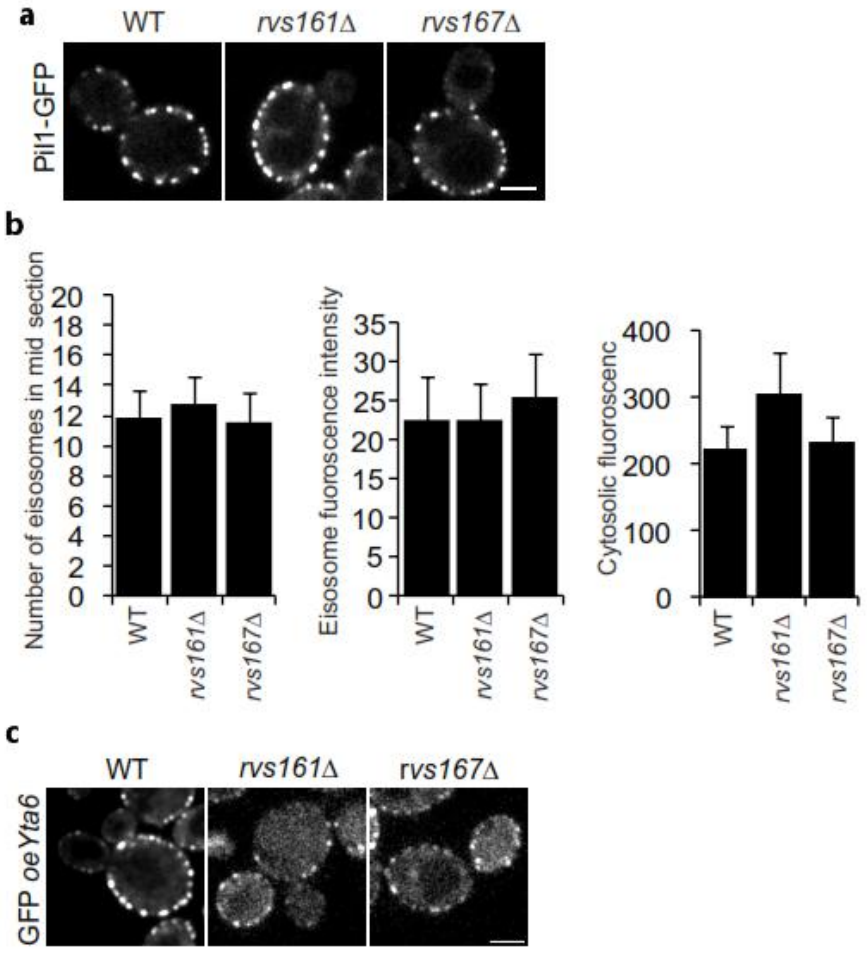

Fig 25. Reduced FM4-64 foci in *oeYta6rvs161* and *oeYta6rvs167Δ* are not dependent on eisosomes. (a) Eisosomes localization is not affected in RVS mutants. (b) Quantification of number of eisosomes, eisosomes fluorescence intensity and cytosolic fluorescence in WT, *rvs161Δ* and *rvs167Δ*. (c) *oeYta6* localization is affected in *rvs161Δ* and *rvs167Δ* (Bar = 2.5 μm).

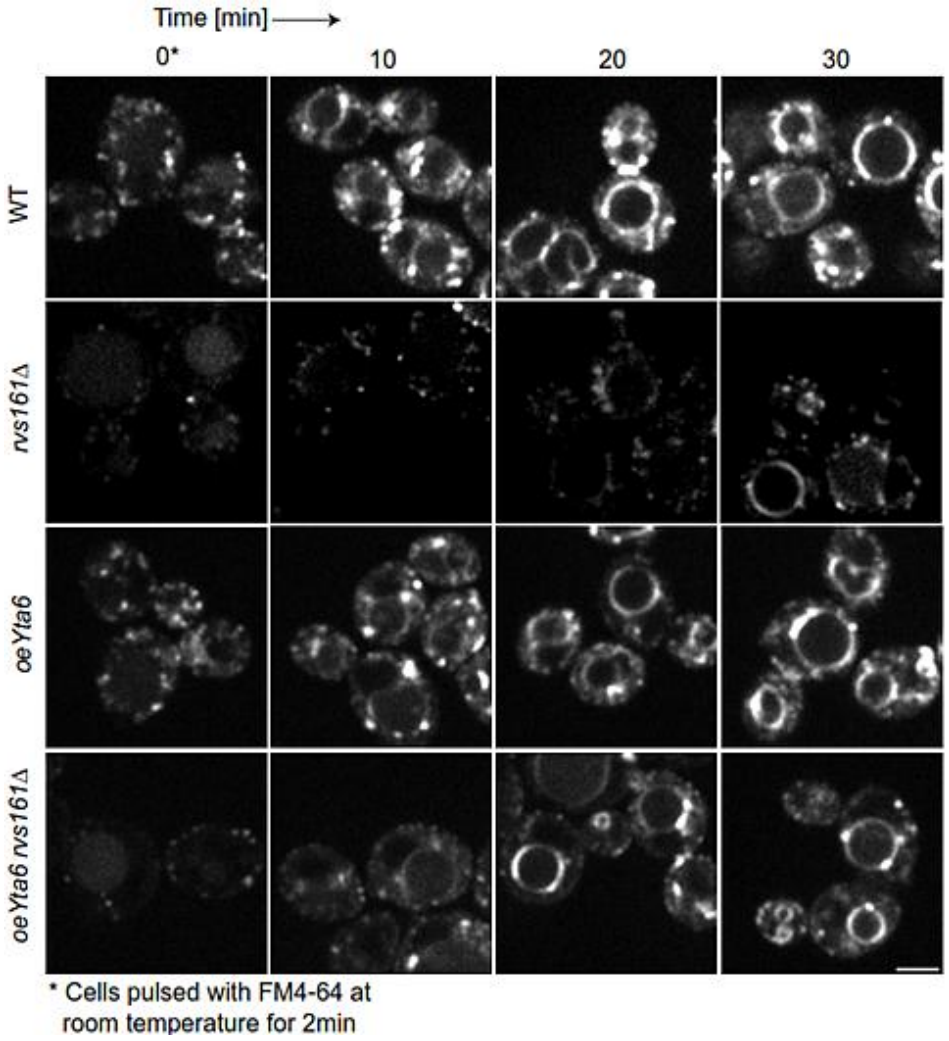

Fig 26. Endocytic rescue mediated by *oeYta6* occurs efficiently in room temperature in cells pulsed with FM4-64. Representative confocal midsections of a 30 min FM4-64 chase experiment is shown in WT, *rvs161Δ, oeYta6, oeYta6rvs161Δ* (Bar = 2.5 μm).

6.1.15. Eisosomes are not required for rescue of endocytosis mediated by Yta6 overexpression

To test if eisosomes are required for rescue of endocytosis mediated by Yta6 overexpression in amphiphysin mutants, we observed FM4-64 uptake in *oeYta6rvs161Δpil1Δ*. We compared the FM4-64 uptake in WT, *rvs161Δ*, *oeYta6rvs161Δ* and *oeYta6rvs161Δpil1Δ*. Consistent with previous results we found that *oeYta6* rescued FM4-64 uptake defects in *rvs161Δ* but combination

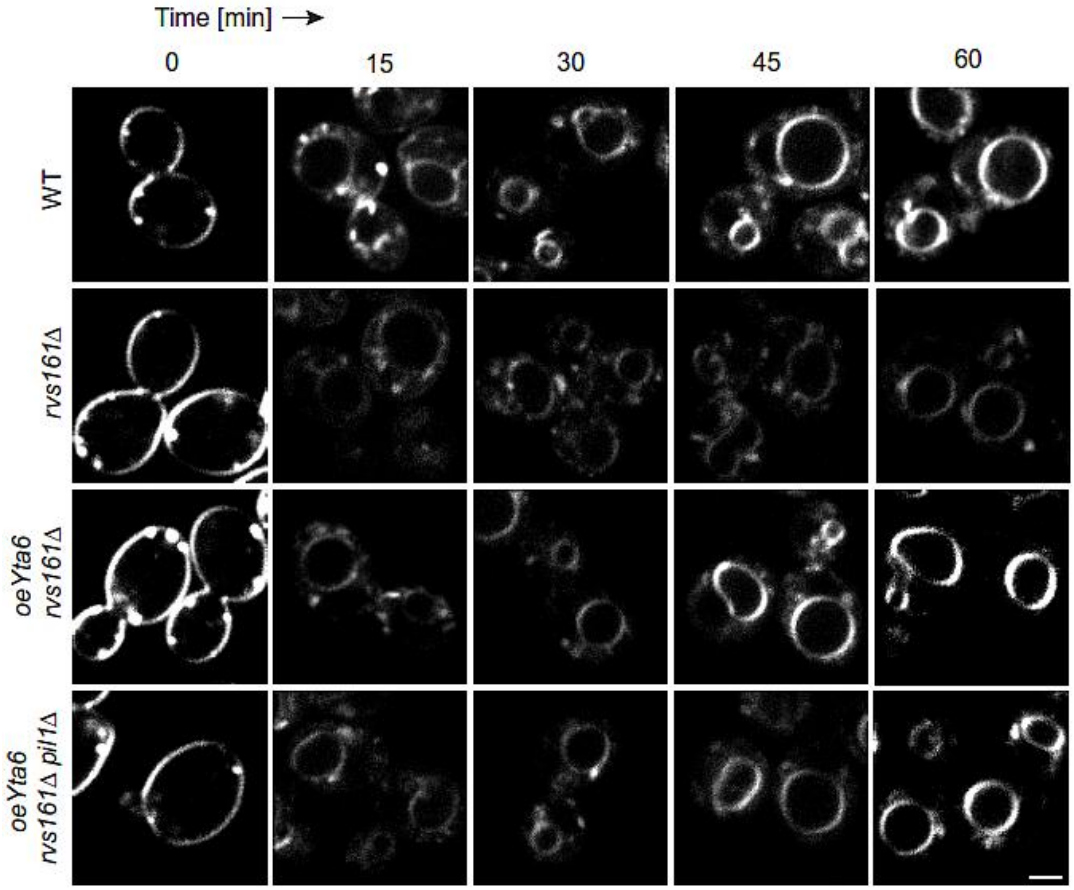

Fig 27. Endocytic rescue mediated by *oeYta6* is independent of eisosomes. Representative confocal midsections of FM4-64 chase in WT, *rvs161Δ, oeYta6rvs161Δ and oeYta6rvs161Δpil1Δ* are shown for a 60 min chase experiment (Bar = 2.5 μm).

*pil1*Δ did not reduce the delivery of FM4-64 uptake. We thus conclude that *PIL1* is not required for rescue mediated by Yta6.

6.1.16. Yta6 overexpression endocytic defects of protein cargoes in amphiphysin mutants

To test whether the effect of Yta6-overexpression is specific just for the FM4-64 dye or may be relevant also for endogenous protein cargoes, we investigated the uptake the plasma membrane arginine transporter Can1, which is internalized by endocytosis. To this end, we blocked Can1 synthesis and delivery to the plasma membrane, by addition of the translation blocking drug cycloheximide (CHX), which induces its endocytosis. Time course analysis of Can1-GFP internalization after CHX treatment by microscopy showed its uptake and delivery to the vacuole. As expected, Can1 endocytosis was efficiently delayed and the protein stabilized at the plasma membrane in *rvs161Δ* cells. Analogous to experiments using FM4-64, over-expression of Yta6 in otherwise WT cells had only a mild effect, if any, on Can1-GFP uptake and transport to the vacuole. However, over-expression of Yta6 in *rvs161Δ* cells rescued the defects in Can1-GFP uptake.

To confirm these results, we probed for Can1-GFP degradation after endocytosis by Western blot. At the beginning of the CHX chase, WT, *rvs161Δ*, Yta6 overexpressing and Yta6 overexpressing *rvs161Δ* cells all expressed similar levels of Can1-GFP. After 4 h CHX chase, Can1-GFP was almost completely degraded in

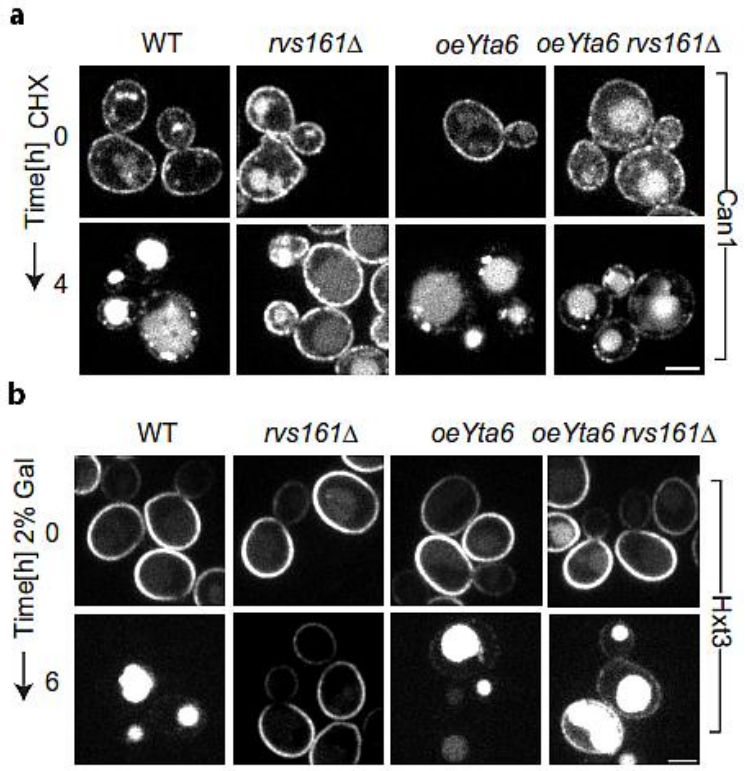

Fig 28. *oeYta6* can rescue endocytosis of protein cargoes in yeast amphiphysin mutants. (a) Representative images of midsections of cells expressing Can1-GFP are shown in the time course experiments in WT and mutants. (b) Representative images of midsections of cells expressing Hxt3-GFP are shown in the time course experiments in WT and mutants (Bar = 2.5 μm).

wild type cells, consistent with our observations by confocal microscopy. Can1-degradation was almost completely blocked by *rvs161Δ* and this could be reversed by Yta6 over-expression, similar to our observation for FM4-64 uptake.

To test whether suppression of the endocytic defects of rvs-mutants by elevated levels of Yta6 is specific for Can1, or maybe is more general, we also investigated other cargoes, such as the sugar transporter Hxt3-GFP. This protein mostly localizes at the plasma membrane in high glucose containing medium,

but is internalized after shift to galactose containing medium. Hxt3-GFP uptake after such a shift in conditions was strongly reduced in *rvs161Δ* cells, but rescued by over-expression of Yta6 **(Fig 28)**.

6.1.17. Deletion of Yta6 does not affect rate of endocytosis of Can1 and Ste3

Our data on the rescue of Hxt3 and Can1 endocytic defects in *rvs*-mutants indicate that both proteins can access an uptake pathway activated by increased Yta6 levels. We next determined the contribution of this pathway,

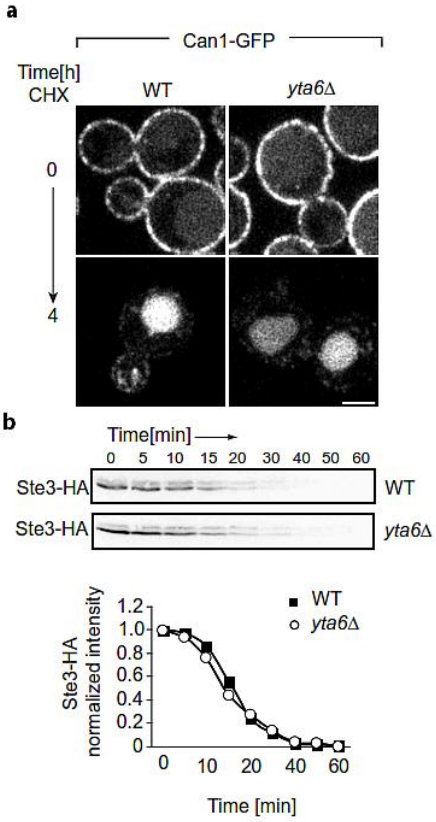

Fig 29. Yta6 deletion does not affect the endocytosis of Can1 and Ste3. (a) Representative confocal midsections of Can1-GFP are shown in WT and *yta6Δ* cells. Can1-GFP levels on the plasma membrane are shown before (upper panels) and after (lower panels) 4 h chase. (b) Western blot analysis of GalP::Ste3-HA shut down (shift to 2% glucose containing medium) in WT and *yta6Δ*. Quantification of the Ste3-HA degradation as shown in the lower panel (Bar = 2.5 μm).

and specifically Yta6, to the endocytosis of these transporters. When we analyzed uptake of Can1 in *yta6Δ* cells in the presence of CHX, we found no significant reduction. Similarly, constitutive uptake of the a-factor pheromone receptor Ste3 was not impaired in *yta6Δ* cells **(Fig 29)**.

6.1.18.Yta6 mediated rescue does not affect early markers of clathrin dependent endocytosis

Two interpretations might explain the suppression of the endocytic defect due to *RVS161* deletion by Yta6 over-expression: i) increased Yta6 levels could lead to re-activation of actin patches defective in endocytosis due to absence of Rvs161 or ii) Yta6 could activate an actin patch-independent pathway operating in parallel. If mutant actin patches are re-activated by Yta6, we expect that their distribution, lifetimes or dynamics, which are compromised in the *rvs161Δ, rvs167Δ* and *vrp1Δ* mutants, are rescued by increased Yta6 levels. We first tested the effect of Yta6 overexpression on actin patch distribution in WT or *rvs161Δ* cells. Compared to WT cells, *rvs161Δ* mutants have depolarized actin patches, but this was not affected by the overexpression of Yta6. We next investigated the lifetime of actin patches marked with Sla1, which is an early arriving component of actin patches and indication of endocytic efficiency. Consistent

with previous reports, we observed an increased average residence time of Sla1-RFPmars foci at the plasma membrane of *rvs161Δ* cells, but increasing Yta6 levels had no influence on this phenotype of *RVS161* deletion **(Fig 30)**.

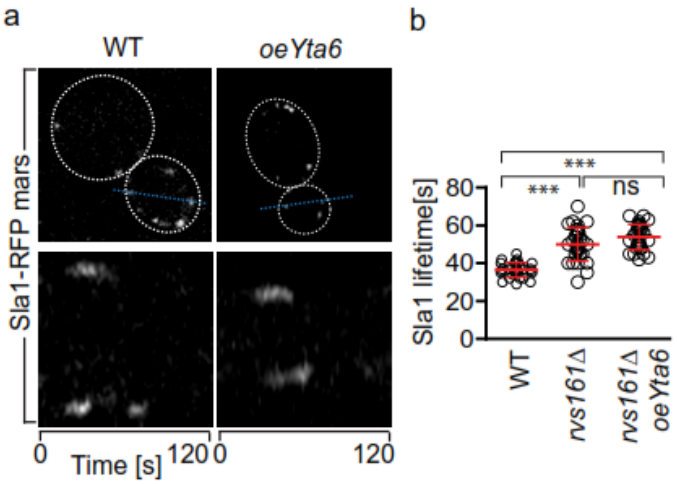

Fig 30. Overexpression of Yta6 has no effect on stalled Sla1-RFPmars patches after LatA treatment. (a) WT cells or cells overexpressing Yta6 (*oeYta6)* harboring Sla1-RFPmars were imaged by confocal time lapse microscopy before or after LatA treatment. Representative confocal midsections (top row) or kymographs (lower panels) are shown. (b) Quantification of Sla1-RFPmars life time in WT, *rvs161Δ*, and *rvs161ΔoeYta6* is shown (n=31 (wt), 31 (*rvs161Δ)*, 31 *(oeYta6 rvs161Δ)* (Bar = 2.5 μm).

6.1.19. Yta6 mediated rescue does not affect late markers of clathrin dependent endocytosis

To also confirm our findings for a component of actin patches that arrives later during the endocytic reaction, we also determined the lifetime of Abp1-GFP (Kaksonen et al., 2005). Consistent with prior reports, we observed increased lifetime of Abp1-GFP in *rvs161Δ* cells compared to WT, but overexpression of Yta6 had no effect on this defect. Another prediction from the hypothesis that overexpression reactivates actin patches in the investigated mutants is that

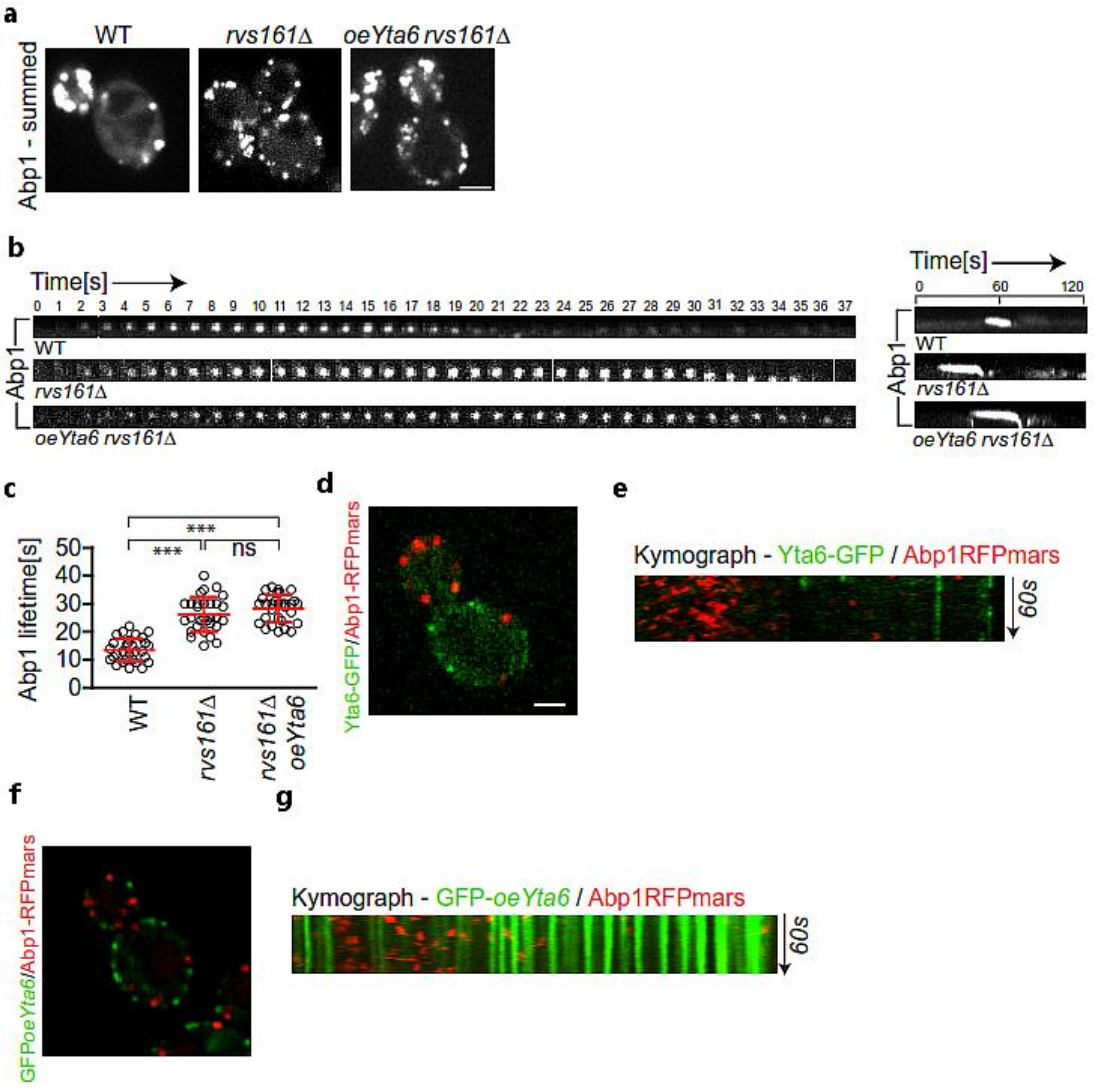

Fig 31. Late marker Abp1 of canonical endocytic pathway in yeast is unaffected by *oeYta6*. (a) Actin patch distribution is not altered in cells overexpressing Yta6 compared to *rvs161Δ* cells. Actin patches labeled by Abp1-GFP were followed for 10 seconds and maximum projections of such a movie are shown. (b) Actin patch life time is not altered by overexpressing Yta6. Representative actin patches are shown over time in WT, *rvs161Δ* cells overexpressing Yta6 (*oeYta6)* cells as indicated. Right panel shows the kymograph of time series as shown in left panel. (c) Quantification of Abp1 life times as shown in (c) (n=31 (wt), 31 (*rvs161Δ), 31 (oeYta6 rvs161Δ)*. (d) Yta6 does not colocalize with Abp1. A representative picture of a cell expressing endogenous Yta6-GFP and Abp1-RFPmars is shown. (e) Representative kymographs are shown of the cells in (d) (f) Right panel shows a representative picture of a cell overexpressing GFP Yta6 and Abp1-RFPmars. (g) Representative kymographs are shown (Bar = 2.5 μm).

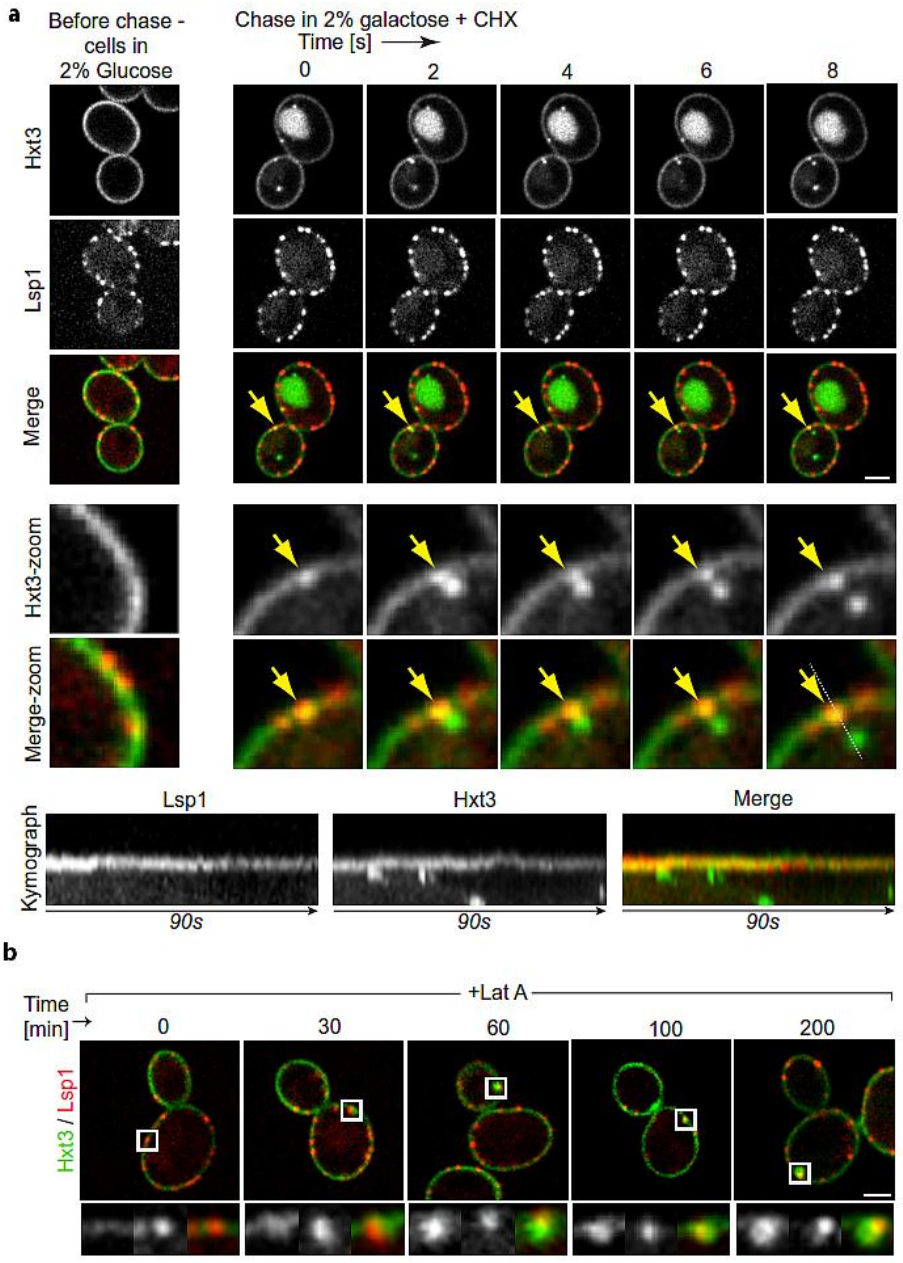

Fig 32. Hxt3 endocytic intermediates colocalize with eisosomes. (a) Live imaging of single cell expressing Lsp1-RFPmars and Hxt3-GFP is shown in mid sections to show colocalization of uptake of Hxt3 at eisosomes. Zoomed panel (bottom) shows the cargo aggregation at the eisosomes at 0 sec, invagination at 2 sec, scission at 4 sec, internalization of cargo containing vesicle at 6 sec. Scale bars = 2.5 μm. A kymograph of the marked region is shown below. (b) Hxt3 accumulates at eisosomes upon chase in LatA (Bar = 2.5 μm).

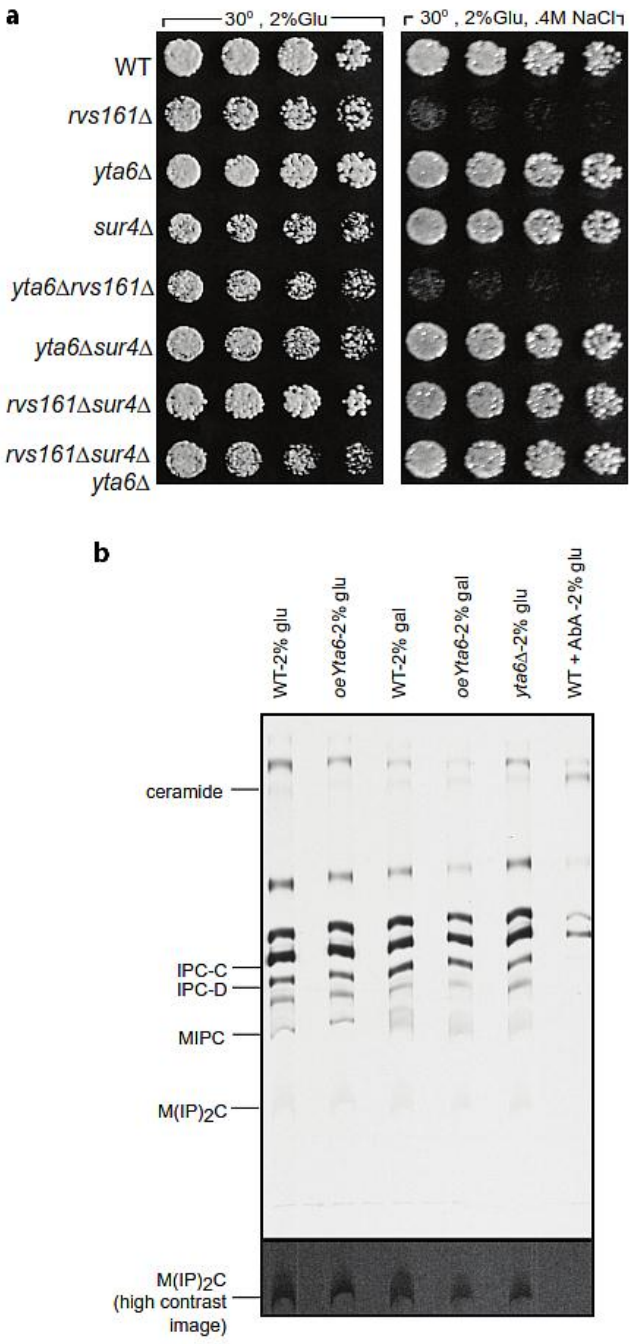

Fig 33. Yta6 is not involved in the pathway of rescue of *RVS* mutants which is mediated by *SUR4*. (a) Plating of serial dilutions WT or combinations of *yta6Δ, sur4Δ, rvs161Δ* is shown for the study of any crosstalk with Sur4 mediated rescue of *RVS* mutants. (b) Yta6 mutants do not affect sphingolipid levels. The bands were assigned after comparison with previously published work (Tabuchi et al., 2006).

these proteins colocalize. However, our analysis of the localization of Yta6-GFP expressed at either endogenous or strongly increased levels in respect to Abp1 showed no overlap in single images or time series. These data together show that there is no effect of increased Yta6 levels on dynamics or localization of actin patches under conditions where uptake of FM4-64 is rescued and that Yta6 is not a component of actin patches. We therefore rule out that the suppression of *rvs161Δ* cells endocytic defects by increased Yta6 is due to re-activation of actin patches, but instead is most likely due to a bypass of actin patches by activating an alternative endocytic pathway **(Fig 31)**.

6.1.20. Yta6 colocalizes with endocytic intermediates of protein cargo Hxt3

To determine the localization of Hxt3-GFP during internalization from the plasma membrane, we followed it by fluorescence microscopy. Before the chase period, Hxt3-GFP is localized uniformly in the plasma membrane. During the chase period, when its uptake is induced, however, Hxt3-GFP formed clusters that localized at eisosomes marked with fluorescent Lsp1-RFPmars. When we followed the fate of these foci by fluorescence time-lapse microscopy, we found that many of these clusters connected with internal signal and apparently were internalized within few seconds, whereas other persisted for a longer and variable time. **Fig 32** shows that the internalization of Hxt3-GFP from the one such cluster at the plasma membrane at eisosomes into the cell interior during a 90 sec time course. Importantly, the Hxt3-GFP signal inside the cells is does not

reflect an internal pool of the protein that is recruited to the plasma membrane because in kymographs we see clusters appear in the plasma membrane, but never localizing from a previously existing cell-internal pool. After their appearance, Hxt3 clusters are also seen to migrate into the cell interior, apparently reflecting their internalization. To test whether Hxt3 uptake still requires actin, we performed Hxt3 endocytosis experiments in the absence of polymerized actin due to the presence of Latrunculin A (LatA). Under these conditions, plasma membrane clusters still formed, often with brighter signal, but their internalization was blocked. In addition, Yta6 was not localized to the plasma membrane any longer. This shows that the Yta6 and actin patches intersect and suggests that endocytosis of cargo mediated by Yta6 might also require the actin cytoskeleton after initial cluster formation. The formation of Hxt3-GFP clusters at eisosomes during its uptake together with the requirement for eisosome proteins and Yta6 for this reaction strongly suggests that Hxt3-GFP is endocytosed by a pathway originating there.

6.1.21. Yta6 mediated rescue does not require *SUR* genes

One potential mechanism of the rescue of endocytosis by Yta6 could occur similar to that mediated by *SUR* genes. We tested this by employing mutants of Sur4. First we observed if Yta6 is involved in the mechanism of rescue of Sur4 of the *rvs161Δ*. To this end we compared the growth of WT, *sur4Δ, rvs161Δ, sur4Δrvs161Δ, rvs161Δ yta6Δ, sur4Δyta6Δ* and *sur4Δ rvs161Δ yta6Δ*. As expected we observed the rescue of growth of *sur4Δrvs161Δ* but this was not affected in combination with *yta6Δ* **(Fig 33a)**. Independently we performed

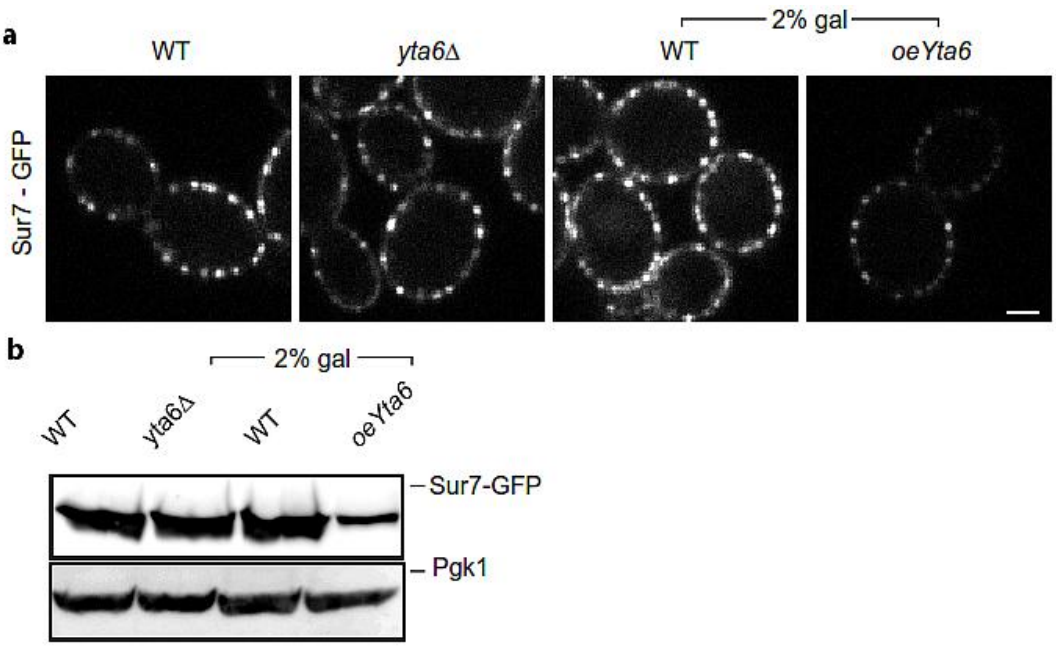

Fig 34. Yta6 overexpression shows reduced local and total amounts of Sur7. (a) Representative mid sections of cells expressing Sur7-GFP is shown in WT, *yta6Δ,* WT (galactose grown) and *oeYta6* (galactose grown). (b) Lysates of cells expressing Sur7 –GFP in WT, *yta6Δ,* WT (galactose grown), *oeYta6* (galactose grown) were prepared and subjected to immunoblotting and probing with anti-GFP and anti-Pgk1 (Bar = 2.5 μm).

semiquantitative lipid analysis by thin layer chromatography (TLC) and found that Yta6 deletion or overexpression mutants do not show any changes in the lipid levels **(Fig 33b)**. Next we tested if Yta6 has any crosstalk with Sur7 as overexpression of Sur7 is known to suppress RVS defects. We performed western blot to quantify the total amount of Sur7 in *oeYta6* and found that its total levels are reduced suggesting that Sur7 may be another cargo that is endocytosed at eisosomes. Microscopy of Sur7 foci further revealed its lower amounts per foci in comparison to WT **(Fig 34)**. It is thus likely that endocytic rescue effect mediated by Yta6 overexpression is independent of Sur7 and it is possibly a cargo which requires Yta6 for endocytosis.

6.2. Emp70 is required for organization of intracellular compartments in trafficking

6.2.1. Emp70 dynamically localizes to eisosomes

To address functional relationships between plasma membrane processes, genetic interactions among a set of 374 genes involved in plasma membrane biology were selected (Aguilar et al., 2010). In the *PIL1* genetic interaction network of the plasma membrane E-MAP, we found that *EMP70* is the strongest candidate for a functional relationship with *PIL1* since: i) the two genes have a high genetic profile correlation (Correlation = 0.366; highest score for *PIL1*; ii) the two genes are part of a triangle of positive interactions, with all partners showing positive interactions with each other iii) the Emp70 homologue Tmn2 was found in a systematic study to be required for normal Pil1-GFP localization (Frohlich, Moreira et al. 2009). In addition, our unbiased statistical analysis identified *EMP70* and *PIL1* as part of the same module. These genetic links prompted us to investigate the *EMP70* in more detail. To this end, we fluorescently tagged Emp70 with GFP and analyzed it's localization by confocal microscopy. We performed quantification of colocalization of Emp70 and eisosome component Lsp1 and found that approximately half of Emp70 foci colocalize with Lsp1 **(Fig 35)**.

6.2.2. Emp70 is an endosomal protein

Emp70-GFP localizes in a complex pattern consisting of central ring reminiscent of vacuoles and several bright foci in the cytoplasm that often seem connected

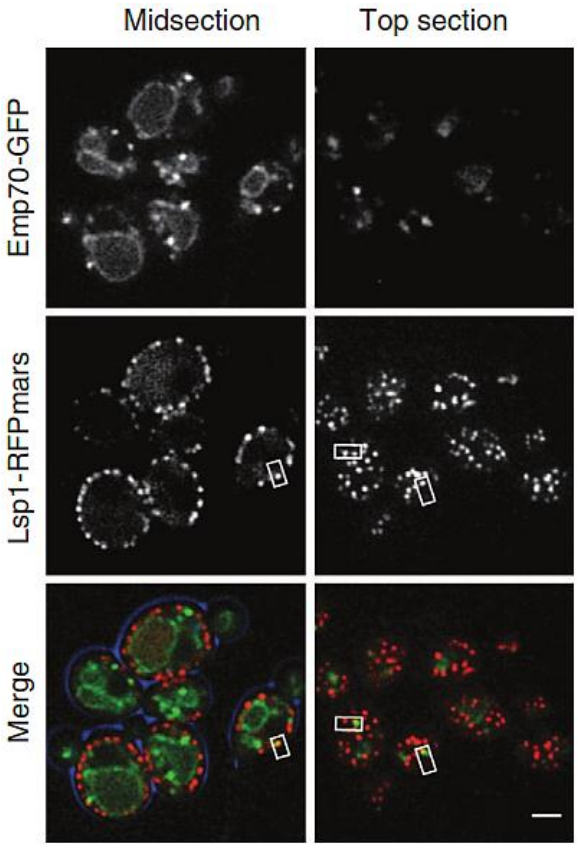

Fig 35. Emp70 foci localize to the cell periphery. Emp70-GFP (green) was expressed in cells harboring the fluorescent eisosomes marker Lsp1-RFPmars. Representatives mid- (left) and top sections (right) are shown. Boxes highlight selected areas of colocalization (Bar=2.5 μm).

to the vacuole. Emp70 was previously found in a membrane fraction enriched for endosomal membranes (Singer-Krueger, JBC 1993). We therefore tested whether the Emp70 foci in the cytoplasm are endosomal compartments. To this end we used a number of endosomal markers and found that Emp70-GFP foci

localize with Kex2 marking the TGN/early endosome, but not for example the late endosomal/ pre-vacuolar marker Vps5 **(Fig 36, Fig 38a).**

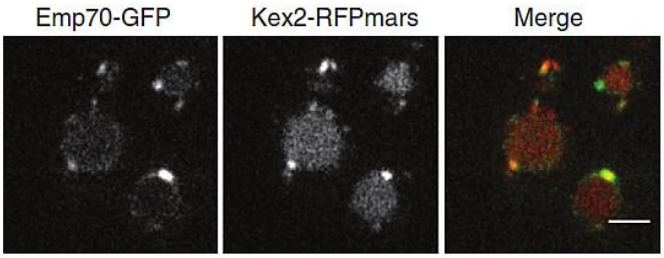

Fig 36. Emp70 colocalizes with Kex2. Emp70-GFP and Kex2-RFPmars were coexpressed and imaged. Representative confocal midsections are shown (Bar=2.5 μm).

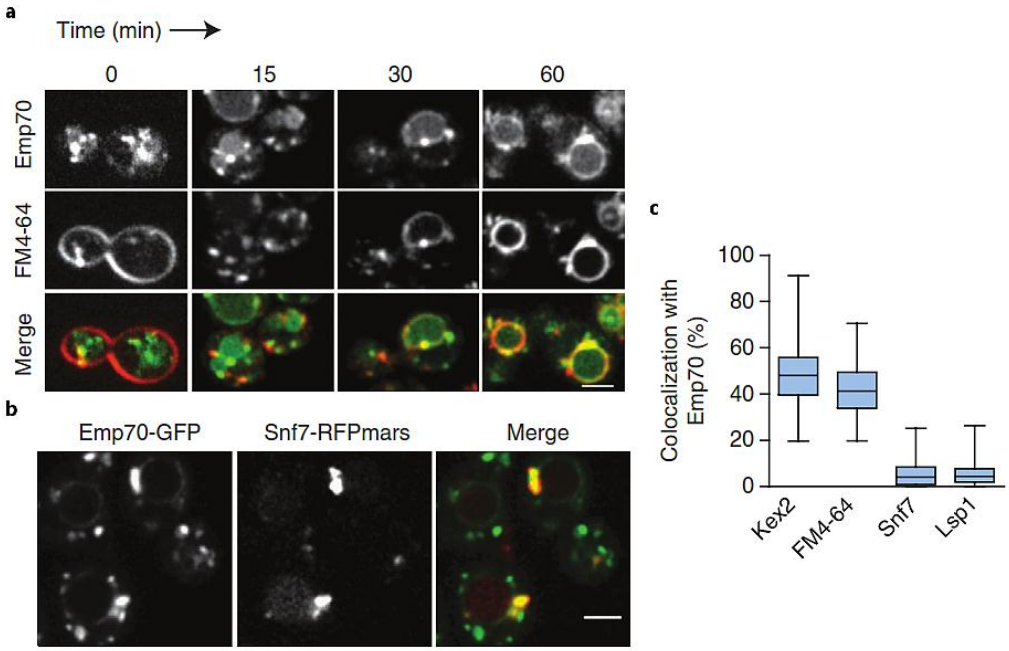

Fig 37. Emp70 localizes to FM4-64 marked endocytic compartment. (a) Cells expressing Emp70-GFP were pulse labeled with FM4-64 (red) and imaged for 1 hr. Images of midsections of cells at selected time are shown as indicated. (b) Quantification of the organelle distribution of Emp70. Emp70-GFP was imaged in live cells and analyzed for colocalization with Kex2-RFPmars (n=100), vacuolar FM4-64 (n=91), Snf7-RFPmars (n=93), diploid strain expressing one tagged Snf7 allele) and Lsp1-Cherry (n=107). The relative area of overlap between signals was quantified as a percentage of total area occupied by Emp70 signal. Box plots representing maxima, 75th percentile, media, 25th percentile and minima are shown for the colocalization with each marker. (Bar = 2.5 μm.)

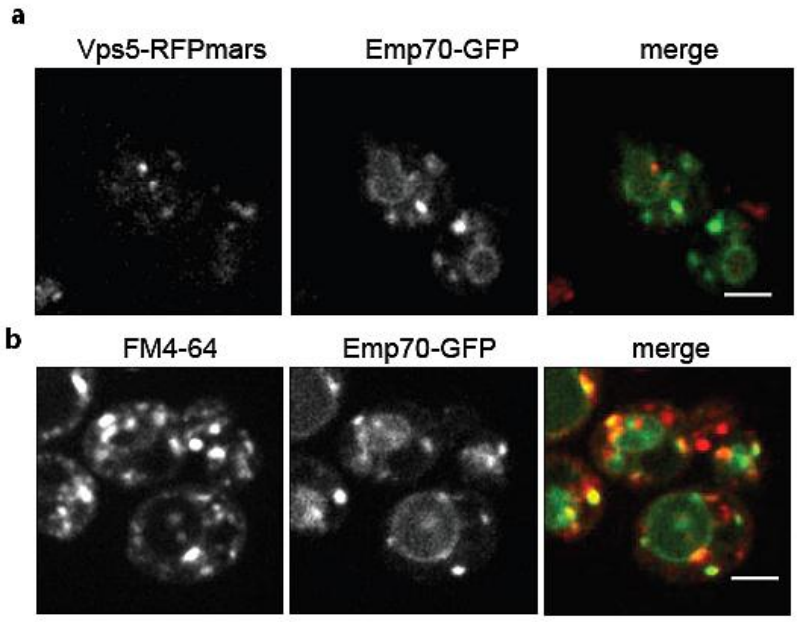

Fig 38. Emp70 localization in respect to endosomes. (a) Strains expressing Emp70-GFP and Vps5-RFPmars from the endogenous locus were imaged by confocal microscopy. Representative images are shown. (b) FM4-64 uptake experiment was performed at 16 ^{0}C and representative confocal midsections are shown. (Bar = 2.5 μm.)

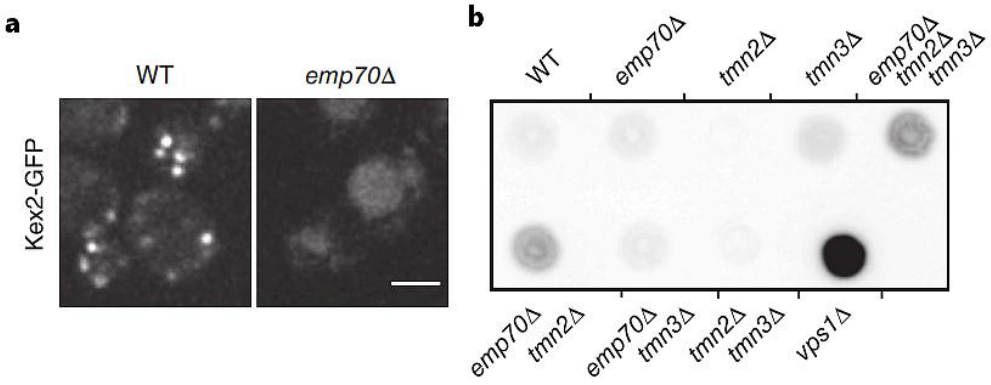

Fig 39. Emp70 is required for normal endosome function. (a) Emp70 is required for normal localization of Kex2-GFP. Kex2-GFP was expressed in either WT or *emp70Δ* cells, and representative confocal midsections are shown. (b) Emp70 family members are required for late endosomal protein retrieval. Mutants of *EMP70*, *TMN2* or *TMN3* were tested alone or in combination for CPY secretion. A representative colony blot is show. (Bar = 2.5 μm.)

6.2.3. Emp70 colocalizes with FM4-64 intermediates at the plasma membrane and intracellularly

To independently test whether the labeled compartments are part of the endocytic route, we used the endocytosis tracer FM4-64 in pulse-chase experiments. FM4-64 uptake experiments in cells expressing GFP-labeled Emp70, revealed co-localization of Emp70 foci with the earliest endocytic intermediates that we could observe **(Fig 35)**. As the dye migrated through the endocytic system, it colocalized with a subset of Emp70 positive foci towards the end of the reaction, but markedly less at intermediate time points. At the final time point, FM4-64 clearly labeled the vacuole delimiting membrane where it colocalized with the Emp70-GFP ring staining. Together this indicates that Emp70 localizes to early endosomes and the vacuolar membrane. Trafficking from the early endosome can be blocked by incubation of cells at 16 ^{0}C, which leads to an accumulation of FM4-64 in this compartment. To confirm that Emp70 indeed localizes with early endosomes, we localized it in cells where FM4-64 was blocked in the 16 ^{0}C compartment and found near perfect overlap between the GFP and the FM4-64 signal, further arguing that Emp70 localizes to an early endosome **(Fig 37, Fig 38b)**.

6.2.4. Emp70 is required for normal endosome functions

To test whether Emp70 is important for the function of early endosomes, we analyzed the localization of Kex2-GFP in *emp70Δ* strain. This deletion resulted in a dramatic re-localization of Kex2 from the steady state early endosome

localization to the vacuole **(Fig 36)**. Under normal conditions, Kex2 sorting depends on signals that send it to the early endosome, which subsequently matures into a late endosome, from where it is actively retrieved. It is therefore possible that the defect in Emp70 results either from a defect in retrieval of the protein from the late endosome, or a complex trafficking defect that results in a defect of early endosomes **(Fig 39a)**. If retrograde trafficking is affected this implies that the functionality of the receptor, Vps10, is impaired leading to a secretion of the normally vacuolar sorted CPY. To test this possibility, we assayed CPY secretion and found that *EMP70* deletion alone did not result in miss-sorting and secretion of CPY. This was in clear contrast to the effect of *vps1Δ*, a mutation in the dynamin-like GTPase known to affect endosomal recycling **(Fig 39b)**.

6.2.5. Emp70 deletion mutant does not affect endocytosis

To test the role of Emp70 in endocytosis we tested its deletion mutant for endocytic defect. We tested the endocytosis of styryl dye FM4-64 and protein cargo Ste3-HA. We did not observe any significant delay of Ste3-HA in *emp70Δ* compared to WT **(Fig 40)**.

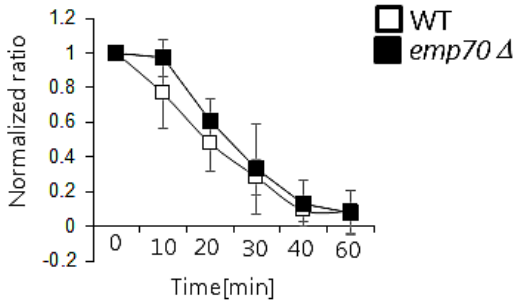

Fig 40. *emp70Δ* does not affect the rate of Ste3-HA degradation. Graph shows the quantification from three independent experiments of the Ste3-HA chase in WT and *emp70Δ* cells.

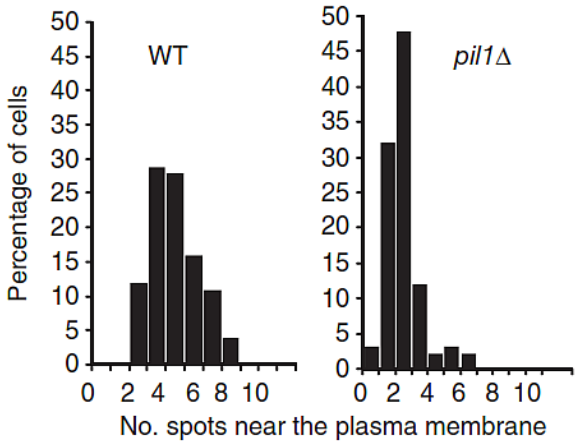

Fig 41. *PIL1* is required for normal Emp70 localization to the cell periphery. Emp70-GFP was expressed in cells expressing the plasma membrane marker Ylr413w-RFPmars, and foci overlaying this marker were counted in more than 100 WT and *pil1Δ* cells. Results are shown as a histogram of number of spots opposed to the plasma membrane in each cell.

6.2.6. Pil1 is required for normal Emp70 localization to the cell periphery

We also detected Emp70 foci in the cellular periphery that did not localize to eisosomes. To test whether this association has a functional relevance, we investigated the localization of Emp70 in *pil1Δ* cells. In these cells we observed a marked reduction of foci close to the plasma membrane. To quantify this effect, we recorded confocal mid-sections, and had several observers count the number of peripheral foci in each cell. The resulting histogram confirmed the visual impression that Emp70 foci in the cell periphery are greatly reduced in *pil1Δ* cells **(Fig 41).**

6.2.7. Yta6 partially colocalizes with Emp70

Finally to test if Emp70 is involved in Yta6 mediated pathway, we tested its colocalization with Emp70. To this end we performed time lapse imaging and observed their colocalization. We found a transient colocalization of Emp70 and Yta6 **(Fig 42).**

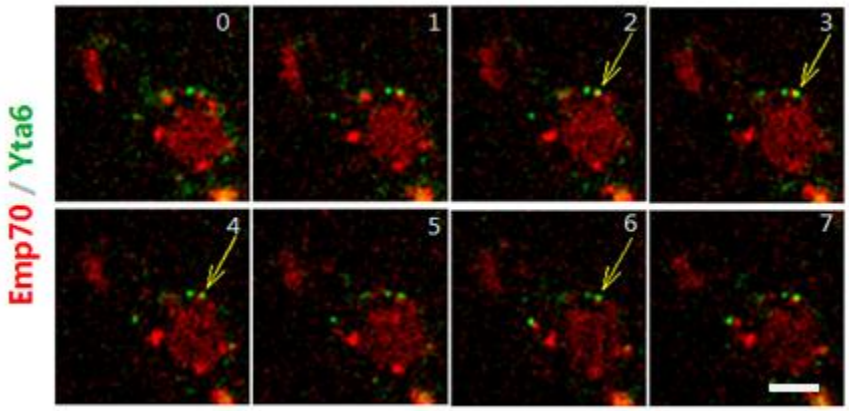

Fig 42. Yta6 partially colocalizes with Emp70. Cells coexpressing Yta6-GFP and Emp70-RFPmars were followed in time lapse imaging. Such a cell showing their colocalization is shown (t = sec; Bar = 2.5 μm).

7. Discussion

In this study we performed detailed analysis of localization and function of AAA-ATPase Yta6 that was earlier shown to localize to the cell cortex (Beach and Bloom, 2001). Previously discovered AAA-ATPase proteins in yeast have been found in almost all cell organelles but only one recently discovered AAA-ATPase AipA was found to localize to cell cortex (Higuchi et al., 2011). AipA was found to colocalize with Abp1 which is a bonafide marker of canonical endocytosis mediated by actin patches. It has been suggested to be a negative regulator of endocytosis as its overexpression displays impaired growth. Sequence homology with other yeast AAA-ATPase proteins revealed its similarity to Yta6 and Sap1. Our studies revealed that Yta6 localizes to the plasma membrane but in contrast to AipA which colocalizes with members of the canonical pathway of endocytosis, Yta6 colocalizes with eisosomes. Due to unique localization of most AAA-ATPase proteins it is likely that they have a targeting sequence and in case of Yta6 – plasma membrane targeting. We found for Yta6 that its N-terminal domain without the AAA-ATPase domain is sufficient for its localization to the plasma membrane. Due to low sequence similarity it is unclear which other AAA-ATPase proteins would likely localize to the plasma membrane and thus better bioinformatic analysis is required to recognize domain if any in its N-terminus. The closest homolog of Yta6 is Sap1 in yeast and that does not localize to the plasma membrane (Noguchi and Noguchi, 2007). Spastin and katanin are its other homologs found in higher eukaryotes. Katanin has been primarily suggested to function in microtubule severing consistent with its

localization. Spastin function is currently unclear. A recent study has implicated its role in endocytosis and intracellular trafficking (Connell et al., 2009). Further studies are required to understand if Spastin does in higher eukaryotes what Yta6 performs in yeasts.

We showed by microscopy and immunoprecipitation experiments that Yta6 specifically localizes and interacts with eisosomes, respectively. Consistent with our immunoprecipitation experiments we observed that endogenous Yta6 localization depends on eisosomes. However, *GAL* promoter driven overexpressed Yta6 did not show mislocalization in *pil1Δ* strain. In light of our data from confocal and TIR-FM imaging, it is likely that punctae of Yta6 first localize to the plasma membrane and then oligomerize to form foci at eisosomes. Interestingly, localization of Yta6 also depends on actin. This could be either by interaction with actin patches or actin cables. We did not observe any colocalization of Yta6 with Abp1 which marks the actin patches, thus it maybe mediated by actin cables.

Previously, we have linked eisosomes to endocytosis primarily based on the observation that intermediates which form at the plasma membrane early during FM4-64 uptake colocalize with eisosomes and such eisosomes are called ‘active eisosomes’. This work showed that Yta6 maybe functions in activating eisosomes and likely functions in an alternative endocytic pathway originating at eisosomes. However, at any given time point, only a fraction of eisosomes carry such an FM4-64 intermediate. This raises the question of what distinguishes

such active eisosomes from inactive ones. Here, we found that the AAA-ATPase Yta6 forms foci that localize to active eisosomes and that Yta6 is limiting for the formation of FM4-64 intermediates. It is therefore likely part of the activation mechanism of eisosomes. Electron microscopy on thin sections of *oeYta6* showed novel membrane infoldings which we call 'membrane swirls'. Interestingly, membrane swirls have dimensions only slightly larger than 'finger like projections', thus they may play a role in endocytosis. They show tubular structures protruding inside the cell.

An important question concerning eisosome function is what happens to FM4-64 intermediates formed there. FM4-64 dye that initially during pulse-chase experiments is located in focal intermediates at eisosomes ends in the yeast vacuole. This suggests that these intermediates are endocytosed. However, actin patches, which mediate the canonical endocytosis pathway in yeast, mostly do not co-localize with eisosomes and, by extension, with FM4-64 intermediates formed there suggesting that either FM4-64 is taken up at sites distinct from eisosomes or that FM4-64 uptake from eisosomes is mediated by an alternative endocytic pathway. Both possibilities are mutually non-exclusive and it has been well established that FM4-64 uptake can be mediated by proteins of the actin patch network. Here, we find that increased Yta6 levels rescue the FM4-64 uptake defect of mutation of genes encoding actin patch proteins, such as Rvs161, Rvs167 or Vrp1. This is not due to some specific properties of FM-dyes, since we obtained similar data for Can1 and Hxt3 uptake. In addition, overexpression of Yta6 does not alter actin patch dynamics in either WT,

rvs161Δ or of Sla1 dynamics in latrunculin A treated cells, arguing that the suppression is due to a bypass of the actin patch requirement. Together, these data strongly suggest that there is an alternative endocytic pathway, which starts at eisosomes to which Yta6 localizes. Intriguingly, only some protein cargoes - such as Hxt3 - require this pathway for efficient uptake, whereas others - such as Can1 or Ste3 - may use it and can access it when Yta6 is over-expressed, but are not dependent on it under the conditions tested.

The suppression of the *rvs161Δ* endocytic phenotype by Yta6 overexpression is reminiscent of its suppression by deletions of genes encoding enzymes of the sphingolipid synthesis pathway, collectively named *SUR* (Suppressors of RVS-deletions) (Germann et al., 2005). Loss of any of these genes' function results in rescue of viability of *rvsΔ*-cells upon starvation. In addition, such deletions also suppress the endocytic defect of *rvs161Δ* or *rvs167Δ* cells. Suppression of RVS-mutations in these cases could be due to Yta6 activation. This could be mediated for example by sphingolipid signaling, since bioactive synthesis intermediates of these lipids accumulate in *sur* mutants. In addition, it was previously demonstrated that sphingoid base synthesis is required for the internalization step of endocytosis and that this requirement reflects a signaling function of sphingolipids (Friant et al., 2001; Zanolari et al., 2000). How these findings relate to actin patch-dependent versus Yta6-dependent endocytosis is yet unclear. Intriguingly, phosphorylation of eisosome components Pil1 and Lsp1 by Pkh-kinases is controlled by alterations in sphingolipid metabolism, particularly evident after a block of complex sphingolipid synthesis. Overexpression of Pkh-kinases also rescues the sphingoid base synthesis

requirements for endocytosis (Friant et al., 2001). It is therefore possible that this sphingolipid signaling network is used to trigger plasma membrane endocytosis after specific stimuli at eisosomes and that at least part of this activation is mediated by Yta6. Consistent with this notion, we found Yta6 phosphorylation strongly decreased after blocking sphingolipid synthesis, maybe reflecting post-translational regulation of the protein's activity (observed by Florian Fröhlich).

Activation of the Yta6-pathway by signals to take-up specific proteins would explain why *YTA6* mutation has only a modest effect on endocytosis of some tested cargoes. Alternatively, another protein could share a redundant function with Yta6, therefore masking its phenotype on the uptake of some proteins. A candidate for such a protein is the highly abundant AAA-ATPase Cdc48, since it and its adaptors Shp1 and Ufd1 are required for suppression of the *rvs161Δ* endocytic defects on some transporters by sphingolipid synthesis mutants (Morgan et al., 2009). Based on known functions of AAA-ATPase domains, both Yta6 and Cdc48 could disassemble oligomeric complexes and therefore perform a mechanical function of disassembling complexes during endocytosis (Sauer et al., 2004). Alternatively and not mutually exclusively, overexpression or inactivation of Yta6 (and maybe Cdc48) may participate in signaling that in turn activates endocytosis. Despite the evidence that endocytic defects of *rvs*-mutants are suppressed by alterations in sphingolipid metabolism, it has not been tested whether this rescue is due to a bypass or re-activation of the Rvs-dependent, actin patch-mediated pathway. Our data now suggests that at least Yta6-mediated suppression of endocytic defects by-passes the normal actin-

dependent uptake machinery because (i) Yta6-mediated uptake functions in the absence of actin polymerization and (ii) Yta6 overexpression does not rescue the Sla1 dynamics after actin depolymerization and (iii) Yta6 overexpression does not restore the dynamics of Abp1-GFP labeled actin-patches in *rvs161Δ* cells.

What could be the physiological function of the Yta6-mediated endocytic pathway? As *YTA6* mutants do not strongly affect endocytosis under normal conditions, it is thus likely that this pathway is activated only in certain conditions. For example, heat shock generates a transient increase of sphingolipid base levels that signals to trigger uptake the uracil permease Fur4 (Chung et al., 2000). Many transporters in yeast, including Fur4, localize to the MCC. If domain organization is disrupted, turnover of some transporters is increased. Domain organization could therefore perform two related functions: A first function could be to sequester and protect proteins from endocytic uptake by the constitutive actin patch machinery under normal conditions. A second function would be to rapidly internalize transporters by the Yta6-mediated pathway after a change in conditions, for example during stress situations.

In yeast, only the canonical endocytic pathway mediated by clathrin and actin patches has been described. Our data now suggest that at least part of this pathway can be by-passed. How does the alternative pathway relate to endocytic mechanisms in other systems? Mammalian cells have at least ten distinguishable pathways. The closest homologues of Yta6 in mammalian cells

are spastin and related AAA-ATPases. In contrast to these proteins though, Yta6 does not have a motif to interact with microtubules and likely does not have microtubule severing activity. Intriguingly though, Spastin is localized to endosomes in mammalian cells, is required for efficient degradation of the EGF receptor and was suggested to couple membrane trafficking to microtubule remodeling (Bakowska et al., 2007; Connell et al., 2009). In addition, depletion of Spastin was found to inhibit BMP-signaling and this is linked to endocytosis of the BMP-receptor II, mediated by NIPA1. Both NIPA1 and Spastin are encoded by genes mutated in hereditary spastic paraplegia and their trafficking functions are likely important for the development of the disease (Fink, 2006). Yta6 might thus share an ancient function in trafficking with these orthologous AAA-ATPases. A better understanding of its molecular function, downstream targets and the pathway that it activates may therefore contribute to our understanding of the cell biological foundations of the development of these diseases.

All cargo after internalization from plasma membrane needs further trafficking from the endosomal pathway to their final destination for either recycling or degradation. In yeast the degradative organelle is the vacuole which performs similar functions as lysosomes in mammalian cells. We found from E-MAP (epistatic mini array profile) analysis of *PIL1* with other genes that a protein Emp70 has strong negative genetic interaction with eisosome component Pil1. Emp70 is a transmembrane protein; specifically it has nine transmembrane regions. Emp70 homologs are present in mammals and show functions related to endocytosis. It has two more homologs in yeast - Tmn2 and Tmn3. Tmn2 has

been found to be required for proper Pil1 localization (Frohlich et al., 2009). Tmn2 and Tmn3 in yeast have also been linked to endocytosis. Although Emp70 was identified in 1975, it was not functionally characterized (Schimmoller et al., 1998). Our studies showed that Emp70 localizes to more than one compartment: plasma membrane, early endosomes and vacuoles. Its localization to plasma membrane is transient but our time course experiments showed reproducibly that its localization time interval is longer when it localizes to eisosomes compared to non-eisosomal region. It is conceivable that during its localization to eisosomes, Emp70 mediates intracellular trafficking by transporting endocytic cargo. In support, we found a strong colocalization of Emp70 with early endosomal marker Kex2 and FM4-64 intermediates. Currently we know that internalized cargo passes from early to late endosomes and finally fuses to vacuoles. We observed Emp70 stained structures that were directly connected from plasma membrane to vacuoles suggesting that there might be another pathway of intracellular trafficking. The Emp70 endosomal intermediates then could carry the vesicles directly to vacuoles. This pathway may be specific for internalization through eisosomes as we observed that deletion of *PIL1* causes reduced Emp70 foci localizing to the plasma membrane. Emp70 has potentially other functions because we also found that it is required for the proper localization Kex2. Kex2 steady-state localization depends on signals that send it to early endosomes, which subsequently mature into late endosomes, from which Kex2 is actively retrieved (Brickner and Fuller, 1997). It is possible that vacuolar mislocalization of Kex2 in *emp70Δ* cells results from a defect in retrieval from the late endosome or a complex trafficking problem

affecting early endosome function. Normally, if retrieval is compromised, vacuolar sorted carboxypeptidase Y (CPY) is secreted. We tested this and found that, in contrast to the control *vps1Δ*, *emp70Δ* alone does not lead to CPY secretion (Robinson et al., 1988; Rothman et al., 1989). EMP70 has two homologs in the genome, TMN2 and TMN3. To address whether they could compensate for Emp70 function in its absence, we tested CPY secretion in strains with different combinations of the family members deleted. TMN2 deletion alone had no effect, and TMN3 deletion alone only a weak effect, on CPY sorting. In contrast, combining *emp70Δ* with either *tmn2Δ* or *tmn2Δ tmn3Δ* resulted in CPY secretion, showing that Emp70 is functionally redundant with Tmn2 in vacuolar protein sorting and that the Emp70 protein family is required for normal endosomal function.

8. Curriculum Vitae

Personal Data

Name:	Michael Rehman
Date and Place of Birth:	28.09.1981, India
Marital status:	Married

Education and research experience:

2002	Bachelor in Biosciences
2004	Masters in Biotechnology
2004-2006	Junior Research Fellow, *National Centre for Biological Sciences, India*
Nov 2006- Feb 2007	Research experience, *Emil Fischer Zentrum, Erlangen*
Mar 2007 – present	Doctorate candidate at the Max Planck Institute of Biochemistry in the group of Prof. Tobias C Walther. *Title of thesis: Analysis of endocytosis at eisosomes*

Publications

1. N E Ziolkowska, L Karotki, **M Rehman**, J T Huiskonen, T C Walther. " Eisosome-driven plasma membrane organization is mediated by BAR domains". *(Nature Structural and Molecular Biology accepted)*

2. **M Rehman**, P S Aguilar, F Frohlich, M Shales, I Ulitsky, A Olivera-Couto, H Braberg, R Shamir, P Walter, M Mann, C S Ejsing, N J Krogan, T C Walther. "A Plasma Membrane E-MAP Reveals Links Between the Eisosome, Sphingolipid Metabolism and Endosomal Trafficking", *Nature Structural and Molecular Biology* 17(7): 901-908 (first author – equal contribution)

3. S Srivastava, B Ramdass, S Nagarajan, **M Rehman**, G Mukherjee, S Krishna. "Notch1 regulates the functional contribution of RhoC to cervical carcinoma progression." *Br J Cancer 102(1): 196-205.* 2010

4. C Choudhary, C Kumar, F Gnad, M L Nielsen, **M Rehman**, T C Walther, J V Olsen, M Mann. "Lysine acetylation targets protein complexes and co-regulates major cellular functions." *Science 325(5942): 834-840*. 2009

5. B Ramdass, TT Maliekal, S Lakshmi, **M Rehman**, P Rema, P Nair, G Mukherjee, BK Reddy, S Krishna, M R Pillai "Coexpression of Notch1 and NF-kappaB signaling pathway components in human cervical cancer progression." *Gynecol Oncol 104(2): 352-361.*2007

9. Declaration of individual contributions in publications

Rehman, M., Aguilar, P. S., Frohlich, F., Shales, M., Ulitsky, I., Olivera-Couto, A., Braberg, H., Shamir, R., Walter, P., Mann, M., Ejsing, C. S., Krogan, N. J.,Walther, T. C. (2010). "A plasma-membrane E-MAP reveals links of the eisosome with sphingolipid metabolism and endosomal trafficking." Nat Struct Mol Biol 17(7): 901-908. (MR, PSA, FF, MS – equally contributed)

✹ **Michael Rehman was responsible for performing all experiments related to Emp70 and Pil1 genetic interaction (Fig 5, Fig 6).**

Choudhary, C., Kumar, C., Gnad, F., Nielsen, M. L., **Rehman, M.**, Walther, T. C., Olsen, J. V., Mann, M. (2009). "Lysine acetylation targets protein complexes and co-regulates major cellular functions." Science 325(5942): 834-840.

✹ **Michael Rehman was responsible for performing experiments of functional importance of Cdc28 K40 acetylation (Fig 4a). He was partially involved in the experiments related to Fig S7, where Cdc28-GFP pulldown was required for mass spectrometry analysis of its acetylation.**

N E Ziolkowska, L Karotki, **M Rehman**, J T Huiskonen, T C Walther. "Eisosome-driven plasma membrane organization is mediated by BAR domains". Nat Struct Mol Biol

✹**Michael Rehman was responsible for bioinformatics analysis figures: Fig 2b, supplementary figure 3. He was also involved in all the yeast work with NE Ziolkowska.**

10. Acknowledgements

This thesis arose out of research that was done in the Walther laboratory from 2007 to 2011. It gives me a great pleasure to acknowledge all the people who helped me during this period. In the first place I would like to thank Dr Tobias C Walter for his wonderful supervision. Before joining Walther laboratory I had gained research experience in India for two years but it not teach me how to design a good experiment. Tobi taught me what types of questions are more important to ask, what are good hypotheses, the importance of making models in science and last but not the least the importance of presenting the work to the outside world. I have already started to apply many of his teachings and they will be remembered for many years from now.

Walther lab also provided a very scientific and friendly atmosphere during those years. I would like to thanks Ulli and Peter for their excellent technical help. Ulli almost got me started into yeast gene tagging by helping me to obtain the endogenous Yta6 GFP tagged strain. I am grateful to Doris who helped me with many microscopy related issues. Her enthusiasm and care of the microscopy setup enabled us to have more data and fewer frustrations. Florian Frohlich's cheerfulness and helpful nature enabled me to get through with SILAC based proteomics experiment. I am also thankful to Pablo Aguilar, Lena, Pablo Mardones, Natalie, Dilip, Jerry, Alvaro, Tina, Anoop, Giesla, Nikola, Tina, Shravan, Christian, Georgios, Romain and Flo W for many discussions. I want to specially thank Felix for many discussions and kicker games mixed with further discussions which made Giesla confused if we were playing or brain-storming. I

gratefully acknowledge Dr Matthias Mann and Dr Chunaram Choudhary for the collaboration work and support.

As is true for any endeavor, my research period also had its tough times. I want to take this opportunity to thank my parents, Elena, relatives and Roshan for their love, care, support and being there at all times.

11. References

Aghamohammadzadeh, S., and K.R. Ayscough. 2009. Differential requirements for actin during yeast and mammalian endocytosis. *Nat Cell Biol*. 11:1039-1042.

Aguilar, P.S., F. Frohlich, M. Rehman, M. Shales, I. Ulitsky, A. Olivera-Couto, H. Braberg, R. Shamir, P. Walter, M. Mann, C.S. Ejsing, N.J. Krogan, and T.C. Walther. 2010. A plasma-membrane E-MAP reveals links of the eisosome with sphingolipid metabolism and endosomal trafficking. *Nat Struct Mol Biol*. 17:901-908.

Alberts, B., Johnson, A., Lewis, J, Raff, M., Roberts, K., and Walter, Peter. 2002. Molecular biology of the cell. . *Garland science*. 4th edition.

Allen, J.A., R.A. Halverson-Tamboli, and M.M. Rasenick. 2007. Lipid raft microdomains and neurotransmitter signalling. *Nat Rev Neurosci*. 8:128-140.

Ammelburg, M., T. Frickey, and A.N. Lupas. 2006. Classification of AAA+ proteins. *J Struct Biol*. 156:2-11.

Ayscough, K.R. 2005. Defining protein modules for endocytosis. *Cell*. 123:188-190.

Bakowska, J.C., H. Jupille, P. Fatheddin, R. Puertollano, and C. Blackstone. 2007. Troyer syndrome protein spartin is mono-ubiquitinated and functions in EGF receptor trafficking. *Mol Biol Cell*. 18:1683-1692.

Beach, D.L., and K. Bloom. 2001. ASH1 mRNA localization in three acts. *Mol Biol Cell*. 12:2567-2577.

Berchtold, D., and T.C. Walther. 2009. TORC2 plasma membrane localization is essential for cell viability and restricted to a distinct domain. *Mol Biol Cell*. 20:1565-1575.

Brickner, J.H., and R.S. Fuller. 1997. SOI1 encodes a novel, conserved protein that promotes TGN-endosomal cycling of Kex2p and other membrane proteins by modulating the function of two TGN localization signals. *J Cell Biol*. 139:23-36.

Chung, N., G. Jenkins, Y.A. Hannun, J. Heitman, and L.M. Obeid. 2000. Sphingolipids signal heat stress-induced ubiquitin-dependent proteolysis. *J Biol Chem*. 275:17229-17232.

Connell, J.W., C. Lindon, J.P. Luzio, and E. Reid. 2009. Spastin couples microtubule severing to membrane traffic in completion of cytokinesis and secretion. *Traffic*. 10:42-56.

Dalal, S., M.F. Rosser, D.M. Cyr, and P.I. Hanson. 2004. Distinct roles for the AAA ATPases NSF and p97 in the secretory pathway. *Mol Biol Cell*. 15:637-648.

Douglas, L.M., S.W. Martin, and J.B. Konopka. 2009. BAR domain proteins Rvs161 and Rvs167 contribute to Candida albicans endocytosis, morphogenesis, and virulence. *Infect Immun*. 77:4150-4160.

Drubin, D.G., K.G. Miller, and D. Botstein. 1988. Yeast actin-binding proteins: evidence for a role in morphogenesis. *J Cell Biol*. 107:2551-2561.

Dupre, S., D. Urban-Grimal, and R. Haguenauer-Tsapis. 2004. Ubiquitin and endocytic internalization in yeast and animal cells. *Biochim Biophys Acta*. 1695:89-111.

Engqvist-Goldstein, A.E., and D.G. Drubin. 2003. Actin assembly and endocytosis: from yeast to mammals. *Annu Rev Cell Dev Biol*. 19:287-332.

Fink, J.K. 2006. Hereditary spastic paraplegia. *Curr Neurol Neurosci Rep*. 6:65-76.

Friant, S., R. Lombardi, T. Schmelzle, M.N. Hall, and H. Riezman. 2001. Sphingoid base signaling via Pkh kinases is required for endocytosis in yeast. *EMBO J*. 20:6783-6792.

Frickey, T., and A.N. Lupas. 2004. Phylogenetic analysis of AAA proteins. *J Struct Biol*. 146:2-10.

Frohlich, F., K. Moreira, P.S. Aguilar, N.C. Hubner, M. Mann, P. Walter, and T.C. Walther. 2009. A genome-wide screen for genes affecting eisosomes reveals Nce102 function in sphingolipid signaling. *J Cell Biol*. 185:1227-1242.

Frye, L.D., and M. Edidin. 1970. The rapid intermixing of cell surface antigens after formation of mouse-human heterokaryons. *J Cell Sci*. 7:319-335.

Germann, M., E. Swain, L. Bergman, and J.T. Nickels, Jr. 2005. Characterizing the sphingolipid signaling pathway that remediates defects associated with loss of the yeast amphiphysin-like orthologs, Rvs161p and Rvs167p. *J Biol Chem*. 280:4270-4278.

Grossmann, G., M. Opekarova, J. Malinsky, I. Weig-Meckl, and W. Tanner. 2007. Membrane potential governs lateral segregation of plasma membrane proteins and lipids in yeast. *EMBO J*. 26:1-8.

Habermann, B. 2004. The BAR-domain family of proteins: a case of bending and binding? *EMBO Rep*. 5:250-255.

Hanson, P.I., and S.W. Whiteheart. 2005. AAA+ proteins: have engine, will work. *Nat Rev Mol Cell Biol*. 6:519-529.

Hartman, J.J., J. Mahr, K. McNally, K. Okawa, A. Iwamatsu, S. Thomas, S. Cheesman, J. Heuser, R.D. Vale, and F.J. McNally. 1998. Katanin, a microtubule-severing protein, is a novel AAA ATPase that targets to the centrosome using a WD40-containing subunit. *Cell*. 93:277-287.

Heese-Peck, A., H. Pichler, B. Zanolari, R. Watanabe, G. Daum, and H. Riezman. 2002. Multiple functions of sterols in yeast endocytosis. *Mol Biol Cell*. 13:2664-2680.

Higuchi, Y., M. Arioka, and K. Kitamoto. 2011. Functional analysis of the putative AAA ATPase AipA localizing at the endocytic sites in the filamentous fungus Aspergillus oryzae. *FEMS Microbiol Lett*.

Hurley, J.H., and S.D. Emr. 2006. The ESCRT complexes: structure and mechanism of a membrane-trafficking network. *Annu Rev Biophys Biomol Struct*. 35:277-298.

Janke, C., M.M. Magiera, N. Rathfelder, C. Taxis, S. Reber, H. Maekawa, A. Moreno-Borchart, G. Doenges, E. Schwob, E. Schiebel, and M. Knop. 2004. A versatile toolbox for PCR-based tagging of yeast genes: new fluorescent proteins, more markers and promoter substitution cassettes. *Yeast*. 21:947-962.

Jonsdottir, G.A., and R. Li. 2004. Dynamics of yeast Myosin I: evidence for a possible role in scission of endocytic vesicles. *Curr Biol*. 14:1604-1609.

Kaksonen, M., C.P. Toret, and D.G. Drubin. 2005. A modular design for the clathrin- and actin-mediated endocytosis machinery. *Cell*. 123:305-320.

Karp, G. 2004. Cell and Molecular biology: Concepts and experiments.

Katzmann, D.J., G. Odorizzi, and S.D. Emr. 2002. Receptor downregulation and multivesicular-body sorting. *Nat Rev Mol Cell Biol*. 3:893-905.

Kilmartin, J.V., and A.E. Adams. 1984. Structural rearrangements of tubulin and actin during the cell cycle of the yeast Saccharomyces. *J Cell Biol*. 98:922-933.

Langer, T. 2000. AAA proteases: cellular machines for degrading membrane proteins. *Trends Biochem Sci*. 25:247-251.

Lin, C.H., J.A. MacGurn, T. Chu, C.J. Stefan, and S.D. Emr. 2008. Arrestin-related ubiquitin-ligase adaptors regulate endocytosis and protein turnover at the cell surface. *Cell*. 135:714-725.

Lingwood, D., and K. Simons. 2010. Lipid rafts as a membrane-organizing principle. *Science*. 327:46-50.

Lombardi, R., and H. Riezman. 2001. Rvs161p and Rvs167p, the two yeast amphiphysin homologs, function together in vivo. *J Biol Chem*. 276:6016-6022.

Longtine, M.S., A. McKenzie, 3rd, D.J. Demarini, N.G. Shah, A. Wach, A. Brachat, P. Philippsen, and J.R. Pringle. 1998. Additional modules for versatile and economical PCR-based gene deletion and modification in Saccharomyces cerevisiae. *Yeast*. 14:953-961.

Malinska, K., J. Malinsky, M. Opekarova, and W. Tanner. 2003. Visualization of protein compartmentation within the plasma membrane of living yeast cells. *Mol Biol Cell*. 14:4427-4436.

Malinska, K., J. Malinsky, M. Opekarova, and W. Tanner. 2004. Distribution of Can1p into stable domains reflects lateral protein segregation within the plasma membrane of living S. cerevisiae cells. *J Cell Sci*. 117:6031-6041.

Mayor, S., and M. Rao. 2004. Rafts: scale-dependent, active lipid organization at the cell surface. *Traffic*. 5:231-240.

McCourt, P.C., J.M. Morgan, and J.T. Nickels, Jr. 2009. Stress-induced ceramide-activated protein phosphatase can compensate for loss of amphiphysin-like activity in Saccharomyces cerevisiae and functions to reinitiate endocytosis. *J Biol Chem*. 284:11930-11941.

Morgan, J., P. McCourt, L. Rankin, E. Swain, L.M. Rice, and J.T. Nickels, Jr. 2009. Altering sphingolipid metabolism in Saccharomyces cerevisiae cells lacking the amphiphysin ortholog Rvs161 reinitiates sugar transporter endocytosis. *Eukaryot Cell*. 8:779-789.

Mullins, C., and J.S. Bonifacino. 2001. Structural requirements for function of yeast GGAs in vacuolar protein sorting, alpha-factor maturation, and interactions with clathrin. *Mol Cell Biol*. 21:7981-7994.

Noguchi, C., and E. Noguchi. 2007. Sap1 promotes the association of the replication fork protection complex with chromatin and is involved in the replication checkpoint in Schizosaccharomyces pombe. *Genetics*. 175:553-566.

Orlando, K., and W. Guo. 2009. Membrane organization and dynamics in cell polarity. *Cold Spring Harb Perspect Biol*. 1:a001321.

Patton, J.L., and R.L. Lester. 1991. The phosphoinositol sphingolipids of Saccharomyces cerevisiae are highly localized in the plasma membrane. *J Bacteriol*. 173:3101-3108.

Robinson, J.S., D.J. Klionsky, L.M. Banta, and S.D. Emr. 1988. Protein sorting in Saccharomyces cerevisiae: isolation of mutants defective in the delivery and processing of multiple vacuolar hydrolases. *Mol Cell Biol*. 8:4936-4948.

Rothman, J.H., I. Howald, and T.H. Stevens. 1989. Characterization of genes required for protein sorting and vacuolar function in the yeast Saccharomyces cerevisiae. *EMBO J*. 8:2057-2065.

Sauer, R.T., D.N. Bolon, B.M. Burton, R.E. Burton, J.M. Flynn, R.A. Grant, G.L. Hersch, S.A. Joshi, J.A. Kenniston, I. Levchenko, S.B. Neher, E.S. Oakes, S.M. Siddiqui, D.A. Wah, and T.A. Baker. 2004. Sculpting the proteome with AAA(+) proteases and disassembly machines. *Cell*. 119:9-18.

Schimmoller, F., E. Diaz, B. Muhlbauer, and S.R. Pfeffer. 1998. Characterization of a 76 kDa endosomal, multispanning membrane protein that is highly conserved throughout evolution. *Gene*. 216:311-318.

Schuck, S., M. Honsho, K. Ekroos, A. Shevchenko, and K. Simons. 2003. Resistance of cell membranes to different detergents. *Proc Natl Acad Sci U S A*. 100:5795-5800.

Simons, K., and M.J. Gerl. 2010. Revitalizing membrane rafts: new tools and insights. *Nat Rev Mol Cell Biol*. 11:688-699.

Simons, K., and W.L. Vaz. 2004. Model systems, lipid rafts, and cell membranes. *Annu Rev Biophys Biomol Struct*. 33:269-295.

Singer, S.J., and G.L. Nicolson. 1972. The fluid mosaic model of the structure of cell membranes. *Science*. 175:720-731.

Smith, M.G., S.R. Swamy, and L.A. Pon. 2001. The life cycle of actin patches in mating yeast. *J Cell Sci*. 114:1505-1513.

Stradalova, V., W. Stahlschmidt, G. Grossmann, M. Blazikova, R. Rachel, W. Tanner, and J. Malinsky. 2009. Furrow-like invaginations of the yeast plasma membrane correspond to membrane compartment of Can1. *J Cell Sci*. 122:2887-2894.

Tabuchi, M., A. Audhya, A.B. Parsons, C. Boone, and S.D. Emr. 2006. The phosphatidylinositol 4,5-biphosphate and TORC2 binding proteins Slm1 and Slm2 function in sphingolipid regulation. *Mol Cell Biol*. 26:5861-5875.

Valdez-Taubas, J., and H.R. Pelham. 2003. Slow diffusion of proteins in the yeast plasma membrane allows polarity to be maintained by endocytic cycling. *Curr Biol*. 13:1636-1640.

Vale, R.D. 2000. AAA proteins. Lords of the ring. *J Cell Biol*. 150:F13-19.

van der Rest, M.E., A.H. Kamminga, A. Nakano, Y. Anraku, B. Poolman, and W.N. Konings. 1995. The plasma membrane of Saccharomyces cerevisiae: structure, function, and biogenesis. *Microbiol Rev*. 59:304-322.

van Meer, G. 2002. Cell biology. The different hues of lipid rafts. *Science*. 296:855-857.

Vanderkooi, G., and D.E. Green. 1970. Biological membrane structure, I. The protein crystal model for membranes. *Proc Natl Acad Sci U S A*. 66:615-621.

Vereb, G., J. Szollosi, J. Matko, P. Nagy, T. Farkas, L. Vigh, L. Matyus, T.A. Waldmann, and S. Damjanovich. 2003. Dynamic, yet structured: The cell

membrane three decades after the Singer-Nicolson model. *Proc Natl Acad Sci U S A*. 100:8053-8058.

Wachtler, V., and M.K. Balasubramanian. 2006. Yeast lipid rafts?--an emerging view. *Trends Cell Biol*. 16:1-4.

Wachtler, V., S. Rajagopalan, and M.K. Balasubramanian. 2003. Sterol-rich plasma membrane domains in the fission yeast Schizosaccharomyces pombe. *J Cell Sci*. 116:867-874.

Walther, T.C., P.S. Aguilar, F. Frohlich, F. Chu, K. Moreira, A.L. Burlingame, and P. Walter. 2007. Pkh-kinases control eisosome assembly and organization. *EMBO J*. 26:4946-4955.

Walther, T.C., J.H. Brickner, P.S. Aguilar, S. Bernales, C. Pantoja, and P. Walter. 2006. Eisosomes mark static sites of endocytosis. *Nature*. 439:998-1003.

Wang, H., B. Kakaradov, S.R. Collins, L. Karotki, D. Fiedler, M. Shales, K.M. Shokat, T.C. Walther, N.J. Krogan, and D. Koller. 2009. A complex-based reconstruction of the Saccharomyces cerevisiae interactome. *Mol Cell Proteomics*. 8:1361-1381.

Wendland, B., S.D. Emr, and H. Riezman. 1998. Protein traffic in the yeast endocytic and vacuolar protein sorting pathways. *Curr Opin Cell Biol*. 10:513-522.

Wendland, B., J.M. McCaffery, Q. Xiao, and S.D. Emr. 1996. A novel fluorescence-activated cell sorter-based screen for yeast endocytosis mutants identifies a yeast homologue of mammalian eps15. *J Cell Biol*. 135:1485-1500.

White, S.R., and B. Lauring. 2007. AAA+ ATPases: achieving diversity of function with conserved machinery. *Traffic*. 8:1657-1667.

Youn, J.Y., H. Friesen, T. Kishimoto, W.M. Henne, C.F. Kurat, W. Ye, D.F. Ceccarelli, F. Sicheri, S.D. Kohlwein, H.T. McMahon, and B.J. Andrews. 2010. Dissecting BAR

domain function in the yeast Amphiphysins Rvs161 and Rvs167 during endocytosis. *Mol Biol Cell*. 21:3054-3069.

Zanolari, B., S. Friant, K. Funato, C. Sutterlin, B.J. Stevenson, and H. Riezman. 2000. Sphingoid base synthesis requirement for endocytosis in Saccharomyces cerevisiae. *EMBO J*. 19:2824-2833.